The investigation of Optical Coherence Tomography as a clinical tool to determine the extent of Molar Incisor Hypomineralisation (MIH) Lesions

Submitted in partial fulfilment of the requirements for the Degree of Clinical Doctorate in Dentistry (Paediatric Dentistry)

Eastman Dental Institute University College London

2015 – 2018

Submitted by:

Dalal Khaled Al Sabah

B.Med.Sc. (Kuwait), B.Dent.Med (Kuwait)

Word count = 32,234

Project Supervisors:

Dr Laurent Bozec (Division of Biomaterials & Tissue engineering, Eastman Dental Institute – University College London)

Dr Susan Parekh (Department of Paediatric Dentistry, Eastman Dental Institute – University College London)

Table of contents

List of Figures:

List of tables

Abbreviations

AI	Amelogenesis Imperfecta
ALARA	As Low As Reasonable Achievable principle
BL	Bucco-lingual
BW	Bitewing radiograph
CPP-ACP	Casein phosphopeptide-amorphous calcium phosphate
CEJ	Cemento-enamel Junction
DDE	Developmental Defect of Enamel index
DICOM	Digital Imaging and Communications in Medicine
DNA	Deoxyribonucleic acid
DPT	Dental Panoramic Tomography
EAPD	European Academy of Paediatric Dentistry
EDH	Eastman Dental Hospital
EDJ	Enamel Dental Junction
FDI	World Dental Federation
FPM	First Permanent molar
FS	Fissure Sealant
GIC	Glass Ionomer Cemenr
HA	Hydroxyapatite crystals
HSBs	Hunter-Schreger bands
LCPA	Long Cone Periapical radiograph
MD	Mesio-distal
mDDE index	modified Developmental Defect of Enamel index
MHSI	Molar Hypermineralisation Severity Index
MIH	Molar Incisor Hypomineralisation

MIH-TNI	MIH Treatment Need Index
MRI	Magnetic Resonance Imaging
OCT	Optical Coherence Tomography
PCB	Polychlorinated Biphenyls
PEB	Post Eruptive Breakdown
PI	Permanent Incisor
PPM	Packs Per Million
SOR	Striae of Retzius
SPM	Secondary Primary Molar
SSC	Stainless Steel Crown
ROI	Region of Interest
TIFF	Tagged Image File Forma

Declaration of work

I, Dalal Khaled Al Sabah confirm that the work presented in this thesis is my own. Where information has been derived from other sources, I confirm that this has been acknowledged and indicated in the thesis.

Dalal Khaled Al Sabah

Eastman Dental Institute, University of College London

September 2018

Abstract

Molar incisor hypomineralisation (MIH) is a qualitative developmental defect in enamel, defined as hypomineralisation of systemic origin affecting first permanent molars and less frequently associated with permanent central incisors. It's prevalence worldwide ranges from 2.4-40%. MIH poses challenges to both patients and clinicians, and a burden on global health. Therefore, prompt diagnosis and treatment is crucial to prevent its complications.

The current diagnostic measures are clinical visual examination by means of indices, and radiographic examination. However, current diagnostic tools are subject to limitations, bias and drawbacks, therefore there is a need for better diagnostic tools to determine the extent and depth of MIH lesions to determine the tooth's prognosis.

The aim of this study is to expand the use of Optical Coherence Tomography (OCT) imaging in dentistry, using it as a routine clinical diagnostic tool in MIH, and to compare the results with conventional clinical methods i.e. radiographs and clinical indices. In addition, to define some markers in the OCT scan and scattering profile intensity plots for both sound and MIH affected teeth, to help aid in their diagnosis.

The major outcome of this study to date came from observing and comparing the OCT scattering intensity profiles for both control and MIH lesions. These were investigated in greater detail and different empirical markers were extracted to stereotype each defect. This led us to establish scattering fingerprints for each type of MIH lesion. A multi-assessors analysis followed by a kappa analysis was done to evaluate the selectivity and accurateness of our makers. In addition, evaluating the lesion as a

whole, progressing it from a 2D to a 3D perspective which helps interpret the data easier.

In conclusion, OCT has been recognised to be a safe and useful diagnostic method when studying MIH lesions, providing an understanding of the lesion in terms of depth and extent, therefore helping in predicting the lesion's prognosis, which is not found in conventional methods. In addition, OCT helps to differentiate between MIH and sound teeth, and additionally between different types of MIH lesions.

Acknowledgment

Alhamdulillah, I am happy that I have managed to finish and submit this final thesis after three years of work and sacrifice. First, I dedicate it to my late father, Baba Khaled, may you rest in peace, whom I know would be proud in this moment. Furthermore, I would like to express my deepest appreciation to my beloved mother, Hessa Al Sabah, and my Aunt, Auntie Bibi, my sisters, Nour and Mariam and brothers, Subah and Athbi for their continuous prayers, encouragement and for being my supporters in all my struggles.

Not to forget, my husband Mubarak Al Sabah who was always my strength and inspiration especially during my difficult times.

Moreover, I would like to express my deepest gratitude to my beloved friends, Mashael Al Omran and Maryam Al Kandari for their continuous help and support throughout my studies and writing up of my thesis; In addition, Amel Behbehani, Shouq Al Rajhi, Awatif Al Sabah, Amira Al Khaja, Fatma Al Baghli and al Anoud Al Mousa for their care, moral support, patience and tolerance throughout the last three years.

I would also like to show appreciation to my supervisors, Dr Laurent Bozec and Dr Susan Parekh, for their excellent guidance and assistance throughout the research. In addition, a special thanks to Dr David Boniface for his help with the statistical analysis. Furthermore, Dr Paul Ashley, the program director for his continuous support throughout the DDent program.

To my dear colleagues, Zoi Tzelepi and Shaima Sarkhoh, thank you both for being supportive and to whom I call a friend who shared all the happy and sorrow moments

during the past three years. To my other DDent colleague, thank you for everything.

To all the staff that I have met and worked with in the Unit of Paediatric Dentistry of Eastman Dental Institute/ Hospital, thank you so much for your lovely companionship.

Last but not least, I would like to give my special thanks to the Ministry of Health Kuwait, for the financial support and the opportunity given to further my studies.

Dalal Khaled Al Sabah

Paediatric Dentistry, Eastman Dental Institute,

University of College London

July 2018

Impact statement

Molar incisor hypomineralisation (MIH) is a common condition causing substantial pain to children, distress to their parents, and a large burden on health care systems around the world (Figure 1). It is predicted that the cost of treatment is potentially the same as the national expenditure on leading cancers. It is one of the more common pandemic health problems in the world, and it can be effectively controlled by early diagnosis, followed by appropriate treatment. Continuing research and development are needed to prevent and manage this important international health problem.

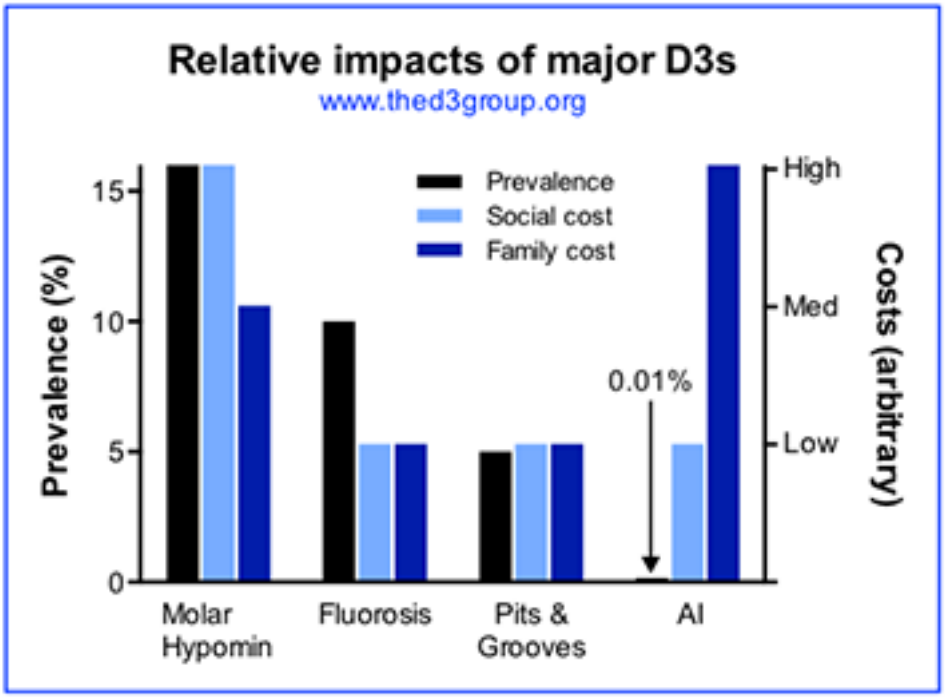

Figure 1 Showing the relative impacts; prevalence, social and family costs of different dental defects, with MIH being the highest (taken from the http://thed3group.org/).

Prevalence of MIH ranges from 2.4-40% worldwide, with an increasing incidence. Recent meta-analysis found that the mean global prevalence is approximately 13%

with 878 million people affected, and 4.8 million cases per year requiring treatment (Schneider, P.M. and Silva, M., 2018).

MIH can be diagnosed both clinically and radiographically, however with limitations. Radiographs not only possess radiation and ionisation defects, but also can be frightening for children who may not be able to tolerate intra-oral films. Therefore a more child friendly, and smaller equipment to scan the teeth without any deterministic defects should be used.

I have presented my research to colleagues and professors in our institute, and proposed a calibration exercise on how to correctly use indices to report MIH lesions (appendix 5). This research was also presented as a poster in the International Dental Association of Research (IADR) in London, United Kingdom 2018, where researches from all over the world attend, interact and exchange new knowledge (Appendix 6).

This research can be a starting point for brining the OCT scanner to the dental clinical chair, as a routine diagnostic tool. Furthermore, the markers we have extracted can be further studied and used as a future research scholarship, to be populated and used within a larger sample size, and to confirm these markers; consequently this can be taken globally as a new index for MIH categorisation. In addition, automate these markers, and make diagnosis of MIH as a 3-D entity instead of characterising it subjectively using 2-d x-rays.

CHAPTER 1

Introduction

Introduction:

Statement of problem:

Enamel is the strongest tissue in the human's body. It is composed of more than 95% hydroxyapatite, with the remaining being water and organic material, which makes it highly mineralised (Avery 2002). Its formation can be affected by genetic, environmental or systemic disturbances, leading to enamel defects.

The most common enamel defect is Molar Incisor Hypomineralisation (MIH), and due to its high prevalence and burden of disease, the lifelong implications and cost to the general community is significant. Therefore the diagnosis and management of MIH is of high importance, especially in the early mixed dentition period, around 6-8 years, due to the limitations in patient co-operation and the diagnostic methods that are not accurate enough to determine the extent of the lesion into enamel.

In this study, our main objective is to expand the use of optical coherence tomography (OCT) as an imaging technique for MIH teeth, brining it to the dental chair. In addition to explore MIH in terms of the type of defect and ultrastructure characteristics, and compare it with clinical and radiographic imaging of teeth. Furthermore, to generate markers as fingerprints to stereotype each type of defect, to aid in the diagnosis of MIH.

CHAPTER 2

Review of Literature

Review of the Literature

2.1 Enamel

Enamel is the (white) visible part of the tooth's crown, which acts as a solid barrier, covering and protecting the dentine and pulp. It is a highly mineralised, and translucent material with well-arranged, packed hydroxyapatite crystals, and is considered the hardest tissue in the human body (Margolis et al., 2006). Human enamel varies in thickness over the surface of the tooth, often thickest at the cusp, up to 2.5 mm, and thinnest around the cervical, approximately 1.3mm (Nanci, 2013).

2.1.1 Enamel formation:

Teeth are formed from an aggregate of ectodermal cells, called the tooth germ, which is composed of the enamel organ, dental papilla and dental sac, as illustrated in figure 2.1. The enamel organ gives us enamel; the dental papilla gives rise to the pulp and dentine, and the dental sac evolves into the tooth supporting tissues (Nanci., 2007). Therefore, the human structure of a tooth is composed of enamel, dentine and pulp as seen in figure 2.2.

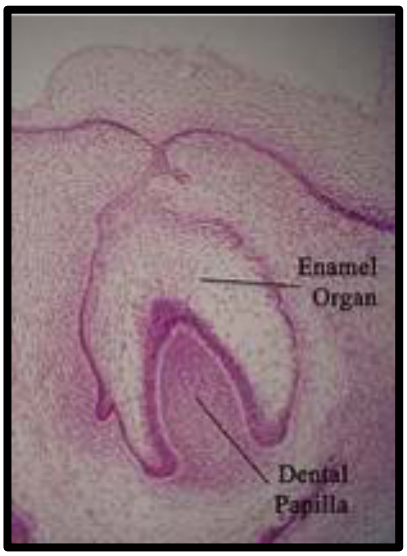

Figure 2.1 Showing histology of enamel organ and dental papilla (Image Courtesy of Nanci, 2013)

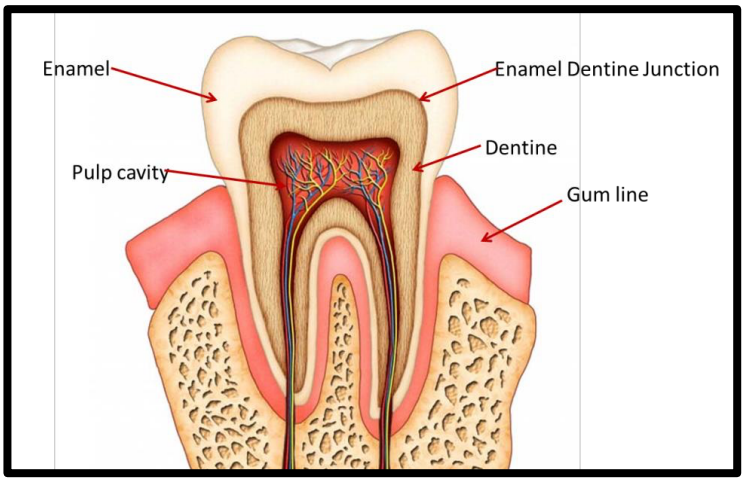

Figure 2.2 Image of the structure of a human tooth (Image taken from http://beta.classmint.com)

Tooth development starts around 6 weeks of gestation period and is divided into stages: the initiation, bud, cap and bell stage, and finally maturation. It's a well-organized process and is strictly under genetic control, any disturbance results from gene mutation. Different dental defects are categorised depending on the type and timing of the insult.

Amelogenesis is the process of enamel formation (figure 2.3), during the advanced bell stage of tooth development and is divided into two stages: secretory and maturation. Around the third or fourth month of gestation, the secretory phase occurs where ameloblasts, the cells responsible for enamel formation, release enamel proteins, which are then mineralised by the enzyme alkaline phosphatase (Fehrenbach et. al., 2015). The proteins are amelogenins, ameloblastins, enamelins, and tuftelins. Primarily the enamel is secreted as a partially mineralised organic matrix, which comprises only 30% of mineral with the residue being organic material and water (Robinson et al., 1995). The enamel minerals in this stage are elongated and thin in shape (Margolis et al., 2006). Following the partial mineralisation, the maturation stage occurs where the ameloblasts remove these proteins from the enamel matrix by proteases such as matrix metalloproteinase-20 in order to finalize the mineralisation. After the

ameloblasts have transported these proteins out of enamel, it is considered fully mineralised and enough space is made for the enamel minerals to expand in thickness and width (Fehrenbach et. al., 2015).

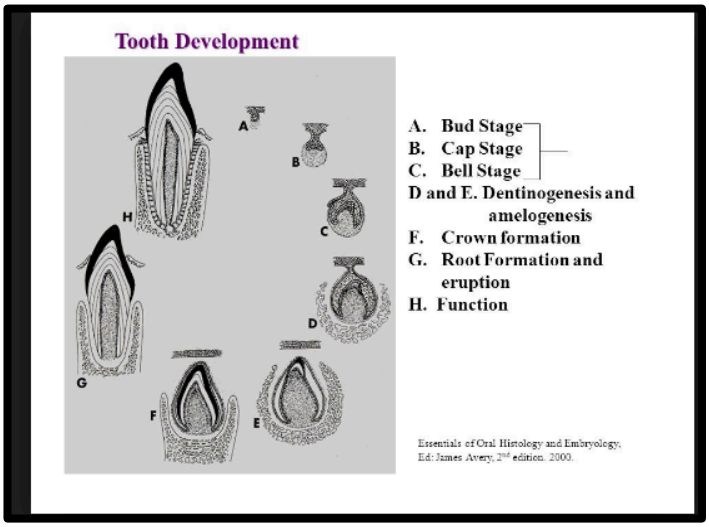

Figure 2.3 Image showing the stages of tooth development, (taken from Essentials of Oral Histology and Embryology, Ed: James Avery, 2nd edition).

Any disturbances during the phase of enamel matrix formation may lead to a quantitative or morphological defect i.e. hypoplasia. On the other hand, if the disturbance occurs in the mineralisation phase, the enamel may have a qualitative defect, i.e. hypo mineralised. (Martinović et al., 2015).

There are three main developmental defects of enamel; hypoplasia, hypocalcification and hypomaturation. Hypoplastic enamel occurs when the enamel layer is not formed into normal thickness. Therefore, clinically the affected tooth appears smaller in size with a smooth or pitting surface and thin but normal enamel (figure 2.4). In hypocalcification, the affected tooth is normal in size and shape however, the color of the enamel ranges from a yellow to brown discoloration due to poor mineralisation process of the enamel matrix (figure 2.5).

The enamel is also very soft and fragile when hypomineralised. On the other hand, hypomature teeth present with normal size and shape with mottled enamel and white to yellow opacities (figure 2.6). Sometimes there are combinations of defect occuring in a single tooth.

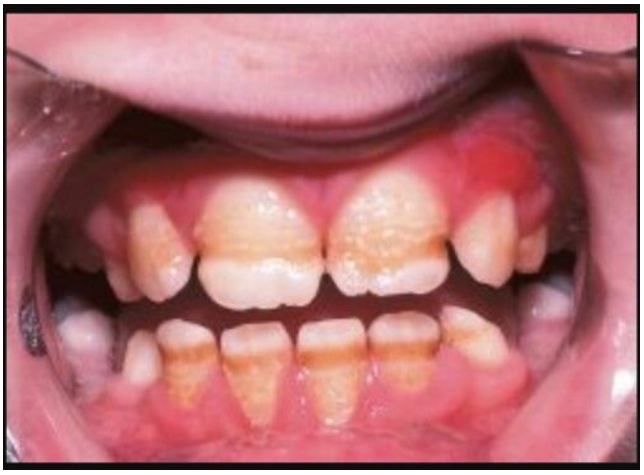

Figure 2.4 Showing a picture of a dentition affected with enamel hypoplasia (image courtesy of Aine, L., et al., 1990)

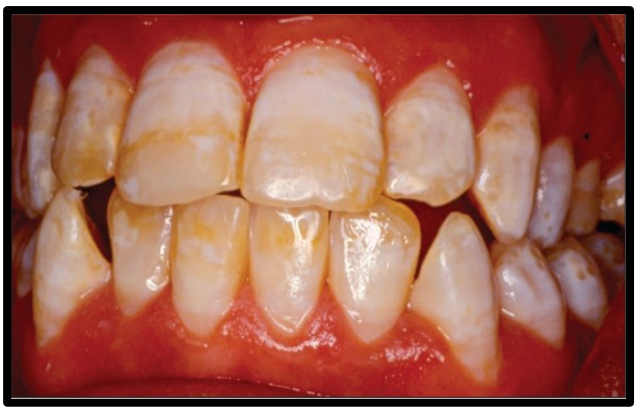

Figure 2.5 Showing a picture of a dentition affected with enamel hypocalcification image courtesy of Student dentaire

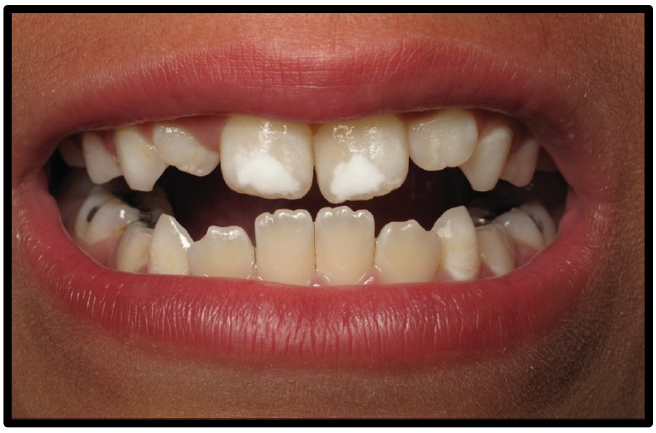

Figure 2.6 Showing a picture of a dentition affected with enamel hypomaturation (Image courtesy of Omar, S.I., 2013.

2.1.2 Composition of enamel

Enamel is composed of both inorganic and organic material. The main inorganic mineral is hydroxyapatite along with some trace elements. Hydroxyapatite is a crystalline calcium phosphate ($Ca_{10}(PO^4)^6(OH)_2$) crystal, comprising more than 95% of the enamels volume (Staines et al., 1981). The crystals are neatly ordered and closely packed, directed from the enamel dentine junction (EDJ) to the occlusal surface of the tooth (Simmer and Hu, 2001).

The organic material constitutes about 1-2% of the enamel matrix, mainly proteins and minor concentrations of proteoglycans and lipoids. The remaining 4% is water, which lies between the crystals and organic material, and its presence is associated with the porosity of the tissue.

Enamel is similar to bone and dentine in some properties, however is considered unique in others, as it is the only hard tissue that does not contain collagen and is avascular with no nerve supply (Fincham et al., 2000). It does contain two unique classes of proteins, whose roles are not fully understood but are said to be important in the development of enamel, these are amelogenins and enamelins (Nanci, A., 2007). Despite the fact that it has no ability of self-regeneration, it is not a static tissue as it can go through mineralisation changes, i.e. demineralisation and remineralisation to a certain degree (Fincham et al., 2000).

Remineralisation is a natural process that occurs in the oral cavity, it helps in managing non-cavitated lesions, by salivary proteins and fluoride, and restores the strength and function of tooth structure. On the other hand, demineralisation is a chemical process where minerals are removed from the hard tissue, by acids, and can lead to cavitation. Together, remineralisation and demineralisation

work as a dynamic process (Li, X. et al., 2014). This is illustrated in figure 2.7 below.

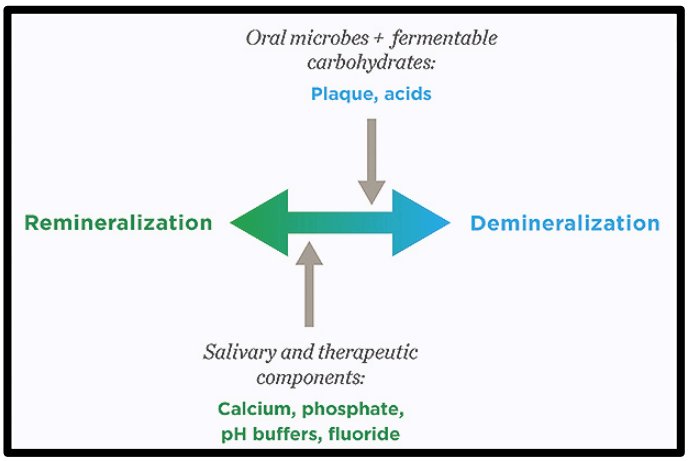

Figure 2.7 The oral equilibrium between remineralisation and demineralisation (Jefferies, S.R., 2014).

2.1.3 Ultrastructure

Enamel is a complex material with an intricate microstructure. The main mineral component is calcium hydroxyapatite, which has a size around 70 nm in width, 25 nm thick and extends across the full width of the enamel (Staines et al., 1981).

Millions of these crystallites conglomerate tightly and are densely packed to form enamel rods (figure 2.8), which are the basic structural unit of enamel. An enamel rod measures approximately 4 μm wide to 8 μm high and when viewed in cross section is compared to a key hole, with its head pointing towards the crown and tail towards the root (Fernandes, C.P. and Chevitarese, O., 1991).

Enamel rods give enamel its rigidity and strength, and because of their interwoven orientation, it gives teeth the ability to withstand masticatory forces up to 20-30 pounds per tooth (Fernandes, C.P. and Chevitarese, O., 1991).

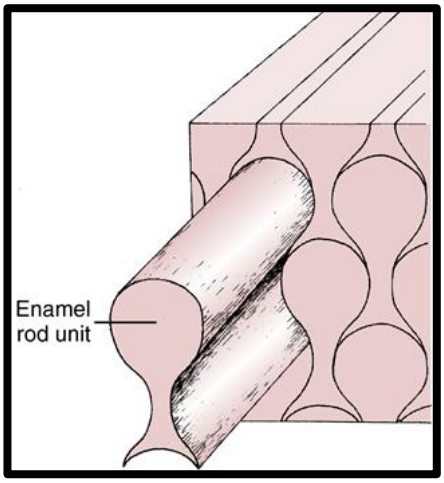

Figure 2.8 Image displaying orientation of enamel rod (From Avery JK: Oral development and histology, 2002)

Hunter-Schreger bands (HSBs)

Under polarised light microscopy, distinctive bands are seen in enamel prisms, which are called ‘Hunter–Schreger bands’ (figure 2.9). These are formed by enamel rods, which are organised in layers of varying thickness, perpendicular to each other. These bands add strength to enamel and prevent any cracks from propagating throughout the tooth (Nanci, 2013). In addition, these band arrangements aid in enhancing enamel resistance to all types of tooth wear, such as attrition, erosion and abrasion (Lynch et al., 2011).

Striae of Retzius (SoR)

These lines are considered as incremental growth lines, which are seen in normal enamel (figure 2.9). They are seen as thick age bands, described like rings on a tree. They present as dark lines, and signify the increments of different layers of enamel during its apposition in crown formation (Brand, et al., 2013).

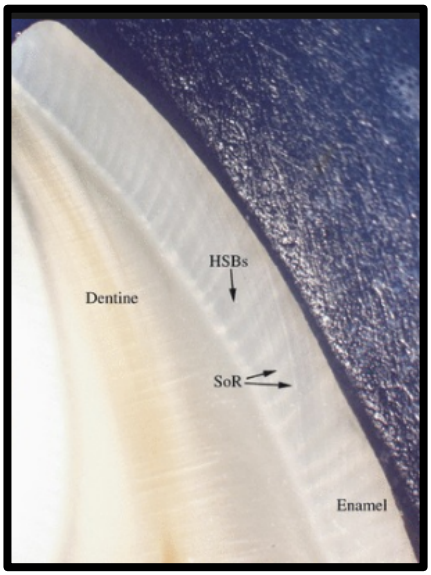

Figure 2.9 Image representing SoR and HSBs (Lynch et al., 2010)

2.1.4 Physical properties

It is the hardness of enamel that permits the teeth to withstand the stresses of heavy masticatory forces (Nanci, A., 2007). Enamel is considered the hardest tissue in the human body, as it compromises approximately 1% of water only (Chun, K.J.,et al., 2014). Studies suggested that enamel's hardness remains homogenous from the outer tooth surface to the enamel dentinal junction (Gutiérrez-Salazar and Reyes-Gasga, 2003). However, as opposed by other studies that it is evident there is a decrease in Hardness and Young's modulus, in addition in between buccal and lingual surface of permanent teeth, as a result of the changes in crystal chemistry (Cuy et al., 2002, Braly et al., 2007).

Enamel's hardness is said to be harder than mild steel, however a lot more brittle (Newbrun, E. and Pigman, W., 1960). Therefore, it is not scratched upon metal cutlery but you can chip it by trying to open a metal can with your teeth.

In relation to the physical properties of enamel, the hardness is the one most widely studied. The values of enamel hardness have been reported either by Knoop Hardness Number (KHN) or Vickers Hardness Number (VHN) depending on the method used. However, the numbers obtained from both methods were not significantly different, with an average ranging from 270 to 350 KHN, or from 250 to 360 VHN (Gutierrez-Salazar and Reyes-Gasga, 2001).

When enamel hardness was measured, sound enamel ranks as 5 on Mohs scale of mineral hardness, compared to 4.5 for bone and 3-4 for dentine, and 83 GPa on Young's modulus (Staines et al., 1981).

Another important property is its high resistance to wear and abrasion. These properties are significant as enamel is unable to self-repair or replace (Berkovitz et al., 2009).

2.1.5 Developmental Enamel Defects

Enamel is characterised by a lack of metabolic activity, thus when it is formed any disturbances occurring during its development can lead to permanent defects, which can act as records of early life events or exposures (Crombie et al., 2009). Developmental Enamel Defect is defined as “disturbances in hard tissue matrices and their mineralisation that arise during odontogenesis” (Vargas-Ferreira, F. and Ardenghi, T.M., 2011). Enamel defects can occur at any stage of tooth development and are usually associated with the development stage when the defect occurs. They have a complex aetiology with multiple pathways, and can have several interconnected factors (Masterson, E.E.,et al., 2017). Causes are either idiopathic, local factors, such as trauma and infection to primary teeth, or general factors, i.e. genetic, systemic.

Dental anomalies are categorised as affecting tooth number (supernumerary teeth and hypodontia), size (macrodontia and microdontia), shape (peg shaped) or structure (MIH) (Pinkham et al., 2005). The most common development enamel defects are molar incisor hypomineralisation (MIH), Amelogenesis Imperfecta and fluorosis (Mohd Noor, M., 2014).

2.2 Molar Incisor Hypomineralisation (MIH)

MIH is defined as ” a qualitative defect of systematic origin of the enamel, involving one or more first permanent molar, which is frequently associated with affected incisors ” and was first introduced in 2001 (Weerheijm et al., 2001).

The disease was presented at the European Academy of Paediatric Dentistry (EAPD) Assembly in 2000, by four different groups of researchers who each named

the condition differently. The four different names were as follows; ‘hypomineralised FPMs’ (Beentjes et al., 2002), ‘idiopathic enamel hypomineralisation in FPM’ (Jälevik et al., 2000), ‘non-fluoride hypomineralisation in FPM’ (Leppäniemi et al., 2000) and ‘cheese molars’ (Weerheijm et al., 2000). Therefore, to avoid confusion an agreement on the name has to be reached, thus the definition was made.

A relationship as well has been found between the occurrence of hypomineralised second primary molars (HPSM) and MIH, which is suggested that, clinically, HSPM can be used as a predictor for MIH (Elfrink et al., 2012).

2.2.1 Epidemiology

Worldwide many prevalence studies related to MIH have now been published (summarised in table 2.1), ranging from 2.4% to 40% (Jalevik, 2010), which may be due to the use of different indices, criteria, examination variability, lack of standardised methods of recording lesions and different age groups (Elfrink et al. 2015).

Previously, diagnosis of MIH affected teeth was concealed by the presence of carious lesions, whereas currently, MIH has become more evident as a separate entity as caries experience decreases in many populations and clinicians’ awareness increases (Gambetta-Tessini, K., et al., 2016). Studies regarding data about prevalence in North America, Africa and the Middle East are very uncommon, with the majority of studies clustered in Europe where they reported prevalence from 3.6% to 37.5%, (Jälevik, 2010.), with the prevalence in UK being 15.9% (Balmer et al., 2012). With regards to the Middle East, only few data is found accounting for the prevalence of MIH, however it was found to be common amongst children in Iraq

(Ghanim et al., 2011). A study in 2008 reported that the prevalence of MIH in Hong Kong as only 2.8%, (Cho et al., 2008) while another study in Brazil reported a prevalence of 40.2% (Soviero et al., 2009). These variations might be due to differences in environmental, socioeconomic status or genetic factors associated with each population (Balmer et al., 2012).

The increase in prevalence may be due to the fact that as caries rates in the past were higher, MIH lesions might have been concealed, and as caries levels have now decreased; MIH lesions became a clearer entity (Ogden et al., 2007). In addition, global awareness of the condition has increased. Meanwhile, the prevalence of MIH is likely to be underestimated as some examiners failed to include MIH teeth with post-eruptive break down that required atypical restorations or were extracted (Jalevik 2010).

Another study showed that primary second molar hypomineralisation is around 9% in Netherlands, suggesting that there is a relationship between primary second molar hypomineralisation and MIH, thus it can be used as a predictor for permenant molars (Elfrink et al., 2012).

A study in 2008 found that there was no significant difference in prevalence between males and females (Willmott et al., 2008). In addition, it was found that children with severely affected FPMs would more likely have affected incisors (Jalevik et al., 2001a).

Country	Prevalence	Study
Worldwide	2.4% to 40%	Jalevik, 2010
Europe	3.6% to 37.5%	Jälevik, 2010
UK	15.9%	Balmer et al., 2012
Hong Kong	2.8%	Cho et al., 2008
Brazil	40.2%	Soviero et al., 2009
Netherlands	9%	Elfrink et al., 2012

Table 2.1 Summarizing prevalence of MIH across different countries as presented in different studies

2.2.2 Aetiology

The exact cause of MIH is not known, and there is currently not enough evidence in the literature to establish the aetiological factors for MIH (Crombie et. al., 2009). Different aetiologies suggested include health problems during pregnancy and the first few years of life, or other environmental factors (Fragelli et al., 2015).

Ameloblasts, the cells that deposit enamel, are sensitive and susceptible to very minor changes in their environment, disrupting Amelogenesis. Disrupting factors include increases in temperature, hypoxia, hypocalcaemia, and any changes in pH (Allazzam et al., 2014).

MIH can occur at any time before birth, or during the first three years of life, as this is the crucial development time for both the first permanent molars and permanent incisors (Alaluusua, 2010). During the fourth month of intra-uterine life, the first permanent molars start to develop and mineralisation starts at birth and continues up to a thousand days, explained in table 2.2. As for the incisors, calcification starts at the age of three to four months and enamel formation is complete at the age of 4-5 years old (Nanci, A., 2007). Therefore, any disturbance in this period can lead to a hypomineralisation defect in the molars and incisors, leading to MIH (Alaluusua, 2010).

	Calcification begins		Crown completed		Eruption	
Tooth	Maxilla	Mandibula	Maxilla	Mandibula	Maxilla	Mandibula
I_1	3 months	3 months	4 _ year	3 _ year	7 _ year	6 _ year
I_2	11 months	3 months	5 _ year	4 year	8 _ year	7 _ year
M_1	32 weeks in utero	32 weeks in utero	4 _ year	3 _ year	6 _ year	6 year

I_1= permanent central incisor; I_2= permanent lateral incisor; M_1= first permanent molar

Table 2.2 Development of first permanent molars and incisors as described by Proffit 1993

Pre-natal causes

It was thought that MIH could be related to any medical problem during pregnancy, as it was more common in children with mothers who had problems during pregnancy than those who were healthy (Whatling and Fearne, 2008; Lygidakis et al., 2008). A study in 1980, demonstrated urinary infection during the last trimester was found to be associated with MIH (Fredén et al., 1980).

Peri-natal

Any traumatic birth event, e.g. an abnormal delivery such as a Caesarean section, can lead to metabolic changes in the formation of the enamel causing clinical defects (Alaluusua, 2010). Hypomineralisation was more prevalent in preterm children compared to those born after week 37, and children with low birth weight (Prokocimer et. al., 2015). However, another study stated that there is no association between MIH with birth prematurity or complications, low birth weight, or breast-feeding duration (Allazzam et al., 2014).

Post-natal causes

Illness during the first four years of life have been linked to MIH (Allazzam et al., 2014). In addition, a Greek study showed that complications during the first year of life were clearly more common in MIH children than in those without (Lygidakis et al., 2008). Diseases can affect enamel mineralisation either by direct influence of the disease on the ameloblast activity, or indirectly by its complications such as hypoxia, hypocalcaemia, fever, and/or malnutrition due to the illness (Sui et. al., 2003).

A study in 1995 showed that children with respiratory illnesses had a higher prevalence of hypomineralised permanent molars (Van Amerongen et. al., 1995). Respiratory diseases which result in hypoventilation and respiratory acidosis, affect the enamel matrix pH which in turn inhibit the action of proteolytic enzymes and the development of the crystal hydroxyapatite, therefore leading to enamel hypomineralisation (W. Sui et. al., 2003). For example, asthma is said to have a link with MIH. This can be due indirectly to hypoxia or respiratory acidosis, or due to the fact that asthmatic patients require corticosteroid therapy, which in turn suppress ameloblast activity (Pawlicki et. al., 1991). However, most children have asthma, but not all children have MIH.

Amoxicillin use in the first year of life has been linked with a higher risk of MIH (Laisi et al., 2009). However, the association of MIH with antibiotics use is controversial, as antibiotics are commonly used with upper respiratory infections, so it is not possible to confirm whether the disease or the drug itself caused MIH. This is the same case as with fever, as it's a common symptom associated with most childhood respiratory infections so it is difficult to conclude if it is the illness or the fever that is causing the defect (Allazzam et al., 2014).

In addition, a correlation was made between exposure to high levels of dioxins and Polychlorinated biphenyls (PCBs), which are both environmental pollutants often formed as waste in industrial processes, to enamel formation defects. Exposure to these environmental toxins in early childhood has been linked with hypomineralised opacities (Alaluusua et al., 1996). It was found in Sloavenia that children living in a PCB contaminated area had a higher prevalence of enamel defects compared to those in a control area (Jan and Vrbič, 2000). Several animal experiments have shown that teeth are amongst the most sensitive organs to the effects of dioxins. In addition, a study associated prolonged breastfeeding with MIH (Alaluusua et al., 1996) and it suggested that pollutants, such as dioxins, in breast milk, could be the cause. On the other hand, other studies found that there was no relation between MIH and breast-feeding, and may in fact reduce the risk of MIH (Jalevik et al., 2001a, Whatling and Fearne, 2008). The main aetiological factors associated with MIH are summarised in table 2.3 below.

Author, Year	Type of Study	Cause
Pre-Natal		
Whatling and Fearne, 2008; Lygidakis et al., 2008	Epidemiological Study	Any disease during pregnancy
Peri-Natal		
Alaluusua, 2010	Systematic review	C-section
Prokocimer et. al., 2015	Cross-sectional study	Preterm baby
Prokocimer et. al., 2015	Cross-sectional study	Low birth weight
Fredén et al., 1980	Systematic review	Urinary infection
Post-Natal		
Allazzam et al., 2014	Cross-sectional study	Illness during first 4 years of life
Lygidakis et al., 2008	Retrospective clinical study	Illness during first year of life
W. Sui et. al., 2003	Experimental study	Hypoxia, hypocalcaemia, malnutrition, fever
Van Amerongen et. al., 1995	Retrospective clinical study	Respiratory disease
Pawlicki et. al., 1991	Experimental study	Asthma
Laisi et al., 2009	Retrospective clinical study	Amoxicillin use in first year of life
Allazzam et al., 2014	Cross-sectional study	Fever
Alaluusua et al., 1996	Retrospective clinical study	Dioxins and Polychlorinated biphenyls (PCBs),
Alaluusua et al., 1996	Retrospective clinical study	Prolonged breast feeding

Table 2.3 Table summarising different studies conducted on the aetiology of MIH

2.2.3 Clinical features

Hypomineralisation is clinically manifested as enamel opacities, which are the effect of disturbances in the enamel's translucency. The enamel is of normal thickness, however the surface, which can be white, white- yellow or yellow-brown, and there is typically, a demarcated line between the lesion and healthy enamel. Under masticatory forces, affected teeth may exhibit loss of enamel, namely post eruptive breakdown (PEB), as seen in figure 2.10; however, this breakdown does not tend to affect incisors, as they are not subject to occlusal load. Clinically, this resembles enamel hypoplasia but the difference is the margins of the MIH lesions are irregular, whereas those in hypoplasia are smooth and rounded (Don Santos et al., 2012).

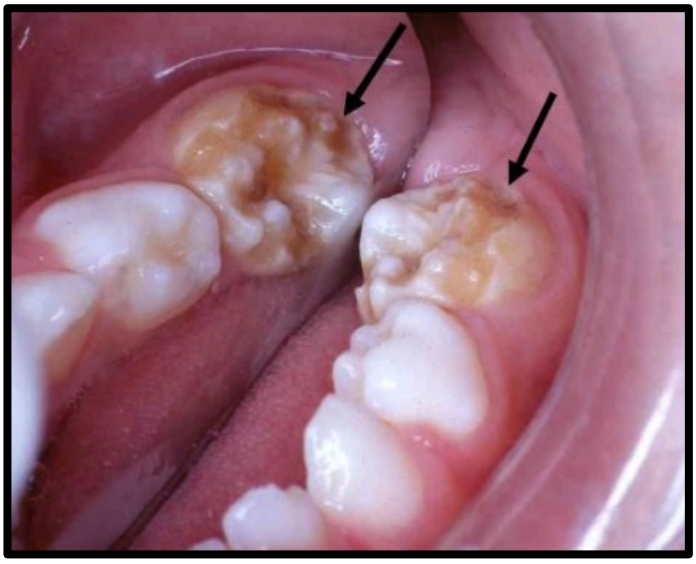

Figure 2.10 Showing a FPM with PEB, taken from www.kidz-teeth.com

Although MIH can affect multiple teeth, it is not considered chronological as seen in tetracycline staining or linear enamel hypoplasia, nor does it affect the entire dentition as seen in Amelogenesis Imperfecta. MIH lesions are usually seen on the cusps of molars and buccal surfaces of incisors (Jalevik B, Noren JG. 2000). Remarkably, enamel in the cervical area of the tooth usually keeps its normal structure (Farah RA et al., 2010). MIH can also involve the second primary molars, cusps of permanent canines and permanent second molars to a lesser extent, when the condition is very severe (Weerheijm et al., 2003b, Lygidakis et. al., 2010). Affected first permanent molars are not confined to a specific arch or quadrant, and are usually asymmetrical, but lesions affecting permanent incisors showed a predilection for the maxillary (Oliver et al., 2014). This difference might be contributed to the differences in susceptibility and timing of the development of the dentition.

2.2.4 Classifications

A classification by European Academy of Paediatric Dentistry (EAPD) to describe the severity of MIH has been suggested, where mild is considered a lesion with only colour change (white / opaque, yellow or brown) with smooth enamel surface. When the surface is rough, with enamel breakdown it is considered moderate. Severe relates to lesions affecting both enamel and dentine, or atypical restorations usually on the buccal replacing affected hard tissue (Leppaniemi et al., 2001). This is summarised in table 2.4 below.

Lesion	Classification
Mild	Smooth surface, with white-yellow opacity
Moderate	Rough surface, brown-yellow opacity, with breakdown of enamel
Severe	Lesion affecting enamel and dentine, atypical restoration

Table 2.4 Definitions of the criteria used for classifiying the severity of MIH lesions (Leppaniemi et al., 2001).

Another classification was by Oliver in 2014 (table 2.5), where mild is only colour change, moderate is sensitivity, breakdown or atypical restoration, and where severe is a combination of all (Oliver et al., 2014).

Lesion	Classification
Mild	Smooth surface, with colour change
Moderate	Sensitivity, breakdown or atypical restoration
Severe	Sensitivity, breakdown and atypical restoration (combination)

Table 2.5 Criteria used for classifiying MIH lesions (Oliver et al., 2014).

Another classification by Mathu-Muju and Wright in 2006, divided the defects into three different severity levels:

Mild MIH:

- Demarcated, isolated opacities
- No enamel loss
- No history of dental hypersensitivity
- No caries associated with the affected enamel
- Incisor involvement is usually mild if present.

Moderate MIH:

- Intact atypical restorations
- Demarcated opacities are present on occlusal/incisal third of teeth without PEB
- PEB/caries are limited to 1 or 2 surfaces without cuspal involvement
- No dental sensitivity

Severe MIH:

- PEB is present and frequently occurs as the tooth is erupting
- History of dental sensitivity,
- Widespread caries is associated with the affected enamel
- Crown destruction can progress to involve the dental pulp, defective atypical restoration is present

2.2.5 MIH lesions types

MIH can show in different types, but the main types usually seen, mostly studied and understood and furthermost prevalent in our every day life are the types 1 and type 2 MIH lesions, in addition lesions that further deteriorate into PEB. Thus in this research we are focusing on these 3 types. Type 1 is where the lesion/ tooth appears chalky white, or has a creamy opacity and is usually the mildest. Type 2

MIH is where the lesion is darker, and shows a yellow/ brown discolouration. As mentioned previously, the darker the colour the more the protein and carbon content, thus the more severe the form. The third type, which is PEB is not at entity by itself, although a mixture of both with signs of breakdown. Lesions with PEB can be either creamy white or yellow/ brown, so a type 1 or type 2 lesion however with loss of enamel as part of the post eruption breakdown, thus considered the most severe type with poor prognosis.

2.2.6 Differential Diagnosis

Differential diagnosis is required not to confuse MIH with other diseases such as fluorosis or hypomineralised amelogenisis imperfecta (Mast, P.,et al., 2013). PEB can be also misdiagnosed as enamel hypoplasia. However, it can be differentiated from fluorosis in the medical history, as fluorosis is associated with a history of high fluoride intake. In addition, MIH has opacities that are demarcated although in fluorosis the lesions are more diffused and affects the dentition in a symmetrical and bilateral manner. In addition, fluorosis is caries resistant due to the high fluoride, however MIH lesions are caries prone.

In relation to hypomineralised AI, there is usually a family history. Furthermore, AI is more symmetrical and usually affects both primary and permanent dentitions as a whole, and is far less common as it has a prevalence of only 1 in 7000. Additionally, radiographically molars in AI show taurodontism, which is enlarged pulp chambers, however are normal in MIH.

In hypoplasia, the enamel loss is more regular with smooth borders indicating lack of enamel formation, however in PEB the borders are more irregular and sharp that is

due to the breakdown of weak enamel (Ghanim A. et al., 2017).

2.2.7 Ultrastructure of MIH teeth

Knowledge of the microstructural changes of hypomineralised enamel improves the understanding of some of the complications associated with the clinical management of these teeth. Hypomineralised enamel shows disorganised orientation of prismatic structure with wide inter-prismatic areas and loosely packed crystals (Fagrell et al., 2010). In addition, extremely porous enamel in MIH affected teeth, which helps the penetration of bacteria deep down close to the EDJ.

When comparing lesions affected with MIH to sound enamel, differences in the ionic composition have been found, such as reduced concentrations of mainly calcium and phosphorus by 5-20%, in addition to oxygen and phosphorus level. On the other hand, the carbon and carbonate concentration was higher, with nitrogen levels being the highest (Martinović B et al., 2015).

It was found that MIH affected lesions had higher levels of serum albumin, antitrypsin and serum anti-thrombin than sound enamel, but almost the same level of residual amelogenins; this characteristic helps differentiate MIH from other hypomature lesions that contain high residual amelogenins such as Amelogenesis Imperfecta or Fluorosis (Dos santos et al., 2012).

In addition, there was a difference within different MIH lesions, as it was found that chalky white lesions had less protein compared to yellow-brown ones (Farah et al., 2010b). When compared to sound enamel, brown lesions show a 15-21 fold higher and yellow or chalky enamel around 8-fold higher protein content.

The colour of the lesion reflects the extent of hypomineralisation and protein content, where brown defects most frequently occur on molars, and white defects mostly on smooth surfaces of incisors (Oliver et al., 2014). The significance of these proteins is

that albumin inhibits crystal growth, and the other two are responsible for the inhibition of kalikrin 4 proteolytic activities, which in turn can explain the clinical difference in structure between MIH and sound teeth (Farah et al., 2010b). Crombie et al have also demonstrated the difference in physical and chemical properties. They found that micro-hardness and modulus of elasticity of MIH affected teeth were reduced by 80% compared to sound enamel. In addition, the mineral content was less, which explains the PEB. On the other hand, teeth with MIH showed higher porosity. They also suggested that yellow-brown lesions showed more severe forms of MIH compared to chalky white, and are more likely to suffer PEB (Crombie et al., 2013).

Mahoney et al., suggested that due to the increased protein content of MIH enamel, acid access through the hydroxyapatite crystals is limited as he observed that the classic etching patterns obtained with sound enamel were absent in MIH lesions, thus the decrease in bonding (Mahoney, E et al., 2005).

2.2.8 MIH Complications

Clinically, MIH can create serious complications for the dentist as well as for the child affected and pose a costly burden on the public health. As for the dentist, the drawbacks are due mainly to the fast progression of breakdown, which leads to difficulty in anaesthetising and bonding to enamel, and complexity of treatment. In addition, the roughness of the enamel in the erupting molars can lead to eruption difficulties, leading to uneruption or eruption with pain (Ghanim A. et al., 2017). For the patient, it can cause pain, sensitivity, disturbance in aesthetics, carious lesions and breakdown, which may lead to the loss of the teeth affected, as well as psychological distress (dos Santos et. al., 2012).

MIH lesions vary in severity from being minimally affected to more severe. The opacities in severe MIH are porous, resulting in teeth that may break down as soon as they are exposed to masticatory forces after eruption, i.e., PEB, exposing the dentine and enabling dental caries lesions to develop (Weerheijm et al., 2003). PEB leads to poor long-term prognosis of the teeth, which may lead to their extraction early in life. Brown and yellow opacities have a higher risk of breakdown when compared to the white (Costa-Silva CM et al., 2001). MIH lesions can affect aesthetics, as the incisors tend to show opacities and discolouration, which can lead to psycho social effects, especially in teenage girls, as studies showed they wont feel comfortable smiling and are prone to bullying, which can lead to depression (Silva-Junior, M.F et. al., 2016).

In addition to aesthetics, MIH can put enamel at risk of developing carious lesions, which progress rapidly and make it more difficult to diagnose as they are concealed by the change in colour and breakdown. They are usually more sensitive to cold and hot stimuli compared to sound teeth, either due to the porous enamel or exposed dentine, which puts the patient at risk of poor oral hygiene due to difficulty brushing (Beentjes et al., 2002). Moreover, the hypersensitivity leads to eating difficulties, which can affect the child's nutritional balance and growth.

Additionally, they tend to have porous enamel, which leads to inflammatory changes in the pulp, thus making it more difficult to anaesthetise (Weerheijm, 2003). Patients with severe MIH may display dental anxiety, fear and concern, which act as an additional barrier to having the treatment due to the hypersensitivity (Jalevik and Klingberg, 2002). A study in 2007 compared pulps of MIH teeth with controls, and concluded that despite their small sample size, the results they found suggested the presence of inflammatory changes in the pulp (Rodd et al., 2007).

Considering all aspects mentioned above, MIH is considered one of the biggest challenges in dentistry with a great impact on the oral health and quality of life of the patient affected.

2.2.9 Clinical examination of teeth

Based on the manual published in 2017 by A. Ghanim et al., the ideal way to examine MIH teeth is as follows, not to miss any lesions, and to guide clinicians into accurate MIH scoring:

- Dental chair is preferred, or for children knee to knee examination
- Charting should be done in a systematic way, starting with quadrant 1 then 2, 3 and 4 consequently.
- Teeth should be examined wet, or slightly dried with cotton roll.
- Good light source with a disposable non-magnifying, front surface mirror head is recommended.
- The use of a probe to check for any irregular surfaces, but ensuring not to further deteriorate the lesion (Ghanim A. et al., 2017).

2.2.10 Clinical indices

MIH as a clinical entity has become more evident over the past recent years and its diagnosis and management are challenging, therefore early examination is crucial. The most suitable time to examine the teeth, thus diagnose MIH is around the age of 8 where all of the four permanent first molar and incisors have fully erupted.

Different definitions for diagnosing MIH have been developed, such as the one developed at EAPD (Weerheijm et al 2001a), shown in table 2.6 below.

Criteria	Definition
Opacity	A defect involving an alteration in the translucency of the enamel, variable in degree; the defective enamel is of normal thickness with a smooth surface and can be white, yellow or brown in colour. The border of the lesions is demarcated.
Post eruptive breakdown	A defect that indicated deficiency of the surface after eruption of the tooth, this may be caused by such factors as trauma and attrition.
Atypical restoration	Size and shape of restoration do not conform to typical restorative characteristics. In most cases, restorations will be extended to the buccal or the palatinal smooth surface. At the border of the restoration, opacity may be noticed.
Extraction due to MIH	Absence of a molar should be related to the other teeth of the dentition. Absence of a first permanent molar in a sound dentition is suspected to have been an MIH molar

Table 2.6 Definitions of the criteria used for diagnosing MIH, courtesy of Weerheijm et al 2001a.

Despite clear assessment criteria, molar incisor hypomineralisation (MIH) is inconsistent in outcome measurements. Different clinical indices have been designed to help clinicians in assessing enamel defects, these include the

Developmental Defect of Enamel index (DDE), modified Development Defect of Enamel index (mDDE), Molar Hypomineralisation Severity Index (MHSI) and a more recent one the MIH Treatment Need Index (MIH-TNI). These indices are described below in detail and their limitations discussed.

The Developmental Defect of Enamel index:

In 1977, a World Dental Federal (FDI) group established an international epidemiological index system for classifying developmental defects of enamel. After reviewing different studies, the Developmental Defects of Enamel index (DDE) was officially accepted in 1982. This index was helpful in understanding a full range of defects in term of the clinical features, shape and colour of the defect. However, it was a descriptive rather than a causative index as it only describes the lesion without identifying the exact cause.

In order to accurately diagnose the tooth, it was recommended to use visual tactile examination with good lighting, using natural or artificial light, and a probe to detect any irregularities in the enamel surface, should be used.

The DDE is based on the type, number and location of the defect, with each being given a code individually (table 2.7). In addition, it describes the lesions as either affecting both dentitions, or only primary or permanent, with denoting the permanent teeth as numbers and primary as letters. Defects can be single or multiple, localised or more generalised, with a code pertaining to each. If there is any uncertainty on diagnosing the surface abnormality, it should be noted as normal. Furthermore, if the lesion is clear, but does not fit any of the above categories then it should be recorded as ‘Other’.

The major drawback of this index is that it is time consuming and complicated, as for each tooth surface two codes have to be described (type and number), and sometimes an additional code for the location. In addition, it is considered bias as it depends on the clinician's opinion on how he characterises the lesion, which can be different from one person to another, thus the ability of different clinicians to understand and therefore use the index could be questionable. Another major drawback of the DDE is its lack of measuring the severity/ extent of the lesion; in addition, the level of hypersensitivity is not accounted for (Steffen, R. et al., 2017). However, based on studies, the DDE index is the most commonly used amongst the various indices available (table 2.6) (Clarkson J., 1989).

1. Type of Defect	**Code**	
	Permanent teeth	**Primary teeth**
Normal	0	A
Opacity (white/ cream)	1	B
Opacity (yellow/ brown)	2	C
Hypoplasia (pits)	3	D
Hypoplasia (grooves: horizontal)	4	E
Hypoplasia (grooves: vertical)	5	F
Hypoplasia (missing enamel)	6	G
Discoloured enamel (not associated with opacity)	7	H
Other defects	8	J
Combination of defects	Each is given a code individually same as mentioned above	

2. Number and demarcation of defects		
Single	1	A
Multiple	2	B
Diffuse, fine white, lines	3	C
Diffuse, patchy	4	D
3. Location of defect		
Gingival one-half	1	
Incisal one-half	2	
Gingival and Incisal halves	3	
Occlusal	4	
Cuspal	5	
Whole surface	6	
Other combinations	7	

Table 2.7 Criteria used in Developmental Defect in Enamel index, proposed by FDI working group in 1982, Modified from FDI Commission on Oral Health, Research and Epidemiology (1982)

The Modified Developmental Defect of Enamel index

To solve the complications of the DDE, in 1988 the Committee on Commissions of FDI organised a group to review the DDE and make some modifications to a simpler version. After several modifications, in 1992 the Modified Developmental Defect of Enamel (mDDE) index was published, summarised below in table 2.8.

The differences between the DDE and mDDE are that it is a single scoring system, unlike DDE, which for each lesion 2 or 3 codes have to be noted. In addition, regardless of the change in colours, in the mDDE hypoplasia was the main weight and was broken down into pits, grooves, linear grooves and missing enamel. Another difference is that the mDDE has a category of combination of lesions, which is excluded in the DDE. In addition, the defect must be greater than 1mm in diameter for it to be included in the mDDE index, or else it is considered normal.

The main advantages of mDDE over the DDE are that it is less complicated and time consuming, and increased efficiency for data collection. In addition, it measures the severity or extent of lesion. Therefore the mDDE is an appropriate index to be used for recording and analysing the type and severity of enamel defects in children (Clarkson et al., 1989). It helps present the lesion in a more meaningful manner.

Type of Defect	Code
Normal	0
Demarcated opacities	
White/ cream	**1**
Yellow/brown	**2**
Diffuse opacities:	
Diffuse lines	3
Diffuse patchy	4
Diffuse confluent	5
Confluent/ patchy + staining + loss of enamel	6
Hypoplasia:	
Pits	7
Missing enamel (PEB)	**8**
Any other defects	9
Combinations	**Code**
Demarcated and diffuse	A
Demarcated and hypoplasia	B
Diffuse and hypoplasia	C
All three defects	D

Table 2.8 Modified DDE (mDDE) index used to characterise dental defects of enamel; the criteria marked in bold are related to defects in MIH This table has been taken from the FDA working group report (1992).

The Molar Hypomineralisation Severity Index (MHSI)

The MHSI is a recent index developed by an Australian working group developed in 2014, and is based on the European Association of Peadiatric Dentistry (EAPD) judgment and clinical characteristics (Oliver et al., 2014).

This index not only describes MIH lesions, but molar hypomineralisation in general as well due to the increased awareness of molar hypomineralisation in both primary and permanent dentitions. It assesses the severity of MIH by combining the defect size of individual teeth and the entire dentition, and accordingly gives treatment recommendations. It mainly focuses on the colour and location of lesion (Steffen, R et al., 2017).

MHSI helps in diagnosing the lesion based on two different value scales, one for the whole dentition (values 1-52) and the other for individual affected teeth (values 1-13) and accordingly constructing a tailored treatment plan, based on the sum of the characteristics shown on table 2.9, for it. The more severe the lesion, the higher the MHSI score, therefore it receives more treatment with restorations or extractions than those with lower scores which are planned for prevention only with sealants or fluoride (table 2.10) (Oliver et al., 2014).

Characteristics of molar hypomineralisation defects	Severity of characteristic	Weighting assigned
Erutpion status	Unerupted	0
	Erupted	1
Colour of most severe defect	None	0
	White/ cream	1
	Yellow	2
	Brown	3
Location of most severe defect	None	0
	Smooth surface	1
	Occlusal surface (FPMs)	2
	Incisal edges (PIs)	2
	Cuspal involvement (FPMs)	3
Restorations placed/ replaced (prior to study entry)	None	0
	One	1
	Two or more	2
Atypical restorations (prior to study entry)	None	0
	Present	1
Post eruptive enamel breakdown (PEB)	None	0
	Present	1
Sensitive to temperature (child report)	None	0
	Present	1
Sensitive to tooth brushing (child report)	None	0
	Present	1

Table 2.9 Characteristics of hypomineralised defects on affected first permanent molars (FPMs) and permanent incisors (PIs) and severity weightings.

Based on the score, the recommendations is as follows:

Score	Description	Management
3-6 (Mild)	Intact coloured defects, usually on smooth or occlusal surfaces	Preventive therapy with Fissure sealant (FS) and remineralisation or Glass ionomer cement (GIC) if defects are in areas of occlusal load. Some teeth may require restorations if they become carious or develop PEB.
7-9 (Moderate)	Yellow or brown defects on occlusal or cuspal surfaces which may have atypical or previous restorations, PEB, or sensitivity.	Provide Adh restorations, particularly when PEB is present; consider stainless steel crowns (SSC) if PEB is extensive. Stabilise enamel surfaces using remineralisation, FS, and/or GICs. If defect is extensive, consider optimal timed extraction with orthodontic advice to encourage space closure.
10–13 (Severe)	Brown or yellow defects with a combination of PEB, sensitivity, and atypical restorations or previous restorations	Provide Adh restorations or extraction. If FPMs have been restored unsuccessfully on several occasions, consider placing either a SSC or extract after orthodontic advice. Consider remineralisation. Stabilise enamel surfaces with GIC until a definitive treatment plan is made or while waiting optimal timed extraction with orthodontic advice to encourage space closure.

Table 2.10 Recommendations for treatment based on severity score (Oliver et al., 2014).

The MIH Treatment Need Index (MIH-TNI)

In 2016, during the meeting of the German Society of Paediatric Dentistry an international MIH group developed a new MIH index. This index was designed to create a new straightforward index for scoring and treating MIH.

The aims of the index were to detect both the extent of the defect and account for hypersensitivity. It should also be suitable for the investigation and description of lesions on both individuals and for larger populations, and therefore be used for treatment planning (Steffen, R et al., 2017). The grading used in this index is guided by the lesion's destruction and hypersensitivity. The index values are shown in table 2.11.

Index	Definition
Index 0	No MIH, clinically free of MIH
Index 1	MIH without hypersensitivity, without defect
Index 2	MIH without hypersensitivity, with defect
2a	<1/3 defect extension
2b	>1/3 <1/3 defect extension
2c	>2/3 defect extension or/ and defect close to the pulp or extraction or atypical restoration
Index 3	MIH with hypersensitivity, without defect
Index 4	MIH with hypersensitivity, with defect
4a	<1/3 defect extension
4b	>1/3 <1/3 defect extension
4c	>2/3 defect extension or/ and defect close to the pulp or extraction or atypical restoration

Table 2.11 Index values used in scoring lesions with MIH-TNI (Steffen, R et al., 2017).

Scoring should be made with the patient facing the front and done in a clockwise direction, starting with the maxillary right. The index is based on sextants, so given that the mouth is divided into 6 sextants (table 2.11), 6 values are recorded with the highest value for each sextant (table 2.12).

MIH-TNI		
Maxillary right	Maxillary front	Maxillary left
Mandibular right	Mandibular front	Mandibular left

Table 2.12 Table showing the sextants and how indices are scored in MIH-TNI for epidemiological studies

Description MIH	Affected teeth	Intervention
MIH index I Without hypersensitivity, without defect		
MIH index IIa, b, c, d MIH without hypersensitivity, with defect		
MIH index III MIH with hypersensitivity, without defect		
MIH index Iva, b, c MIH with hypersensitivity, with defect		

Table 2.13 Table showing how indices are scored in MIH-TNI for an individual risk assessment on each tooth affected by MIH

Due to the availability of many different indices and their deficiency in reliability there isn't a standardised system for recording MIH data. Therefore, it was agreed to have a more standardised system to ensure a unified practical scoring form for the classification and diagnosis of MIH lesions. This agreement was reached in a MIH workshop that was held in association with the 12th EAPD Congress in Sopot, Poland in 2014. Scoring sheets were thus developed that describe MIH lesions on the clinical visual appearance and the extent of enamel destruction. It integrates the components of the EAPD criteria and the modified Developmental Defects of Enamel index (mDDE) for scoring mainly MIH, but incorporates other enamel defects as well. This scoring method is composed of two scoring sheets, a short and long form (tables 2.14 and 2.15 respectively). The first is for simple and fast screening, whereas the long is for more detailed prospective longitudinal studies where causation is included.

In the short form only MIH index teeth secondary primary molars (SPM), first permanent molars, and permanent incisors are scored.

Recording of data is divided into two main sections, and one minor one. The main sections are the visual clinical presentation of enamel lesions, namely clinical status criteria, and the second section pertaining to the size of the tooth surface area affected by the lesion, known as lesion extension criteria. The remaining minor section is related to the eruption status of the tooth (eruption status criteria) (Ghanim, A.,et al., 2015).

	MAXILLA RIGHT				MAXILLA LEFT			
	16	55	12	11	21	22	65	26
Tooth								

	MANDIBLE RIGHT				MANDIBLE LEFT			
	46	85	42	41	31	32	75	36
Tooth								

Table 2.14 The short form of MIH/HSPM clinical data recording sheet

	MAXILLA RIGHT		55	54	53	52	51	61	62	63	64	65	MAXILLA LEFT	
Surface	17	16	15	14	13	12	11	21	22	23	24	25	26	27
Buccal (labial)														
Occlusal (incisal)														
Palatal														

	MANDIBLE RIGHT		85	84	83	82	81	71	72	73	74	75	MANDIBLE LEFT	
Surface	47	46	45	44	43	42	41	31	32	33	34	35	36	37
Buccal (labial)														
Occlusal (incisal)														
Lingual														

Table 2.15 MIH/HSPM clinical data recording sheet, permanent and primary dentitions (long form)

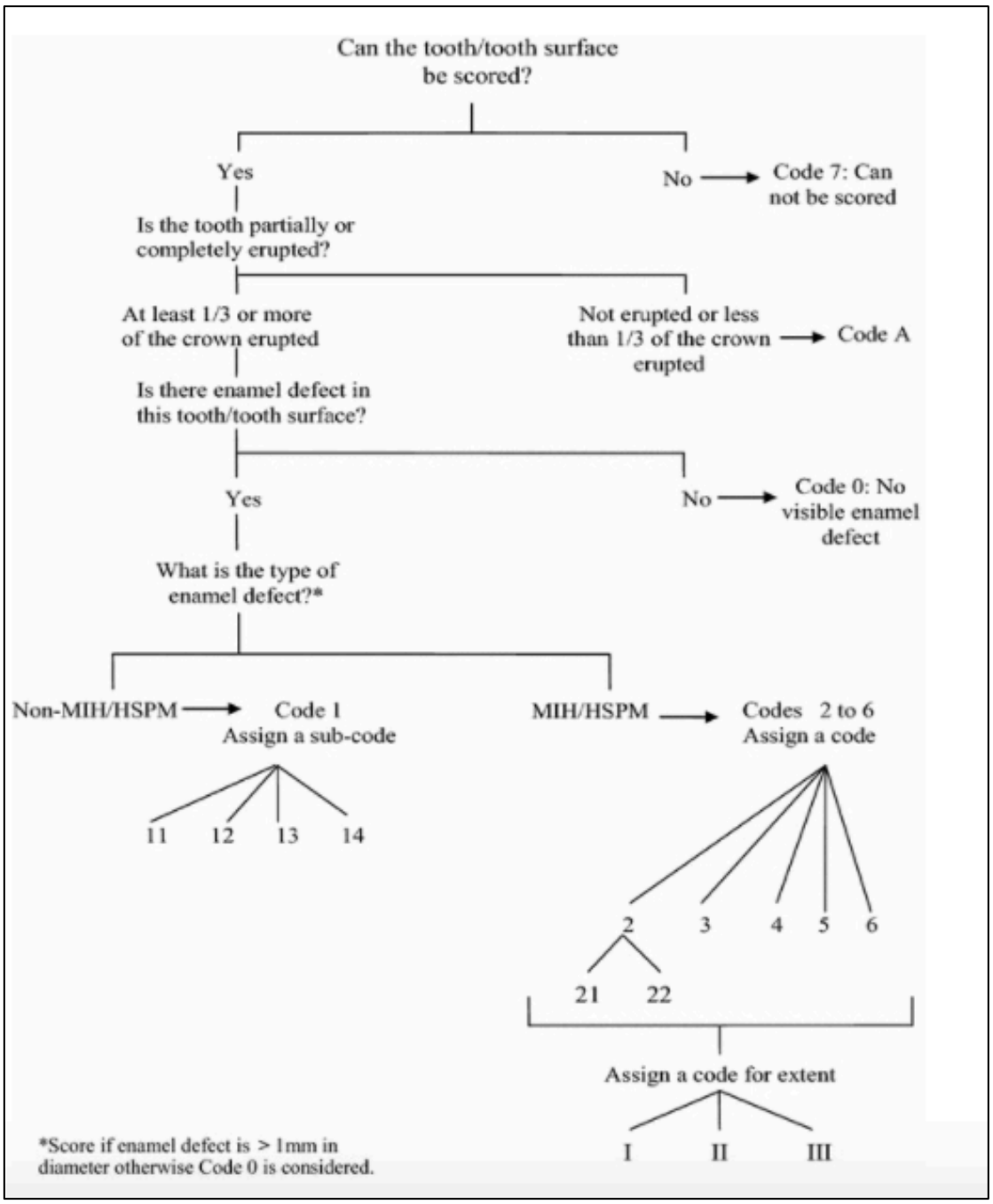

Figure 2.11 Flow chart representing the recommended sequence for diagnosis of MIH/ HSPM and other enamel defects.

In order to use this scoring method, some points have to be put in mind (figure 2.11). Firstly, only teeth that has at least 1/3 of its surface erupted is scored, elsewise it is scored as code A and there is no need to continue with its scoring.

Next, a child is only diagnosed with MIH or HSPM when at least one FPM or one SPM is found to have hypomineralisation, however if only the permanent incisors then this is not considered as MIH. As hypomineralised permanent incisors can be due to turners tooth, which is an infection or trauma to primary incisors which in turn affects the permanent successor. Furthermore, a small defect that is less than one millimetre or if the examiner is in doubt if it is defective or sound, the lesion is excluded and scored as sound. Similarly, when there is any uncertainty regarding the severity of the lesion severity, the less severe rating is to be recorded.

When MIH or HSPM is diagnosed, any full coverage restorations should be scored as atypical restorations. On the other hand, areas with lost restorations with no cavities present should be coded as PEB (code 3). In addition, when more than one lesion exists per tooth, i.e. white and brown opacities, the more severe rating is to be recorded, and in regards to the extent of the lesion, visually all lesions are combined and the extent is scored.

The advantage of this scoring system is that it yields the most information of all indices by having many different subcategories, thus it includes information on the tooth's eruption status, the extent of the lesion status, and the tooth surface area affected, giving a full picture of the lesion.

In addition, hypomineralisation can fall under different diagnoses, so by assigning these defects as present or absent allows their differentiation from MIH. Furthermore it is not time consuming and very convenient.

Indices help in epidemiological screening procedures for assessing MIH and also for the screening and recording of lesions by dental practitioners. However, all indices have their drawbacks as they are subject to bias, subjectivity and are not reproducible. Currently, no index is fully valid to guide clinicians in managing affected

teeth, and treatment is based on individual clinical judgment. Indices help in characterising the lesions, however no information is given on the prognosis of the tooth, or the amount of PEB. Therefore, more objective measures to diagnose enamel defects are required to overcome these drawbacks.

2.2.11 Radiographs

Not all oral diseases are visible to the naked eye; therefore radiographs aid in their diagnosis and are important in developing a treatment plan. Since their discovery by Röntgen in 1895, X-rays have been used widely to investigate oral health problems at their earliest stages, such as cavities, gingival disease, oral infections, and some tumours (Smith J.C., 1971). Whilst MIH is mainly diagnosed clinically, radiographic imaging can be used as an aid to detect the extent of the lesion.

The radiographs requested for aiding the diagnosis of MIH are usually dental panoramic tomography (DPT), bitewings (BW) or peri-apical images (PA). DPT is an extra-oral radiograph, which shows the teeth in both dental arches along with the adjacent bony structures. It uses a minor dose of ionising radiation in order to capture the whole mouth in a single image. However, limitations of DPT are that it does not give detailed information of the teeth as the resolution is low, and the image tends to be distorted, with super imposition of different anatomical structures (Murray et al., 2002). It is mainly requested when the dentition is needed to be seen as a whole, before planning to extract the affected teeth, to ensure the patient has his second and third molars.

While panoramic radiographs detect more extensive lesions, bitewings and periapical radiographs yield more information regarding the dental lesions and surrounding periapical region (Gundappa et al., 2014). Bitewings and periapicals are

small intra oral images, which tend to show the whole posterior region, or individual teeth with their periapical region respectively. Bitewings are good in detecting interproximal lesions, with high resolution, however are of a little value when detecting occlusal lesions. Regarding their radiation, literature shows that the exposure dose from bitewing and periapical images is very low compared to background radiation and other medical exposures. However, because dentists tend to request them routinely, the total dose becomes the problem (Pitts, N.B., 1996). Other than that, despite these are the xrays requested to diagnose MIH lesions, they have their drawbacks of being 2d images thus the lesion is superimposed and can be concealed, this is discussed further in chapter 5 below.

Radiation can affect the biological tissue either directly or indirectly. When the energy of a photon ionises the atomic cell, the effect is termed direct. On the other hand, the photon can indirectly affect the biological tissue. By indirect, it is meant that the photon is absorbed into the cell, ionises the water and forms free radicals, which in turn affect the biological tissue. Both direct and indirect effects take seconds to cause the defect, however it takes hours to decades for the damage to show (White, S.C. and Pharoah, M.J., 2014).

Radiation alters the biological deoxyribonucleic acid (DNA) by either causing a breakage of the DNA strands, disrupting their hydrogen bonds, changing or deleting a base, or cross linking a DNA strand with another strand or a protein. These alterations in turn kill the cell or lead to mutations that can be carcinogenic or hereditable. When the damage is great, killing number of cells, it is termed deterministic. Examples of deterministic effects are mucositis or radiation induced cataract formation. On the other hand, damage can be sub-lethal where it only causes cancer or a hereditable mutation instead of killing the cell, i.e. stochastic. In

order to have a deterministic effect, the threshold dose has to be reached, and the effect is directly proportional to the dose. However, stochastic effects have no certain threshold, any single dose can lead to an effect, and the probability of damage increases with the dose (White, S.C. and Pharoah, M.J., 2014).

Due to the risks of ionising radiation, all exposures must be justified and kept as low as reasonably achievable (ALARA) for both the patient and the staff (Strauss et al., 2006). The risks and benefits of the radiograph should be weighed, and the purpose of it should be to add to the diagnosis and facilitate the treatment plan, based on the lesion severity, caries risk and the patient. Therefore, dentists should aim in maximizing the benefits, and minimizing the risks. Children tend to be as much as 10 times more radiosensitive than adults, therefore optimising the radiation especially in the peadiatric field is very important (Strauss et al., 2006).

Special precautions should be taken in order to protect both the patient and personnel from the risks of radiation. As mentioned previously, justification and using the ALARA rule is very important. In addition, the patient to protect the thyroid should always wear lead collars as it is considered the most radiosensitive organ in the head and neck region along with the brain, salivary glands and bone marrow (White and Mallya, 2012). Studies showed that children are more prone to radiation risks compared to adults, and that 25% of tumour types, which include leukaemia, thyroid, skin, breast and brain cancer occur in children (Kleinerman, R.A., 2006).

Regarding the type of film, using E or F speed film or digital imaging tends to have a lower dose compared to D- speed film or conventional imaging. In order to reduce the scatter of beam, rectangular collimation for peri-apical and bitewing images is required. For panoramic imaging, rare earth screen is indicated, which is an xray-intensifying screen used to enable lower radiation doses to be used while producing

adequate film densities (Long et. al., 2015). Distance from the exposure beam is also important; clinician or any other people in the room should stay at least 1.8m away from the beam and patient. Automatic processors to develop films show less risk than manual film processing, however if manual is the only choice, time temperature method should be used (White and Mallya, 2012).

2.2.12 Management of MIH

There are only a few studies evaluating the restorations in MIH affected teeth. Prognosis is unpredictable and the risk of breakdown and caries in these teeth is very high, therefore early diagnosis and intervention is very important.

Treatment can be painful as it is difficult to anesthetise these teeth because the porous enamel tends to lead to subclinical inflammation of the underlying pulp (Allazzam et al., 2014). In addition, children with MIH may have higher levels of anxiety towards dental treatment on affected teeth, due to the hypersensitivity caused by the lesions, leading to barriers in treatment (Willmott et al., 2008).

Management should focus on elimination of pain, desensitisation, restoration of aesthetics and providing adequate function. In order to consider the present and future needs of the child from the intermediate up to the final treatment plan, treating MIH or other dental anomalies should always be a multidisciplinary team decision. The team usually consists of a specialist from paediatric dentistry, orthodontics, prosthodontics, oral surgery, and also involving the patient's local dentist. Involving the patient and his parents or guardians in this decision is important as well. A 6 step approach consisting of risk identification, early diagnosis, remineralisation, prevention of dental caries and post eruptive enamel breakdown, restorations or extractions, and maintenance is the way to manage MIH affected teeth (table 2.16) (William et al., 2006).

Treatment depends on the severity of the lesion, in cases where there is no structural loss; fluoride varnish or sealants can be used. The likelihood of maintaining tooth structure integrity in these lesions and restoring with glass ionomer cement (GIC) was found to be high. In these cases dietary advice and fluoride toothpastes of at least 1450ppm should be used. In addition, the use of a CPP-ACP (casein phosphopeptide-amorphous calcium phosphate) paste helps in desensitising and acting as a source of calcium and phosphate for the erupting teeth affected with MIH (Ghanim A. et al., 2017).

Conservative or invasive restorations are used when the affected area has to be removed and thus restored. For anterior teeth, the main focus is on aesthetics; therefore it can be handled conservatively with micro abrasion, bleaching or with composite restorations. As for posterior teeth, adhesive restorations or full or partial coverage crowns can be used (Ghanim A. et al., 2017).

In more severe cases, extraction is the choice, which is better to be postponed to an age where the patient is aware why the treatment is being carried out, and is able to co-operate (Fragelli et al., 2015). The ideal time for extraction is indicated by the calcification of the furcation of lower second permanent molars in order to produce the best occlusal position (Cobourne, M. et al., 2009). The timing of the extraction is more important for mandibular first permanent molars than maxillary as they are a problem. For space closure the maxillary tooth tends to rotate around its palatal root, whereas the mandibular needs bodily movement to close the space, which is more difficult. Orthodontic consideration should be made to know how many molars to be extracted for balancing and compensation reasons (Williams and Gowans 2003).

Steps	Recommended procedure
Risk identification	Assess medical history for putative aetiological factors
Early diagnosis	Examine at risk molars on radiographs if applicable
	Monitor these teeth during eruption
Remineralisation and desensitization	Apply localised topical fluoride
Prevention of caries and post-eruptive breakdown (PEB)	Institute through oral hygiene home care programme
	Reduce cariogenicity and erosivity of diet
	Place pit and fissure sealants
Restorations or extractions	Place intra-coronal (Resin composite) bonded with a self-etching primer adhesive or extra-coronal restorations (Stainless steel crowns)
	Consider orthodontic outcomes for post extraction
Maintenance	Monitor margins of restorations for PEB
	Consider full coronal coverage restorations in the long term

Table 2.16 A Clinical Management Approach for PFM Affected by MIH (William et al., 2006).

Due to the limitations of current diagnostic tools, there is a need to investigate other techniques for MIH.

2.3 OCT:

Optical coherence tomography (OCT) is an established medical imaging technique that is considered non destructive as it uses near infrared light to investigate the internal biological structures to a depth of up to 2-3 mm' (Jones et al., 2006b). It is limited to this depth as at greater depths the amount of light that is reflected rather than scattered is too small to be detected. Simplified, it uses light waves to take cross-section images of an anatomic tissue to give us thickness and accurate measurements to assess in diagnosis and treatment planning by measuring their optical reflections. OCT is considered a safe method in imaging the internal structure of the tooth without possessing any radiation or having to cut or prepare the tooth. It has been used as a diagnostic method in ophthalmology and dermatology (Fercher, 1993). OCT has the same concept as ultrasound imaging, with the exception that it uses light instead of sound (Fujimoto et al., 2000).

OCT is based on the concept of using low coherence interferometry, which is the technique where waves are superimposed to obtain information by optical sensing technology. It uses relatively long wavelength light, therefore allowing it to penetrate into the medium and then measuring the reflected light (Riederer, S.J., 2000).

Low Coherence Interferometry has two different techniques, time-domain (TD-LCI) and Fourier domain (FD-LCI). It was showed that they are the same in terms of resolution and in that both can be used to generate low coherence *a*-scan signals and *b*-scan images (Fercher et al., 1991). Conversely, it was demonstrated that the Fourier domain OCT (FD-OCT) technique had better sensitivity than Time domain OCT (TD-OCT) (Leitgeb et al., 2003).

Different diode lasers were used as light sources for the OCT in the past, which produced confusing results. Later these were substituted to superluminescent light diodes (SLDs), which have a wider spectral emission giving an improved depth resolution (Fercher et al., 1993).

The light beam hits the object, and light is reflected and back scattered. OCT rejects the scattered light and collects the light reflected from the region of focus. The light is reflected in different ways relating to their different optical properties; therefore it is captured by the OCT as different reflections (Fujimoto et al., 2000).

The principle on how OCT works as mentioned previously is by capturing off back-reflected light. Accordingly, light is produced from a swept source, which is then split, by a beam splitter into two beams; one is directed to a reference mirror arm and another to a sample arm. Both beams are then coupled by a fibre coupler and detected by a photo detector (Michelson interferometer) and an interference signal is identified. A cross sectional image is then produced by transversely scanning the beam across the sample and collecting a reflectance versus depth profile at each transverse location giving us depth-resolving signals (a-scans). An a-scan is a graph with the x-axis corresponding to depth in the tissue versus intensity of the collected reflections (Y-axis). As the position of the reference mirror is known, the depth into the sample can be determined. Multiple A-scans are then transferred into a digital signal transferring unit, where B-scans are created.

This is illustrated in detail in figure 2.12 below.

Figure 2.12 Principle of OCT. Where (SS) is swept source or tuneable laser, (BS) beam splitter, (REF) reference mirror, (SMP) sample, (PD) photo detector, and (DSP) digital signal processing.

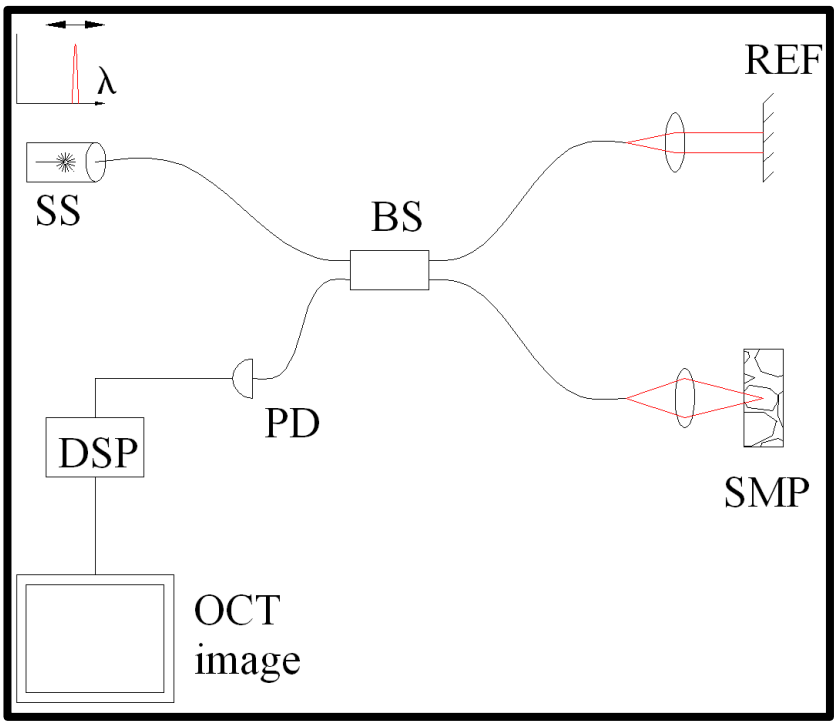

OCT produces both 2 dimensional (2D) and 3 dimensional (3D) images. The 2D image is a grey scale image, which is called a B-Scan shown in figure 2.13a. It is in cross sectional depth, in a XZ plane, thus giving a 2D image. The other type is created by multiple B-Scans together in a Y-plane direction, therefore giving a 3 dimensional image (XYZ) (Fercher et. al., 2002). Plotting signal intensity of an object against unit distance can create a profile or a graph of a B-Scan, and this is called an A-Scan shown in Figure 2.13b, which imitates the intensity of reflected light at different depths.

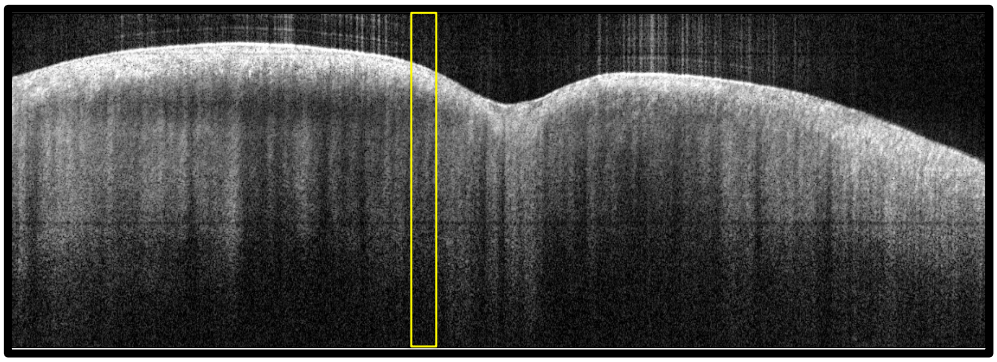

Figure 2.13a

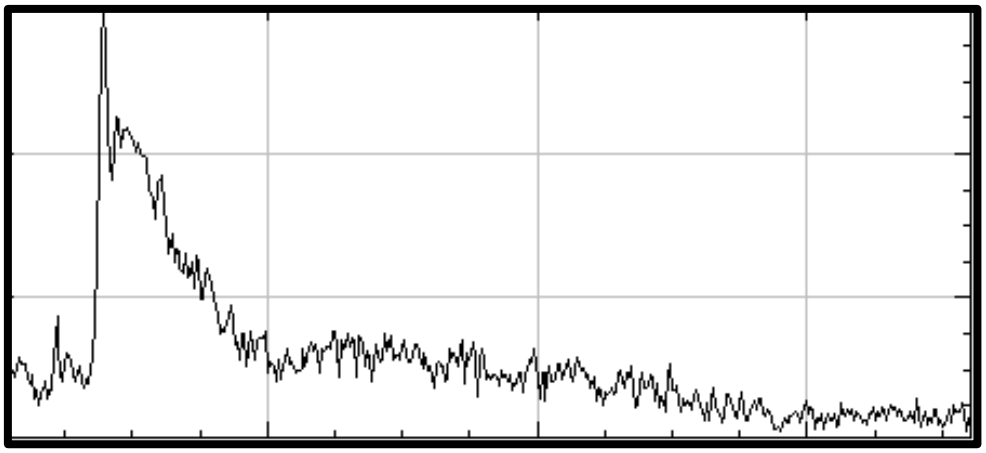

Figure 2.13b

Figure 2.13 Shows examples of (A) B Scan image of a sound tooth, and its corresponding A-Scan with X-axis being depth against OCT signal on Y-axis (B).

2.3.1 Applications of OCT

OCT is an established medical imaging technique and has been used in several medical specialties including dermatology, gastroenterology, ophthalmology and cardiology, and is widely used in scientific research. In 1990, Fercher used the OCT in ophthalmology, investigating the human's eye fundus as a two-dimensional image for the first time (Fercher, 1993). He reported that OCT produces high-resolution images in a non-contract invasive free technique (Fercher, 2010). OCT has also been used in cardiology to assess coronary heart disease (Bezerra et al., 2009) and in gastroenterology, for the early diagnosis of gastrointestinal tumors (Li, X.D., et al., 2000). In addition, it has been shown to be an invaluable diagnostic tool in inflammatory and bullous dermatological condition (Welzel, 2001).

In dentistry, OCT was used in several hard and soft tissue imaging. It has been used in investigating caries, root fractures, interfacial gaps in restorations, oral cancer and mineral loss and is becoming more popular these days. It was first used dentally in 1998 where in vitro images of dental hard and soft tissues were taken (Colston, B.W. et al., 1998). Otis et al. presented the first in vivo OCT images of human dental tissue in 2000 where they showed visual images of the EDJ and periodontal structures and subsequently Feldchteine et al. in 1998 imaged the hard palate mucosa and gingival mucosa. In addition, imaging the dentine pulp complex to record the amount of tooth structure present above the pulp, thus helping in prognosis and dental treatment. OCT has also been used to detect cracks in teeth and micro leakage beneath composite restorations (Hsieh, et al., 2013).

Regarding dental carious lesions, it was first used by Baumgartner and has been found to be capable of capturing early lesions as light propagates through dentinal tubules, and by capturing the changes in enamel rods pattern along with changes in

mineral density (Baumgartner et al., 1998). As dental tissue is unlike resin, secondary caries can easily be seen on OCT as they have different scattering properties. A study by Fried et al., concluded that OCT is an invaluable tool in imaging of interproximal, occlusal, early root caries and secondary caries (Fried et al., 2002).

Gingival mucosa, subgingival calculus and early periodontal disease have been demonstrated using OCT by recording the differences in refractive index between enamel, dentine, cementum and calculus.

OCT has been found to be a valuable tool in the early diagnosis of oral cancer. It helps in understanding the pathological mechanisms, predicting any malignant changes, knowing the risk of tumour recurrence, and predicting the tumour's response to therapy (Hsieh, et al., 2013). Additionally, OCT was helpful in differentiating oral lesions in different carcinogenesis stages (Tsai, M.T. et al., 2009). However, enamel defects such as MIH have not been thoroughly studied using OCT, therefore this study aims to investigate this.

2.3.2 Refractive index:

Refractive index is defined as "The ratio of the velocity of light in a vacuum to its velocity in a specified medium" (Dictionary, O.E., 2007). In simpler words the measure of speed of light as it travels from a medium to another. The larger the refractive index of the medium, the slower the speed of light. Therefore, as light travels through air then into enamel the refractive index changes, and as it goes deeper into the tooth the refractive index either stays the same if the tooth is homogenous, or changes due to the tooth's heterogeneity. Optical scattering in OCT occurs due to differences in refractive index of the different tissue components.

Therefore, materials with similar refractive index will demonstrate similar OCT images. Air has a refractive index of 1, enamel ~1.6 and dentine ~1.5 (Colston, B.W et al., 1998) and this is due to the size of the main scatters in the material.

Knowing the refractive index of biological tissues plays an important role in many biomedical applications, as it characterises their interactions with light. For example, early carious lesions can change the enamel refractive index due do the demineralisation, and thus this scatters differently so assists in diagnosing dental caries. Likewise, malignant tissue can be differentiated from normal tissue by measuring and comparing their refractive index. Moreover, clinically when enamel is dried and turns white, this is due to change in enamel refractive index and how it scatters light (Kidd and Fejerskov, 2004).

2.4 Main research question

Based on the increase in prevalence of MIH, along with the limitations found in the current diagnostic methods, a question raises of “Is there a better diagnostic tool to determine the extent and depth of MIH defects.

CHAPTER 3

Aim and Objectives

Aim and Objectives

3.1 Rational for Research

Based on the increased prevalence of dental anomalies and the importance of their early diagnosis and management, this study is made to acquire more understanding about the phenotypic characteristics, ultrastructure and diagnosis of MIH.

3.2 Aim

To expand the use of Optical Coherence Tomography imaging in dentistry, using it as a routine clinical diagnostic tool in MIH, and to compare the results with conventional clinical methods i.e. radiographs and clinical indices.

3.3 Objectives

1. Characterise Control, Type 1, 2 and PEB lesions using standard diagnostics tools

2. Characterise Control, Type 1, 2 and PEB lesions using OCT

3. Define empirical markers in the OCT scan and scattering profile intensity plot for control, Type 1, 2 and PEB lesions

4. Evaluate the progression of the lesions as a whole, from one a-scan to whole lesion (from 2-D to 3-D)

CHAPTER 4

Patient Recruitment and Selection

Patient Recruitment and Selection

4.1.1 Study registration and ethical approval

This study is designed as a part of a larger group of projects in the Department of Paediatric Dentistry at the Eastman Dental Hospital to investigate different dental anomalies. Ethical approval was obtained from the National Health Services Research Ethics Committee (NHS REC) on August 11 2011, under the reference number 11/LO/0777. Project ID: 11/0223. (Appendix 1)

4.1.2 Patient Selection

In 2011, a dental anomalies clinic was founded in the Department of Paediatric Dentistry at the Eastman Dental Hospital (EDH), where data of patients attending were recorded in order to develop an anomalies database.

Two groups of patients were invited to participate in the project, control patients (without MIH) and patients with MIH. Patients and parents were both given a written information leaflet (Appendix 2) about the project and enough time to think about participating in the study, with the right to ask any questions and understanding that the choice they make had no effect on the treatment given. Written consent (Appendix 3) was obtained from participants willing to take part in this study.

The flow diagram for patient recruitment is shown in figure 4.1 below.

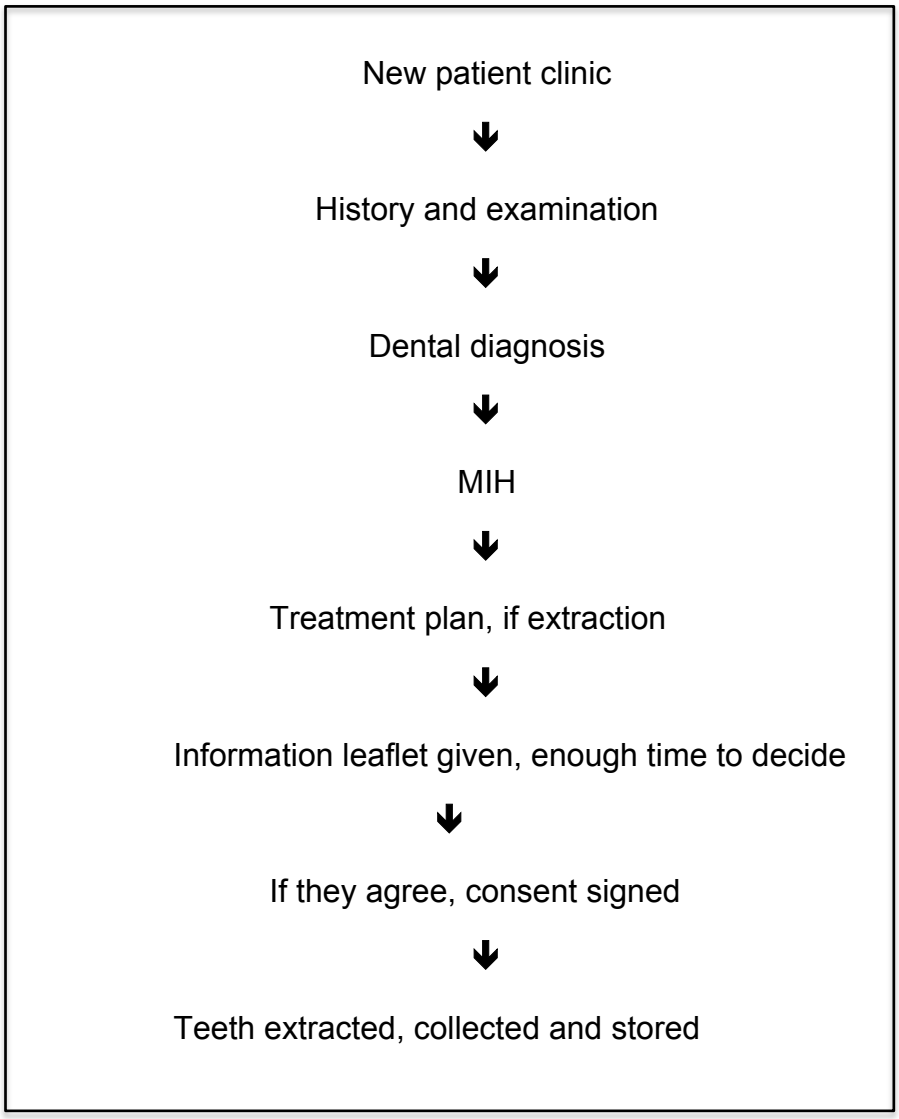

Figure 4.1 Schematic diagram outlining how the sample teeth were collected

The control group, are paediatric patients in the Department of Paediatric Dentistry at the Eastman Dental Hospital, who required extraction of a FPM as part of their treatment plan, either prior to orthodontics or due to caries.

The inclusion criteria for this group were:

- Fit and well
- Without any known illness or syndromes
- Patient requiring FPM extraction as part of treatment plan

The exclusion criteria included:

- Patients with any known relevant medical disease
- Teeth with deep carious lesions
- Patients with dental anomalies
- Patients who did not understand English sufficiently to consent for the study

The second group was MIH patients who needed extractions of their FPMs as part of their treatment plan.

Inclusion criteria was as follows:

- MIH teeth with any of the following:
- White/ cream opacities
- Brown/ yellow opacities
- Atypical restorations
- PEB
- MIH teeth with lesions less than 1mm were excluded, as they were too small to diagnose.

Those who decided to enrol in the study were given three copies of the consent to sign. A copy of each form was kept in a filing cabinet in the locked office of the secondary supervisor, the other copy was given to the patient / parent for his / her reference and the last one was filed in the patient's clinical notes.

4.3.1 Sample collection and storage

The samples obtained were stored in accordance with the Human Tissues Act 2004. All samples collected from the patients were extracted as part of their treatment plan.

After each extraction, the tooth is stored in saline solution until taken to the lab, the same day, where it is debrided from any soft tissue or blood under running water. A scalpel blade was used to debride the tooth from any intact clots, gingival or periodontal tissue.

The tooth is then stored in 70% ethanol at room temperature to be disinfected. After 48 hours the tooth is removed, and placed individually in 0.1% Thymol solution and locked securely in a fridge at 4^{o} C at the Eastman Biomaterial & Tissue Engineering Laboratory, the storage policy was according to the department's policy.

To ensure patient confidentiality and that ethics is reached, each tooth sample was given a unique ID code rather than patients name or hospital number.

CHAPTER 5

Characterise Control, Type 1, 2 and PEB using Standard Diagnostics

Standard Diagnostics

5.1 Method

5.1.1 Clinical Visual Assessment

A samsung galaxy professional camera (16MP, 21x Optical Zoom, Android 4.1 Jelly Bean OS) 4.8 inch HD Touch LCD was used to take photographic images of each of the teeth. Each tooth was wiped off excess moisture using cotton roll, but not thoroughly dried according to the criteria of the mDDE, and placed against black sandpaper, which was used as a background to enhance the contrast, mounted with plasticin. When a photograph was taken, the camera was fixed to a stand about 15 cm away from the tooth, as this was shown to be the best diameter to view the whole tooth with good clarity. Regarding the lighting, the room light was dimmed and used natural sun light to reflect the image without the use of a flash.

Five photographic images were taken for each sample, one for each surface (buccal, mesial, lingual/ palatal, distal, and occlusal). The photographs were close recordings of the teeth. Each photograph was checked for clarity and if the photograph was not clear or if the lesion was not clearly seen, the photograph was repeated until the appearance on the photograph matched the clinical view. The images were then uploaded to a computer where all the data were saved, and labelled according to sample identification code and surface.

The photographs were then printed, and the hard copies served as a mean for characterising the lesions of each MIH defect by 2 different examiners. Each tooth surface was subdivided according to the number of lesions present, and each lesion was described instead of a surface as a whole, for e.g. as illustrated below in figure 5.1 this surface has 2 different lesions, marked in blue boxes.

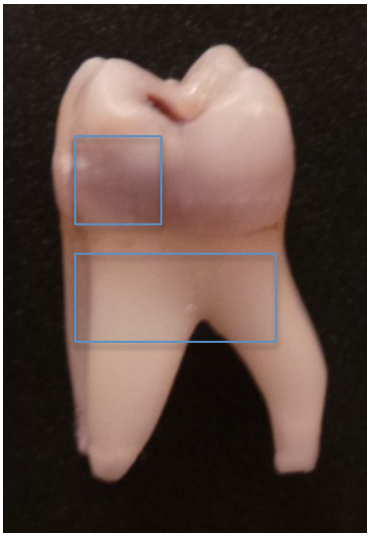

Figure 5.1 Showing a clinical photograph of a FPM illustrating how lesions were divided

The index used to characterise the lesions was the Modified Developmental defect of enamel (mDDE) index (table 5.1), as mentioned previously it is the most common index used in children, and supplemented by using the MIH charting criteria proposed in 2015 (table 5.3) to give a bigger spectra. With regards to the mDDE, each lesion received four different codes and recorded on the dental anomaly proforma (Appendix 4) accordingly. The codes were location (L), demarcation (D), extent (E), and type of lesion (T) as previously described in the mDDE index.

	Code
Type of Defect	
White/cream	1
Yellow/brown	2
PEB	8
Location	
Incisal half	1
Gingival half	2
Both	3
Demarcation	
Diffused	1
Demarcated	2
Both	3
Extent	
Less than 1/3 of surface	1
Between 1/3 and 2/3 of surface	2
More than 2/3 of surface	3

Table 5.1 Showing mDDE Index to record the type of developmental enamel defects

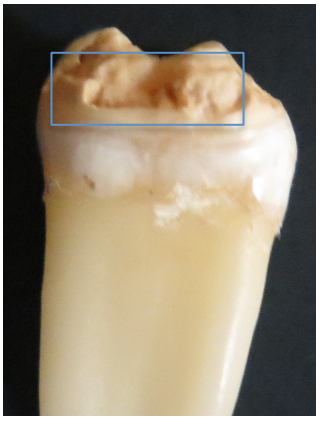

Figure 5.2

Location	Occlusal 1/3= 1
Demarcation	Demarcated= 1
Extent	Between 1/3 and 2/3 of surface= 2
Type	Brown 2 with PEB= 8

Table 5.2

Figure 5.2 Showing clinical photograph of PFM with lesion marked in blue box

Table 5.2 showing an example of how the lesion in figure 5.2 was classified using mDDE

Defect	
No enamel defect	0
Enamel defect non-MIH or HSPM	1
Creamy/ white or yellow/ brown opacity	2
PEB	3
Atypical restoration	4
Atypical caries	5
Missing due to MIH/ HSPM	6
Cannot be scored (Extensive coronal breakdown, where the cause cannot be determined)	7
Extent	
I	Less than 1/3 of tooth surface
II	Between 1/3 and 2/3 of tooth surface
III	More than 2/3 of tooth surface

Table 5.3 MIH charting criteria proposed by Ghanim et al., 2015

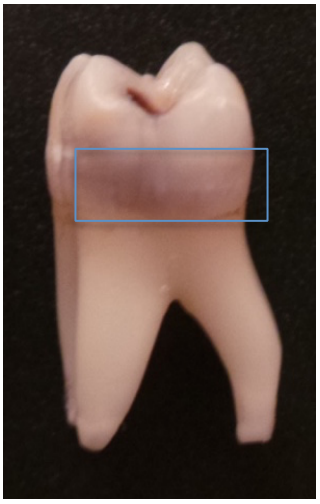

Defect	Yellow/ brown opacity =2
Extent	Between 1/3 and 2/3 of tooth surface = II

Figure 5.3 Table 5.4

Figure 5.3 Showing clinical photograph of PFM with lesion marked in blue box

Table 5.4 Showing an example of how the lesion in figure 5.3 was classified using the MIH charting criteria

Each lesion was characterised separately, instead of a tooth as a whole, and based on the codes they were categorised into different types, as illustrated in figure 5.5. The different categories were type 1, type 2 or type 8 (PEB). And then the lesions were further sub-categorised into either being demarcated, diffuse or both. This would help correlate with the radiographic images and OCT findings.

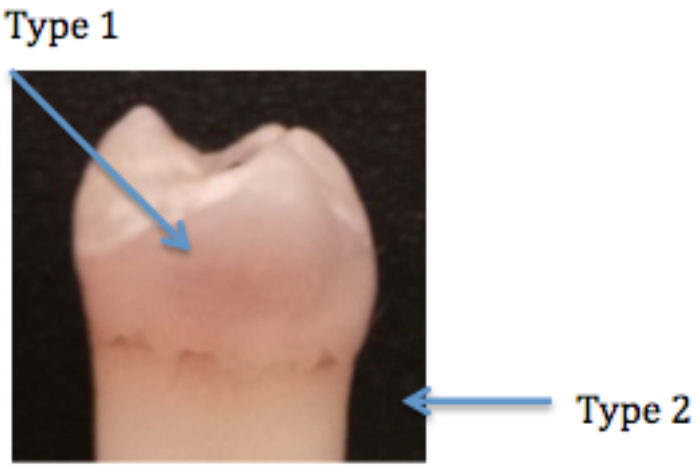

Figure 5.5 Showing how a surface was divided into different lesions to be scanned

5.1.2 Radiographic Assessment

After taking the clinical photograph, excess moisture was wiped off the sample, using a cotton roll, and then the tooth was positioned against an intraoral film on a flat table. The same x-ray machine was used for all samples, using the same settings, type of film and exposure time to ensure no confounding was present. The x-ray machine used was model x-mind by Toshiba, with type F intraoral film and the exposure time used was pre-set for permanent molars, maxillary or mandibular, as noted on the x-ray machine. Two radiographic views were taken for each sample, a bucco-lingual (BL) view to show the mesial and distal surfaces (figure 5.4a), and a mesio-distal (MD) view to show the buccal and lingual surfaces (figure 5.4b) respectively. The images were then scanned and uploaded with their corresponding clinical photographs.

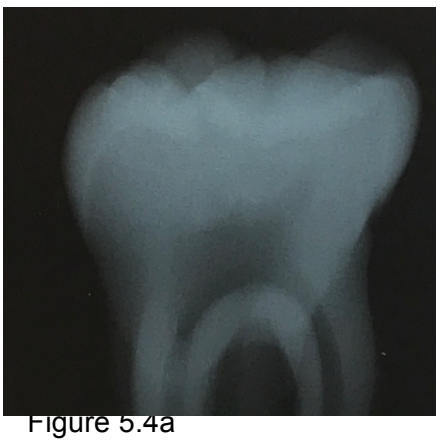

Figure 5.4a

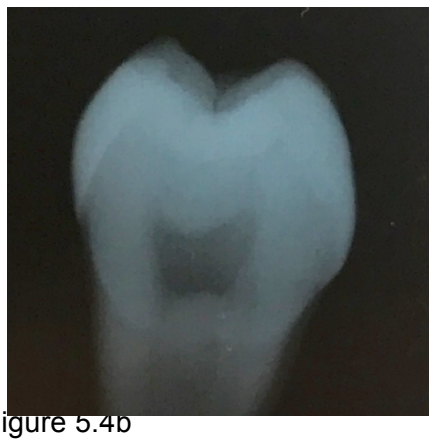

Figure 5.4b

Figures 5.4a and 5.4b Showing x-ray images of a FPM in a BL and MD view respectively.

5.2 Results

From 16 patients, a total of 43 teeth were collected, with 9 (3 patients) excluded due to caries, therefore 34 MIH teeth were included from 13 patients, in addition to 3 sound teeth from 1 patient. Demographic data of patients used is shown below in table 5.5.

Patient ID	Age (Years)	Gender	Ethnicity	Tooth Notation	Sample ID
35	10	M	British	UR6 UL6 LR6	Sound1 Sound2 Sound3
335	9	M	British	UR6 UL6 LL6 LR6	MIH 92 MIH 93 MIH 94 MIH 95
336	10	M	British	UR6 UL6	MIH 96 MIH 97
337	9	M	Black	UR6 UL6 LL6 LR6	MIH 98 MIH 99 MIH 100 MIH 101
338	10	M	Other	UR6	MIH 102
339	11	M	White	UR6	MIH 103
340	12	F	Asian	UL6	MIH 104
341	12	M	White	UR6 UL6 LL6 LR6	MIH 105 MIH 106 MIH 107 MIH 108
342	11	M	Black	UL6	MIH 109

343	10	M	British	UR6 UL6 LL6 LR6	MIH 110 MIH 111 MIH 112 MIH 113
344	9	F	British	UR6	MIH 114
345	8	F	Asian	UR6 UL6 LL6 LR6	MIH 115 MIH 116 MIH 117 MIH 118
346	10	F	Asian	UR6 UL6 LL6 LR6	MIH 119 MIH 120 MIH 121 MIH 122
347	10	M	Black	LL6	MIH 123

Table 5.5 Demographic data of all patients who participated in the study

The remaining 34 used were categorised into 3 being sound and 31 as MIH (figure 5.5). Although the mDDE index is usually applied at a tooth level, in this study it was applied to individual lesions instead, rather than the tooth as a whole, as illustrated previously in figure 5.1, so more than 1 lesion per surface (if present) was used. This was performed to ease the comparison between the uses of the conventional methods with the OCT, based on the type of MIH defect. This yielded a total of 149 lesions, 137 being MIH and 12 being sound.

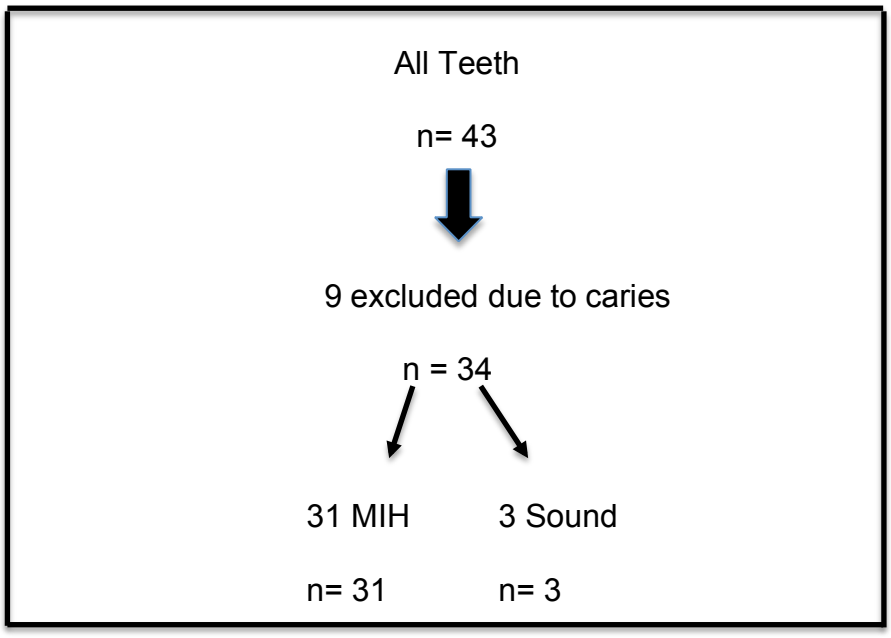

Figure 5.5 Schematic diagram outlining the sample size and allocation criteria for each of the sample groups

A total of 137 lesions were then categorised as 61 being Type 1 MIH, 31 being Type 2 MIH and 45 with PEB based on the mDDE categorisation. Each tooth surface was examined; resulting in 4 or more lesions per tooth (buccal, lingual, mesial and distal), and as some teeth showed breakdown on cusps (occlusal), therefore they were examined as well making them have more than 4 lesions per tooth; In addition to the surfaces that had more than one lesion per surface, which were scanned separately. When the lesions were ready to be scanned, 15 lesions were excluded due to their close proximity to each other, with less than 1mm difference in diameter between them (figure 5.6), which made it difficult to scan them as two different lesions; therefore they were counted as one lesion and described under the more severe type. I.e. if lesion was between type 1 and type 2, it would score as type 2.

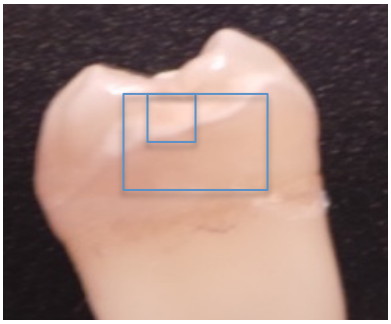

Figure 5.6 Clinical photograph of FPM showing close proximity of lesions, where the small box reflects a type 2, while big box reveals a type 1.

Subsequently, after excluding the 15, the total lesions scanned were 122 lesions, 55 being type 1 and 25 and 42 being type 2 and lesions with PEB respectively (table 5.6).

Lesion	Number
Type 1	55
Type 2	25
Lesion with PEB	42
Total	122

Table 5.6 Summary on the number and categorisation of lesions

The Type 1 and Type 2 groups were further subcategorised to know whether the lesion was demarcated, diffused or both (table 5.7). As for the Type 1 lesions, 39.5% were demarcated, 46% diffused, and 14.5% both. On the other hand, 64.5% of Type 2 lesions were demarcated, 16% diffused, and 19.5% both. From the 45 lesions with PEB, 33.3% were white (Type 1) and 66.7% were yellow/brown (Type 2). There were a low number of control lesions, as only 3 teeth were collected as being sound, due to the rare indication of extraction of sound FPM.

	Type 1	Type 2
Demarcated	39.5%	64.5%
Diffused	46%	16%
Both	16%	19.5%
Total	61	31

Table 5.7 Summary of types of lesions according to DDE

5.2.1 Control Tooth

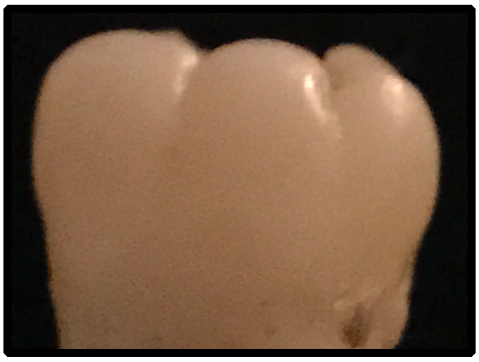

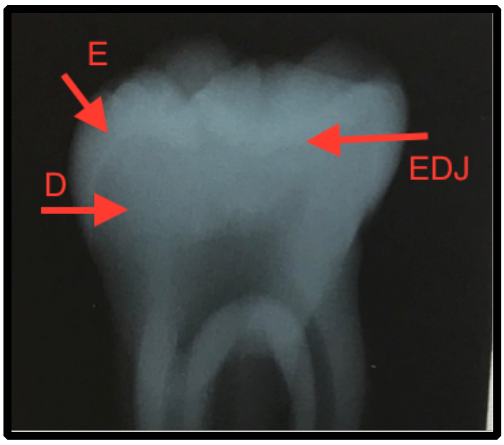

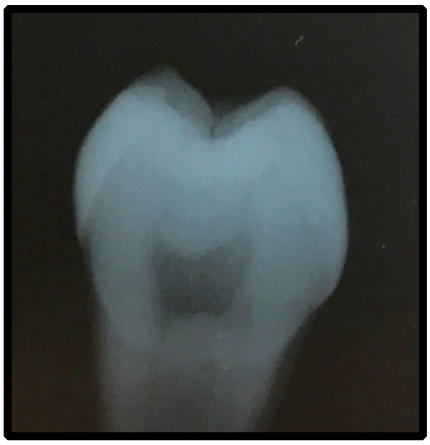

Figures 5.5a, 5.5b and 5.5c Showing a clinical photograph and peri-apicals of a control tooth, a bucco-lingual and a mesio-distal view respectively.

This clinical photograph (figure 5.5a) shows a buccal view of a lower right first permanent molar with smooth sound enamel, of normal colour and no signs of any opacities or breakdown.

Based on the MIH scoring sheets, there is no visible enamel defect, therefore tooth is given a score 0.

In the radiograph (figure 5.5b and 5.5c), we can see that the enamel (E) and dentine (D) are clearly visualised, with a change in contrast between them, where the enamel is highly radiopaque compared to dentine. Between them there is a homogenous continuity of the enamel dentine junction (EDJ).

5.2.2 Type 1 White/Creamy MIH Defect

5.2.2.1- Sample 1

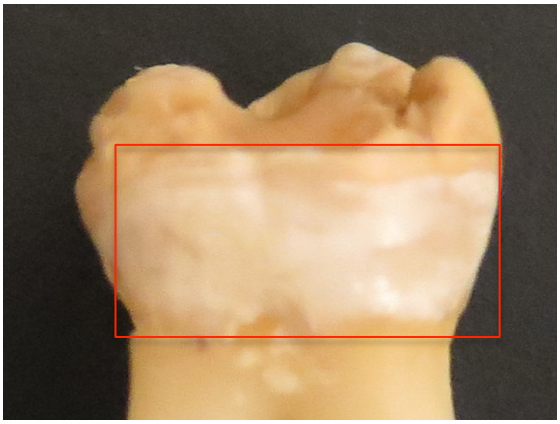

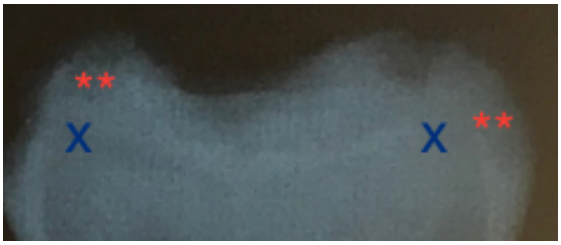

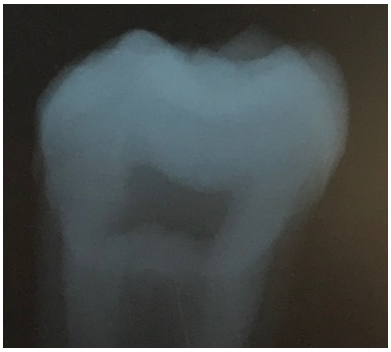

Figures 5.6a, 5.6b and 5.6c Showing a clinical photograph and peri-apicals of a Type 1 lesion, bucco-lingual and mesio-distal views respectively.

This clinical photograph (Figure 5.6a) shows a lingual view of a lower right FPM. When categorising it according to the mDDE, we can see the lesion is demarcated (D1), located on the gingival third of the tooth (L2) with an extent of more than 2/3 of the tooth's surface (E3). As it is of a white/ creamy colour, it is thus a type 1 lesion (T1).

Based on the MIH charting criteria, it's a white creamy opacity with an extent of more than 2/3, therefore scored 2,III.

	mDDE	MIH charting criteria
Location	2	-
Demarcation	1	-
Extent	3	I
Type	1	III

Table 5.8 Summary of classification of mDDE and MIH charting criteria for sample 1

Figures 5.6b and 5.6c show a bucco-lingual and a mesio-distal view of the same tooth. When looking at it from a BL view, the MD can be seen on the image (figure 5.4c), we can see that the enamel shows radiolucent areas on both the mesial and distal (marked with **), and is less radio-opaque than the sound enamel. In addition, there is a loss of the homogenous continuity of the EDJ (marked with x), however this reflects the lesion on mesial and distal, whereas the focus here is the lesion on the lingual. When viewed MD (Figure 5.4), it is difficult to describe as the buccal is superimposed on the lingual, and as the lesion is of a mild type it is not quiet evident on the x-ray image, as its usually underestimated radiographically. In addition, the lesion here is on the lingual, due to the superimposition, the lesion is masked, and therefore cannot be seen.

5.2.2.1- Sample 2

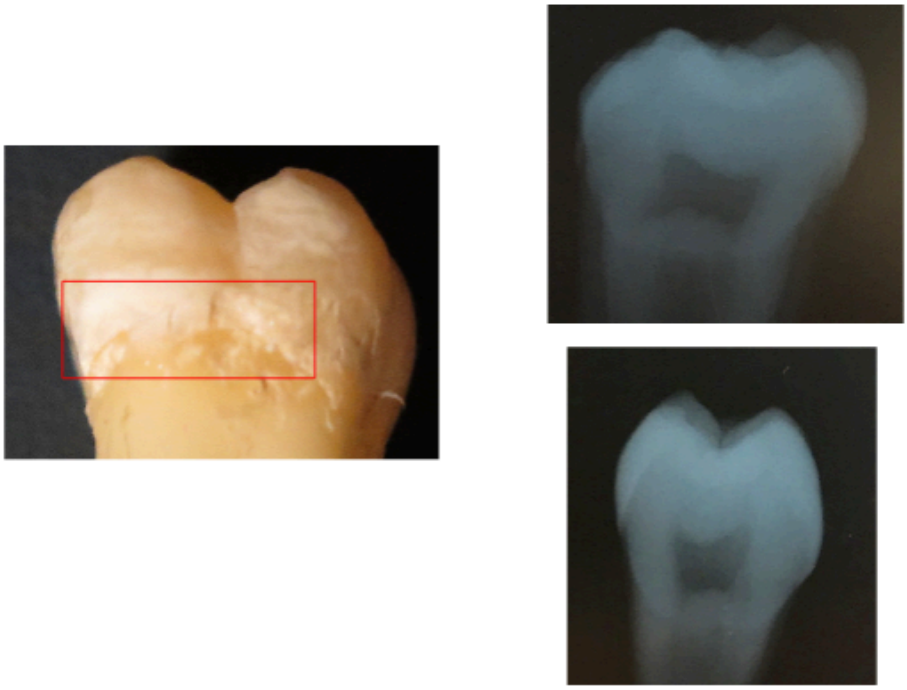

Figures 5.7a, 5.7b and 5.7c Showing a clinical photograph and peri-apicals of a Type 1 lesion, bucco-lingual and mesio-distal views respectively.

This clinical photograph (Figure 5.7a) shows a buccal view of an upper right FPM. When categorising it according to the mDDE, we can see the lesion is demarcated (D1), located on the gingival third of the tooth (L2) with an extent of more than 1/3 of the tooth's surface (E2). As it is of a white/ creamy colour, it is thus a type 1 lesion (T1).

Based on the MIH scoring sheet, it's a white creamy opacity with an extent of between a third and 2/3 of tooth surface, therefore scored 2,II.

	mDDE	MIH charting criteria
Location	2	-
Demarcation	1	-
Extent	2	II
Type	1	2

Table 5.9 Summary of classification of mDDE and MIH charting criteria for sample 2

When viewing the lesion radiographically, it resembles a sound tooth, however with slight radiolucency in the mid-region of the occlusal side of the tooth, symbolising the lesion. However, as the lesion is on the buccal side of the tooth, it is superimposed by the lingual therefore we see a blurred vision, hiding the lesion.

5.2.3 Type 2 Yellow/ Brown MIH Defect

5.2.3.1- Sample 3

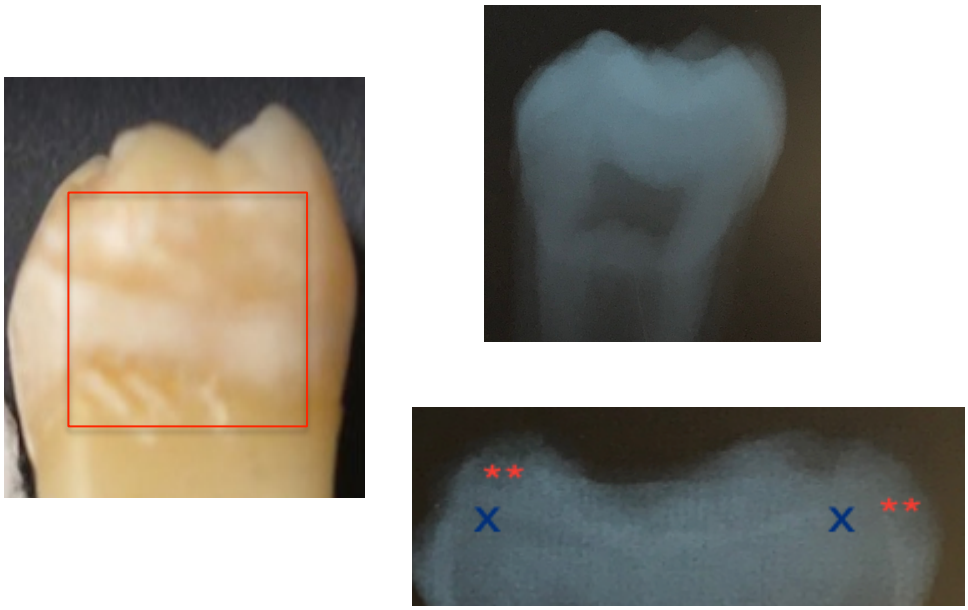

Figures 5.8a, 5.8b and 5.8c Showing a clinical photograph and peri-apicals of a Type 2 lesion, a bucco-lingual and mesio-distal view respectively.

This clinical photograph (Figure 5.8a) shows a mesial view of a lower right FPM, with the lesion affecting the mesial part of the tooth. According to the mDDE index this lesion is considered both demarcated and diffused (D3), affecting the whole tooth surface (L3) with an extent of at least 2/3 of the tooth surface (E2). The lesion is yellow coloured, thus it is a Type 2 lesion (T2).

Based on the MIH scoring sheet, it's a yellow brown opacity with an extent of between a third and 2/3 of tooth surface, therefore scored 2,II.

	mDDE	MIH charting criteria
Location	3	-
Demarcation	3	-
Extent	2	II
Type	2	2

Table 5.10 Summary of classification of mDDE and MIH charting criteria for sample 3

Both figures 5.8b and 5.8c were described earlier in the type 1 lesion, as it is the same tooth however the lesion is of a different area. In the BL view (Figure 5.6b), there is distinctive contrast between enamel and dentine resembling sound enamel, however some radiolucent areas appear on the mesial aspect where it is affected (marked with **). We can also see a break in the EDJ on the mesial side (marked with x), however it is more homogenous on the distal side where it is unaffected. In the MD view (Figure 5.5c), the buccal is superimposed on the lingual therefore we can't clearly see the lesion.

5.2.3.2- Sample 4

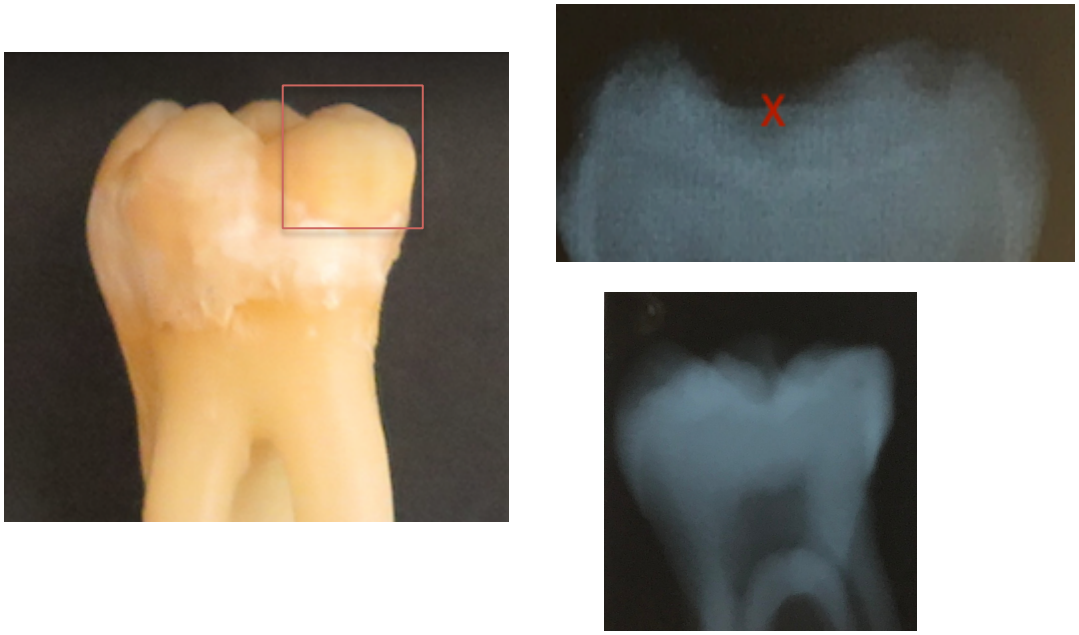

Figures 5.9a, 5.9b and 5.9c Showing clinical photograph and peri-apicals of a Type 2 lesion, bucco-lingual and mesio-distal views respectively.

This clinical photograph (Figure 5.9a) shows a buccal view of an upper left FPM, with the lesion affecting the mesio-buccal cusp of the tooth. According to the mDDE index this lesion is considered demarcated (D2), affecting the occlusal part of tooth (L1) with an extent of more than 2/3 of the tooth surface (E2). The lesion is of yellow colour, thus it is a Type 2 lesion (T2).

Based on the MIH scoring sheet, it's a brown opacity with an extent of more than 2/3 of the tooth surface, therefore scored 2,III.

	mDDE	MIH charting criteria
Location	1	-
Demarcation	2	-
Extent	2	III
Type	2	2

Table 5.11 Summary of classification of mDDE and MIH charting criteria for sample 4

Radiographically (figure 5.9b and 5.9c), the lesion is not shown clearly as it affects the buccal side of the tooth, therefore as mentioned previously, superimposition masks it. There is slight radiolucency on the occlusal side of the xray, which is denoted by X, resembling a lesion.

5.2.4 Lesion with PEB

5.2.4.1- Sample 5

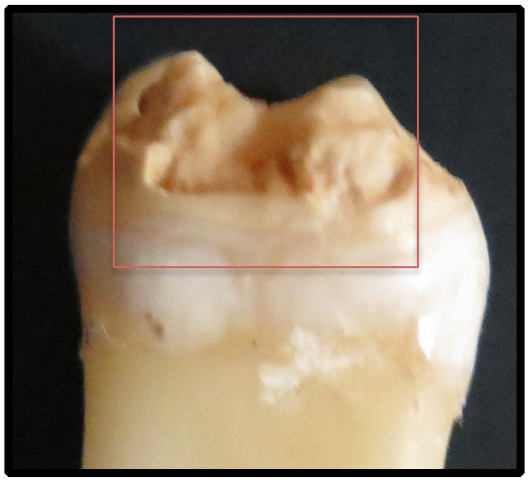

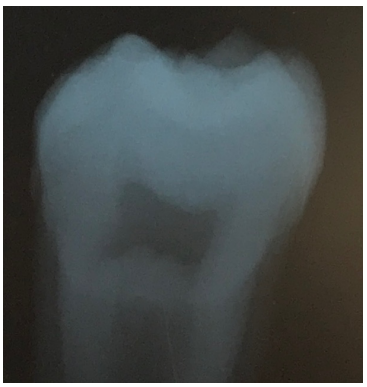

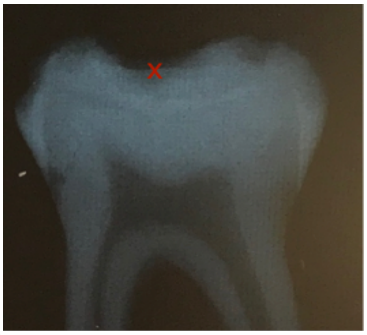

Figures 5.10a, 5.10b and 5.10c Showing clinical photograph and peri-apicals of a lesion with PEB, a bucco-lingual and a mesio-distal view respectively.

The clinical photograph in figure 5.10a shows the mesial aspect of a lower left FPM, with the cusp showing degree of breakdown. Based on the mDDE index, this lesion is considered both demarcated and diffused (D3), with its location being on the incisal edge of the tooth (L1) and extending to only a 1/3 of the tooth surface (E1). As it is showing PEB, it is considered a Type 8 lesion (T8).

Based on the MIH scoring sheet, it's a lesion with PEB with an extent of less than a third of the tooth surface, therefore scored 3,I.

	mDDE	MIH charting criteria
Location	1	-
Demarcation	3	-
Extent	1	I
Type	8	3

Table 5.12 Summary of classification of mDDE and MIH charting criteria for sample 5

Radiographically, one can see the mesial aspect showing PEB, which is clearly shown on both figures (5.10b and 5.10c) as there is loss of definition of the outer structure of the tooth, with radiolucency of enamel, which resembles loss of enamel structure, i.e. PEB.

5.2.4.2- Sample 6

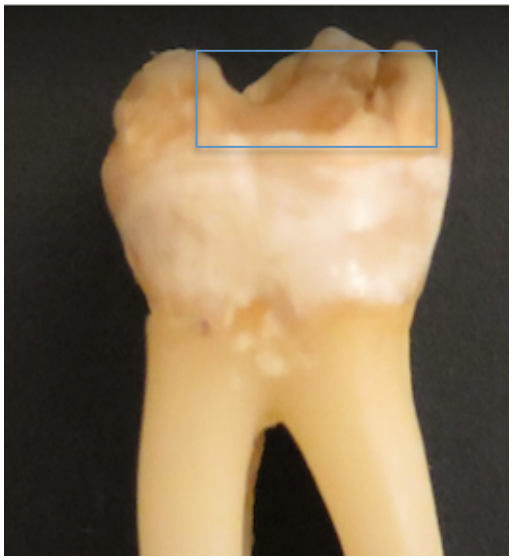

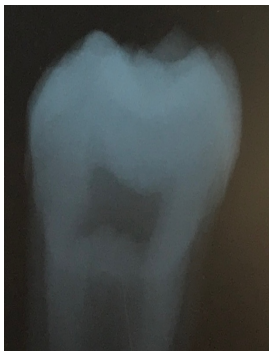

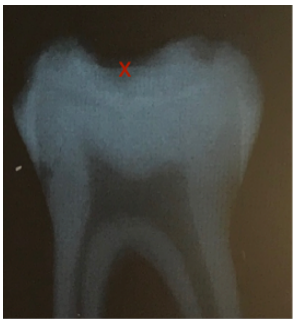

Figures 5.11a, 5.11b and 5.11c Showing clinical photograph and peri-apicals of a lesion with PEB, a bucco-lingual and a mesio-distal view respectively.

The clinical photograph in figure 5.11a shows a buccal view of a lower left FPM, with all the cusps showing breakdown. Based on the mDDE index, this lesion is considered diffused (D1), with its location being on the occlusal edge of the tooth (L1) and extending to only a 1/3 of the tooth surface (E1). As it is showing PEB, it is considered a Type 8 lesion (T8).

Based on the MIH scoring sheet, it's a lesion with PEB with an extent of less than a third, therefore scoring 3,I.

	mDDE	MIH charting criteria
Location	1	-
Demarcation	1	-
Extent	1	I
Type	8	3

Table 5.13 Summary of classification of mDDE and MIH charting criteria for sample 6

Radiographically (figure 5.11b and 5.11c), the lesion is not shown clearly as it affects the buccal side of the tooth, therefore concealed by the superimposition. PEB can be quite seen, as there is radiolucency, which is showing the loss of enamel on the buccal side of the tooth.

5.3 Discussion

Limitations are found in both the conventional methods of diagnosing MIH lesions; therefore this study aims in overcoming these limitations and bringing OCT to the clinical settings as a usual diagnostic tool to know the extent of the lesion and predict its prognosis.

With the clinical method, it was difficult to assess the extent of hypomineralisation and thus the risk of loss of enamel and its severity. Hence it is not easy for clinicians in everyday practice who are faced with questions regarding the degree of hypomineralisation to predict the prognosis and the best management for the affected tooth.

With very mild lesions, for e.g. in type 1 MIH where there is only a slight white opacity, the lesion can be easily missed, especially when the clinician is not looking properly, the tooth is wet, or there is no optimal lighting. In addition, bias can be found as clinicians vary in their ability to diagnose MIH or describe the lesions seen, as it differs from one clinician to another i.e., one might see it as demarcated, while other considers it diffused, or differing between creamy/ white, yellow or a white spot lesion of demineralisation. Furthermore, the number of different indices used possesses difficulties, as there is not one index found which can be used worldwide, thus the wide range of differences in prevalence recorded amongst countries.

All the indices were found to have limitations as well as that they require calibration and training to produce repeatability. The index used here was the mDDE, as mentioned earlier it is the most commonly used worldwide, which helps correlate to different studies. However, the mDDE only describes the location, demarcation, type and extent of lesion, which can be seen superficial on enamel or in cases of PEB, the breakdown. As for the extent, it only describes how it looks externally, i.e. if the

lesion involves less than a third of the tooth (E1), between a third and two-thirds (E2) or at least involves two thirds of the tooth (E3). However, it does not explain to us what is happening to the tooth's ultrastructure, or how severe or deep the lesion is to predict its prognosis and treatment plan, that's why I used MIH scoring system as an adjunct.

In regards to the MIH scoring system, it enables the total spectrum of MIH to be determined by combining both the mDDE and EAPD guidelines to characterise the lesions. In addition, it helps to distinguish it from other enamel defects, by excluding them as non-MIH or HSPM therefore narrowing down the differential diagnosis. Thus it yields maximum information and is not time consuming. However, a drawback of this system is that it only describes the lesion as having a discoloured opacity without specifying if it is doesn't white/ cream or brown/ black.

Furthermore, when taking clinical photographs of the samples, the background lighting, angle of photo taken and usage of flash also possess uncertainty in the outcome of the photographs taken, which can reflect differences to the true lesion. In addition, the use of a ring for the flash can cause a burn out effect on the photo, which can conceal parts of the lesion.

In order to understand how a lesion looks like radiographically, we need to first image a sound control tooth, as to detect the abnormal the normal should first be studied to compare. Thus, when comparing MIH teeth to sound in a radiographic image, different aspects were noticed. As for the sound tooth, the enamel and dentine are clearly visualised, with a change in contrast between them, as enamel is highly radiopaque compared to dentine. Between them we can see a homogenous continuity of the EDJ. However when there has been a change in the density, or a breakdown in the homogenous EDJ, this reflects a lesion.

The severity and type of the lesion dictates its radiographic features, as for the milder type (type 1), the radiographic features are not very distinctive on x-ray images, however in the more severe Type 2 lesions, we can start to see some radiographic changes appearing for e.g., radiolucent areas. On the other hand, in lesions with PEB the tooth surfaces are broken down and destructed, thus they show as radiolucent changes in enamel and in dentine, and if very severe they show loss in tooth structure, which is seen as breakage in the homogenous continuity of the outline. A drawback of this is that x-rays only tend to show radiopaque/ radiolucent areas, and when there is a lesion it tends to be radiolucent therefore it can be confused between caries or an enamel defect. In addition, radiographs cannot distinguish active from inactive disease, for e.g. periodontal disease is not identified until significant bone loss has occurred.

When considering radiographs, they produce ionizing radiation, which is not found in OCT. Radiation as explained earlier can have carcinogenic effects, and other side effects, which were explained previously.

In addition, due to the fact that they are a 2D projection of a 3D object, the amount of breakdown cannot be seen on a bucco-lingual direction. Therefore if the PEB was found on the buccal or lingual surface, it would not be clear on the x-ray image as it would be concealed by the superimposition, as it is a 2D image of a 3D structure.

In addition, lesions shown on x-rays tend to be underestimated, as the actual lesion is usually deeper than what is seen on an x-ray and is usually not seen radiographically until it is 30% into enamel (Woodward et. al., 1996).

Accordingly, it would be helpful for the dentist to have a baseline guide clinically and radiographically to assess the severity and long-term prognosis of the lesion before deciding on the best management approach.

CHAPTER 6

Characterise Control, Type 1, 2 and PEB using OCT

6. Optical Coherence Tomography

6.1 OCT Machine

The OCT machine used was a VivoSight OCT scanner (figure 6.1). This scanner has been initially invented to be used in dermatology. It is a Multi-Beam Swept-source frequency Domain OCT type machine, which is created by Michelson Diagnostics, Kent, United Kingdom. The laser of the OCT is considered a class one eye safe laser, with near-infra red light wavelength of 1305 nm at the centre with optical resolution of less than 7.5 μm and 5μm, laterally and axially, respectively.

The scanned area is 6 mm x 6 mm (width x length) with an image depth of 1.2 mm - 2.0 mm depending on the tissue. The OCT has a scan rate of 10 kHz and a frame rate up to 35 frames per second. The image obtained can be presented as a vertical B scan, En-face image or 3D in TIFF (Tagged Image File Format) stack or DICOM (Digital Imaging and Communications in Medicine) formats.

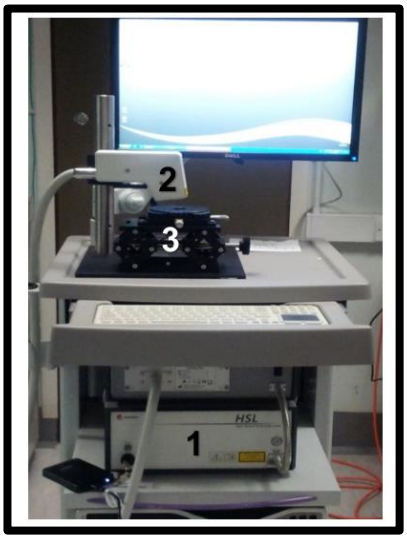

Figure 6.1 Showing the setting of the OCT scanner

The components of the OCT is illustrated in figure 6.1 which are composed of Santec HSL-2000-12-MDL light source (1), Dell Precision T3600 processing system,

Spectrum M2i.4022 4-channel 20 MHz 1-bit data acquisition, and a monitor to display the images along with a hand held scanning probe (2) placed over a mounting platform (3).

6.2 Method

OCT imaging was conducted in the Biomaterials and Tissue Engineering Department at Eastman Dental Institute, University College of London.

The next step after taking clinical and radiographic images was the OCT imaging of the samples. Multiple B scans were taken, depending on the number of lesions present per tooth, imaging each lesion separately, but using the exact same settings for each.

The tooth was removed from the 0.1% thymol solution, excess moisture wiped off using cotton roll, however not fully dried, and then the tooth was placed on the OCT mounting platform, in a vertical position. The tooth was stabilised using plasticin on the position that was best suitable to scan the lesion, making the lesion perpendicular to the laser beam. The distance between the sample and the beam was adjusted using the adjustment knobs, which is used to raise or lower the level of the mounting platform to ensure that the tooth outline is always fully visible on the screen, and that the tooth is not far away from the beam, with optimal clarity. When satisfied with the position, the laser beam is run and the scanning starts. The lesion is scanned starting from the CEJ and runs occlusal ending towards the cusps showing the whole of enamel, as explained in figure 6.2. Each lesion was scanned several times, until the best image was chosen, saved and exported with the other data. Each sample was saved in a separate file named with the ID code, and the file consists of the clinical photo, x-ray and OCT B and A scans.

Each tooth was scanned for the four different surfaces, buccal, lingual/ palatal, mesial and distal in the order described, sparing the occlusal surface. The number of scans per surface was based on the number of lesions present; some had only one while others had more. Each lesion was scored using the mDDE method, 122 lesions were scanned separately. The occlusal surface was spared as the maximum depth of OCT capturing is between 1.2mm - 2mm, making it unclear and difficult to scan and due to the morphology and breakdown of this surface, only the occlusal cusps would be imaged instead of the entire occlusal surface, so not enough information would be gained. The total scan time for each image was approximately 45 seconds.

.

Figure 6.2 Shows a close view of the OCT machine during the imaging procedure.

The tooth is mounted on the mounting platform using plasticin, positioned below the scanning probe. The sample position can be adjusted using the screws indicated with the arrows.

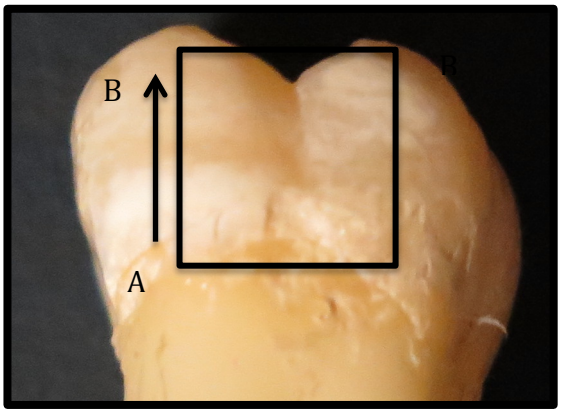

Figure 6.3 Showing a clinical photograph of a FPM with the area of the scan (scanning from A to B)

Figure 6.3 shows an explanation of the scanned area of the tooth surface with 'A' being the start of the scan and 'B' is where it ends, and an arrow showing the direction of laser propagation.

The scan was 2mm deep with a surface area of 6mm x 6mm (figure 6.3), this was the maximum width and depth of the OCT frame that can be scanned, therefore this width was selected for all scans.

The OCT scanner software has two methods of imaging acquisition. The first being free run acquisition where only a single image is captured at an instance. The second method is where multiple frames of a particular area are captured, using either the manufacturer's pre-set system or can be set preferably set by the clinician (accustomed set-up). The pre-set system has two forms, either multi-one or multi-two. Multi-one is where the OCT captures 60 uninterrupted *B*-scan images with 100μm distance between them with a surface area of 6mm x 6mm. On the other hand the multi-two form captures 500 consecutive *B*-scan images with an interval of 4μm distance between them using a scanning widow of 2mm x 2mm. In this study the accustomed set- up method was used in order to capture the maximum information from the samples. Each scan had the same number of frames. The

frames had a distance of 0.01 mm (10μm) distance between each frame, making a total of 500 frames. Each scanning frame measured 1482 pixels X 460 pixels resultant to 6000 μm (6 mm) X 1840 μm (1.84 mm) with each 1 pixel corresponding to about 4 μm as the refractive index of enamel was 1.62. The scans were then exported from OCT software as 16 bit TIFF images and saved to the database.

The images were then imported into a software, named imageJ, which is a public domain, Java based image processing program; which helps in analysing and extracting the information needed from three dimensional live images. The software was developed by Wayne Rasband at the National Institutes of Health in Maryland in USA (Schneider et al., 2012). It helps in analysing the data by creating density histograms and corresponding scattering profile plots. The latest version of imageJ was used in the analysis, which was imageJ 1.47 with 64bit Java, 2013.

The scan is then uploaded to imageJ to be analysed quantitatively and qualitatively by studying the light beam as it travels through the depth of enamel structure, and comparing between both control and MIH teeth. From the B-Scans, the region of interest (ROI) is chosen randomly and then a signal intensity profile is plotted (A Scan). The A-scan resembles where the scattered light is plotted against the depth in enamel. Areas of enamel with any signs of fracture or broken down surfaces, or with any signs of increased surface reflectivity were excluded as they affect the scattering properties, leading to inaccurate results. The width of the selected regions was taken as the width of ten pixels in X-axis, which corresponded to 40.5μm, to reduce the noise level of the scattering.

The OCT images were analysed both qualitatively and quantitatively. As for the qualitative, the images were studied and any abnormalities in the enamel structure

was documented, described and compared to sound enamel (B scans).

On the other hand, the quantitative as mentioned earlier, was the study of the light beam as it travels through the depth of enamel structure, via plotting the scattering intensity profile (A scans). The distance measurement on imageJ was changed to micrometres (μm). Then a rectangular region of interest was selected with a 40.5 μm width on the a-scan (10 pixels wide), as shown in yellow in figure 2.13a. Additionally, scattering profiles were extracted from single frames and plotted as a function of the sample's depth using Origin Pro 9.0TM (OriginLab Corporation, Northampton, MA 01060, USA).

6.3 Results

A total of 34 FPM were scanned using the OCT. 31 teeth were MIH affected and 3 were sound, used as control teeth. This gave us a total of 134 lesions, 122 being MIH and 12 sound. The OCT scanning area on each surface was 6 mm x 6 mm and the depth of scan was 2 mm deep.

As mentioned previously, the settings used were the same throughout the scanning procedure of all lesions. The number of frames of images captured was 600 frames with a distance of 10μm (0.01 mm) between the frames. Each frame measured 1482 pixels X 460 pixels analogous to 6000 μm (6 mm) X 1840 μm (1.84 mm) with each 1 pixel corresponding to about 4 μm. As a result of these consecutive frames, a three dimensional image can be presented.

The images were exported from OCT software as 16 bit TIFFTM images to imageJ to interpret the A-scans. Here the length of the lesion (in the X- dimension), its depth (in the Z- dimension) and its extent across the surface or the number of frames (the Y- dimension) all can be measured.

In both types the control and MIH teeth, signal intensity profiles showed a sharp peak in the beginning of the intensity profile as the light hits the tooth surface, showing a change in refractive index between air and tooth structure. These profile plots provide a direct representation of the scattering of light photons as they travel through the tooth and any disruption in the enamel structure results in altered scattering, which could be measured in the profile.

6.3.1 Control tooth

To understand how the lesion looks like on the scan, a control tooth was scanned first, as a comparison. An example of a sound tooth surface scanned by OCT is described in 6.4b. Figure 6.4a shows a clinical photo of the tooth with a box indicating where the OCT frame has been taken. As discussed previously, the surface is free of any defects.

Figure 6.4a

Figure 6.4b

Figure 6.4c

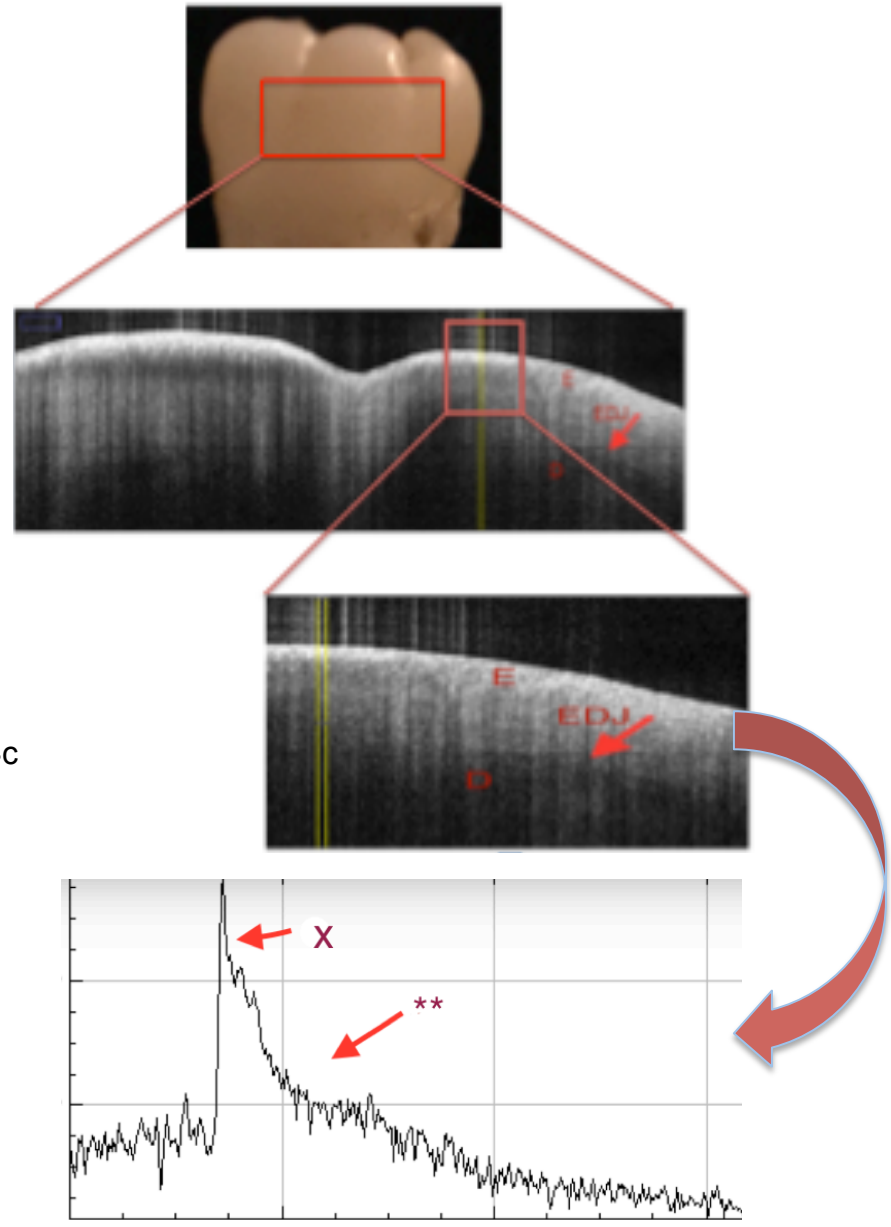

Figures 6.4a, 6.4b and 6.4c Showing a clinical photograph, a B scan and an A scan of a control tooth, respectively

Figure 6.4a shows a B scan of a control tooth. The selected region is highlighted in yellow on the *b*-scan OCT frame, where we can see enamel (E), dentine (D) and clearly a consistent continuity of EDJ between them.

The enamel is rather homogenous with uniform scattering, with no dark areas or any signs of change in contrast. In addition, when the image is viewed as a whole, it shows a well-defined outline of a tooth.

As for the quantitative analysis, figure 6.2b shows an A scan of the tooth. Initially it shows a phase with no scattering where light travels in air. As the light beam hits the enamel surface, a change of refractive index is noted where most of the light is scattered back thus forming a sharp peak in the profile (x), then as it travels deeper into the enamel this back scattered signal intensity decays gradually in an exponential pattern (**), which displays its homogeneity.

6.3.2 Type 1 White/ Creamy MIH Defect

Figure 6.5a

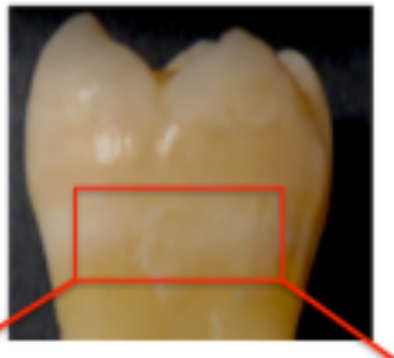

Figure 6.5b

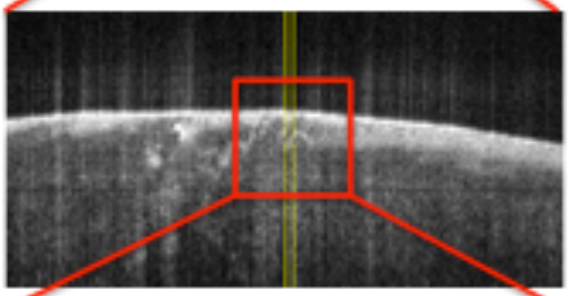

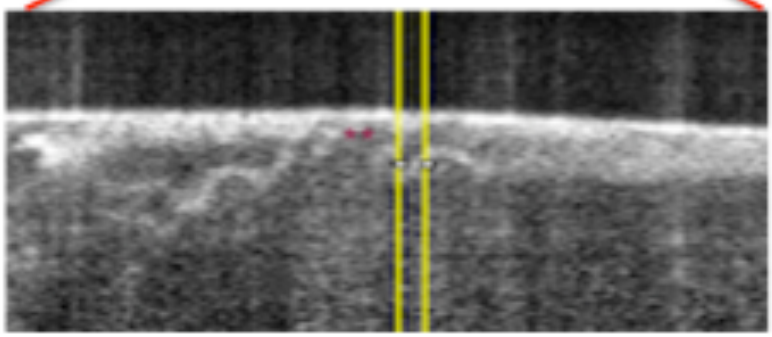

Figure 6.6c

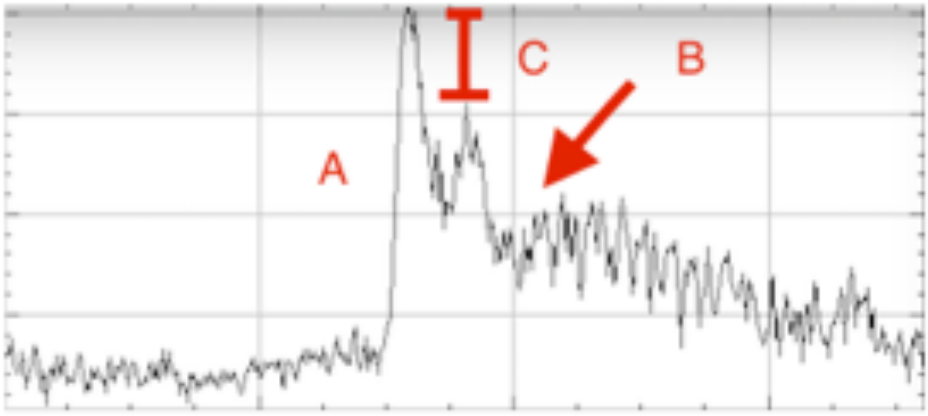

Figures 6.5a, 6.5b and 6.5c Showing a clinical photo, a B scan and an A scan of a Type 1 lesion, respectively.

Figure 6.5a shows a clinical photo of a distal surface of the tooth with a box indicating where the OCT frame has been taken. The selected region is highlighted in yellow on the *b*-scan where the surface of the enamel is smooth and can be recognized by the bright line spanning the length of the section. The area above the tooth is dark due to the lack of scattering in the air (A). On the B-scan one can notice the heterogeneous appearance of the enamel, with areas displaying the natural grey scale contrast reminiscent of control samples, and others area displaying subsurface lesions as show by the stars (**) on the figure 6.5a. The areas of interest (**) shows signs of disrupted enamel conformation and the grey-scale gradient is not uniform in those areas. Indeed, one can notice a brighter region further away from the air/enamel interface suggesting that at this depth within the enamel, the structure is scattering more as a result of structure changes. This is reminiscent of sub-surface lesions.

In order to characterize this lesion in more detail, a scattering intensity profile is plotted, as shown in figure 6.5c. Here the intensity profile does not show a single intensity peak as the case of sound enamel, instead several peaks are shown before it starts to decay, with a wide initial peak (A). Just as the first speak starts; there is another bigger peak, which shows that there is something subsurface. The scatter here is more jagged (B), with more frequent peaks rather than being as an exponential wave appearance. Furthermore, there is a shorter vertical distance between the first peak and the scatter (C).

6.3.3 Type 2 Yellow/ Brown MIH Defect

Figure 6.6a

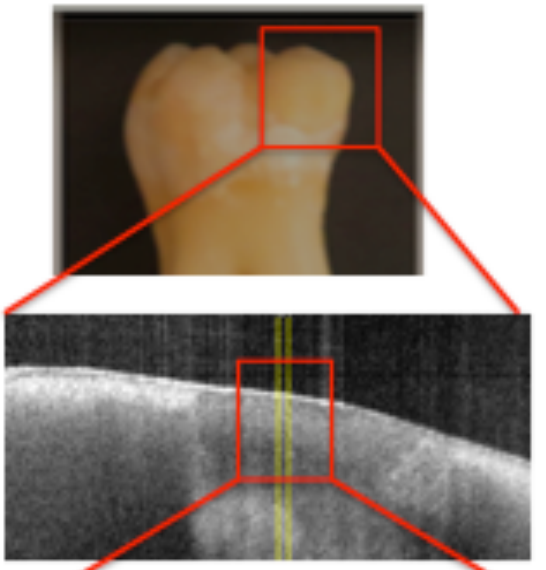

Figure 6.6b

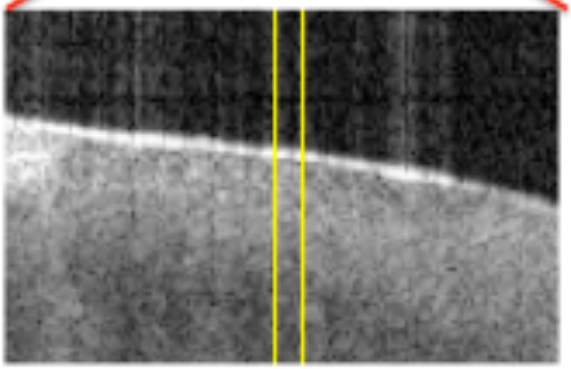

Figure 6.6c

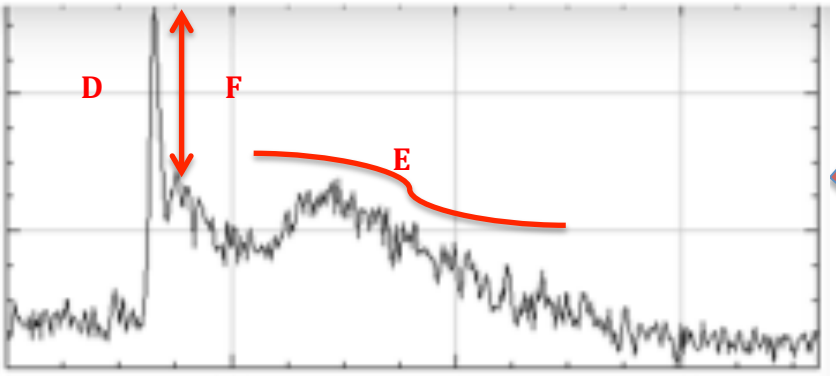

Figures 6.6a, 6.6b and 6.6c showing a clinical photo, B scan and an A scan of a Type 2 lesion, respectively.

In figure 6.6a we can see a clinical photo of a type 2 MIH defect with a box indicating where the OCT frame has been taken. The selected region is highlighted in yellow on the *b*-scan illustrating a homogenous line of enamel in the outer surface of the tooth, showing smooth intact enamel. However, beneath the intact enamel we can see different opacities, which resemble a geographic appearance (**), showing that there is something subsurface that is abnormal. Furthermore, the enamel starts to show roughness towards the mesial of the lesion (x). In addition, no obvious outline can be seen between enamel and dentine, and there is no distinct difference in the contrast, which makes it all diffused with no boundaries.

Figure 6.6c demonstrates a signal intensity profile of a type 2 lesion, where we can see that the signal decay does not show the uniform exponential curve, instead the signal starts with a thin, sharp peak (D), it then shows a significant drop and then starts lingering with a more rounder curve (E), which is more like a wave. In addition, the vertical distance between the first peak and scatter is longer (F) compared to previous lesion.

6.3.4 Lesion with PEB

Figure 6.7a

Figure 6.7b

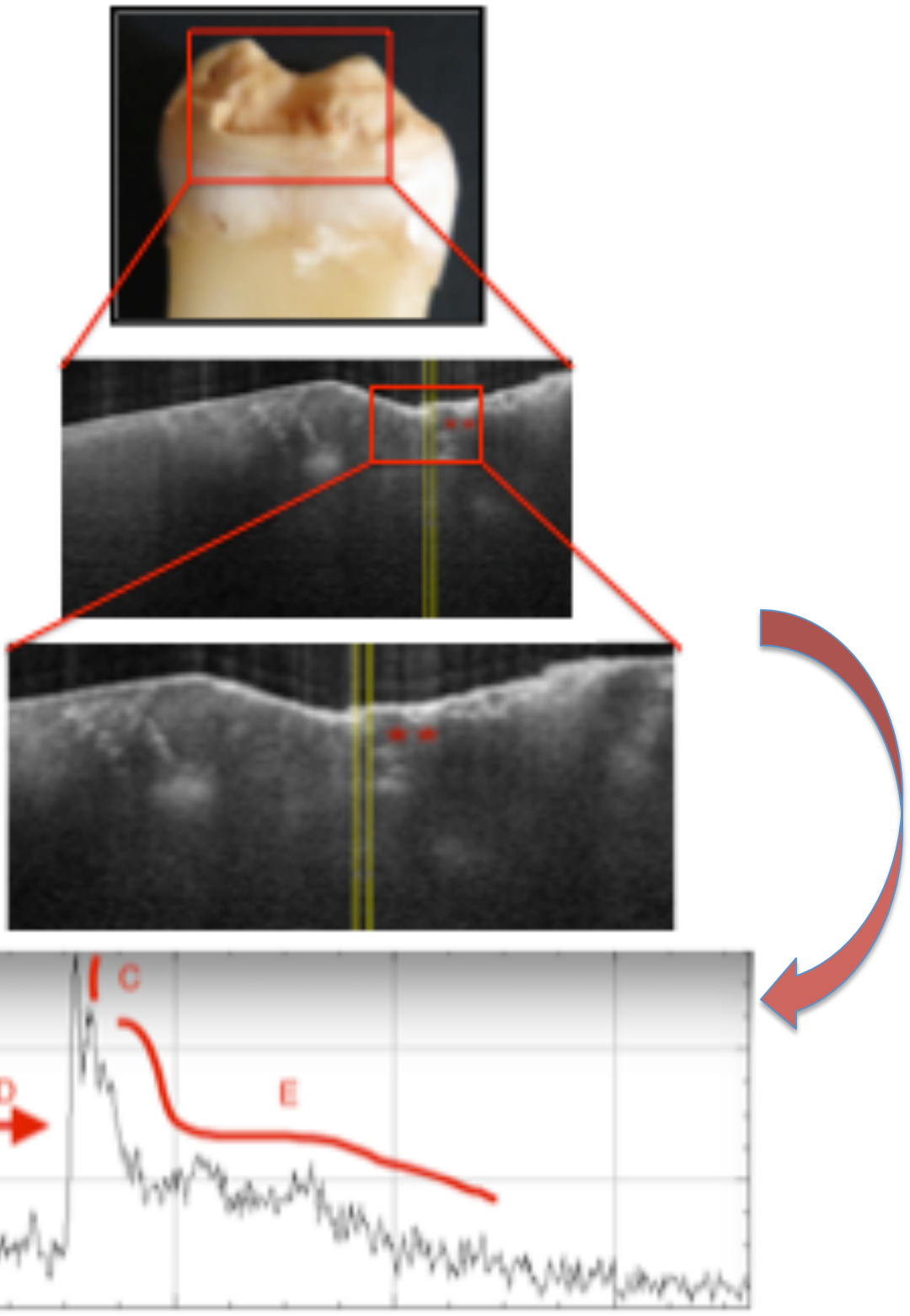

Figure 6.7c

Figures 6.7a, 6.7b and 6.7c Showing a clinical photograph, a B scan and an A scan of a lesion with PEB, respectively.

Here we can see a clinical photo showing an MIH defect with PEB, which is highlighted in a box (figure 6.7a). The selected region is highlighted in yellow on the *b*-scan (Figure 6.7b) where it clearly shows on the start of the scan that enamel is sound and smooth throughout, and then we start to see differences in the contrast with darker areas showing under the white line of sound enamel with cracks beneath which are acting as mirrors reflecting back most of the light leaving dark areas behind (**), furthermore we can see areas of loss of tooth structure where it is seen as breakdown in the continuity of the outline of the tooth, which is reflected clinically as post eruptive breakdown.

Figure 6.7c shows an A scan of the lesion which shows a sharp narrow (D) peak in the commencement which then starts to decay and peak again with many spikes, with a more wave like appearance (E). In addition, the vertical distance between the first and second peak is of short distance (C).

6.4 Discussion

OCT has been proven to be a useful method when studying MIH lesions as it provides images of tissue morphology and ultrastructure at a much higher resolution, better than 10 μm, than other imaging modalities such as magnetic resonance imaging (MRI) or ultrasound. As proven previously, it has been used successfully in medicine in the field of ophthalmology, cardiology, gastro-enterology and dermatology. As mentioned above, OCT possesses no ionizing radiation, in addition it produces real time, instant direct imaging of the tooth with near microscopic resolution therefore showing superiority over conventional methods. In addition, it has been reported that OCT has no detrimental biological effects, thus is safe clinically (Delpy et al., 1988, Otis et al., 2000).

Moreover, no cutting, slicing or preparation of tooth is needed prior to scanning it, and as the frames obtained from OCT scanning are very thin (10μm), this enables

the clinician to detect even the small abnormalities found in the ultrastructure of teeth.

The total time needed to obtain a full scan of the lesion is around 45 seconds, therefore making the OCT scanner a time-effective diagnostic tool.

Another advantage OCT images can be investigated both qualitatively and quantitatively by analysing the B scan and A scan respectively. Signal intensity profile demonstrates the backscatter of light from the tooth structure, which can be studied and compared. As the normal enamel prisms tend to reflect the light, the irregular prisms absorb it, leaving back dark areas. Thus the reflection of light photons as they travel deeper into the tooth structure is complex and depends on the structure of the enamel, i.e. homogenous or not. This can be illustrated in the OCT images, as one can see that the OCT scans of healthy enamel was different from those of the MIH affected enamel. In addition, different types of MIH defects also appeared different from each other. The differences that are seen can be due to enamel porosity in MIH affected teeth, which causes the different signal intensity profiles compared to that of normal enamel. Another cause can be that MIH affected lesions show less mineralised enamel density thus have increased reflectivity (Jones et al., 2006b). This shows that OCT can be a valuable imaging tool in diagnosing enamel defects, as clinicians can use it to differentiate between sound and affected and also between the different enamel defect types.

OCT is a more accurate tool than the conventional methods, and less bias because it is less subject to different clinician's judgments, as it is not based on different indices. Furthermore, it is possible to measure the dimensions of the defects from OCT images using the imageJ software by recording the extent of the lesions into

the depth of enamel without bias.

OCT is a non-ionising and safe method, thus this is an advantage over radiographs, with higher resolution images. The only drawbacks of OCT are the limited depth penetration, which is only 2-3mm and the insufficient scanning range, which is around 6x6mm maximum. In addition, when the surface is smooth, like in sound enamel, the scattering is less thus showing higher resolution. Whereas when there is a lesion, precisely breakdown, the surface is not homogenous, thus the scattering is more, which leads to lower contrast and penetration depth.

Furthermore, when considering the size of the OCT scanner it is difficult to scan posterior teeth intra-orally; therefore an appropriate sized dental scanning probe must be used to help scan posterior teeth.

CHAPTER 7

Defining markers in the OCT scan and scattering intensity plots

7. Defining markers in the OCT scan and scattering profile intensity plots

As mentioned previously, the scattering profile intensity plots between MIH affected enamel and healthy enamel were different, with MIH enamel showing several scattering peaks, instead of a single air-enamel peak. This assumption gave rise to empirical markers, which were described earlier, to describe the A scan profile plots of both the control enamel, and different lesions of MIH. The aim here was to question whether the markers truly fit the stereotyping of the different lesions. This will help clinicians in the future to differentiate between each type easily.

7.1 Methods– multi-examiners evaluation of the markers

7.1.1 Exercise 1: Intra-examiner reliability

Three different lesions were randomly chosen of each group (control, type 1, type 2, and PEB lesions), and their correlated a-scans were printed as hard copies. These were then given to two different examiners (examiners B and C) to study and describe what was seen based on their subjectivity. Both examiners then sat with the main author (examiner A), who had scanned the lesions, and different characteristics were then generated by comparing and contrasting, removing the outliers and leaving back the similarities, which lead to the extraction of similar characteristics, identified as compatible between both. These were then used to extract empirical markers to stereotype each type of lesions differently.

The different empirical markers were as follows;

A. Wide initial peak (figure 7.1)
B. Narrow initial peak (figure 7.2)
C. Jagged like appearance (figure 7.3)

D. Wave live appearance (figure 7.4)

E. Short vertical distance between first and second peak (figure 7.5)

F. Long vertical distance between first and second peak (figure 7.6)

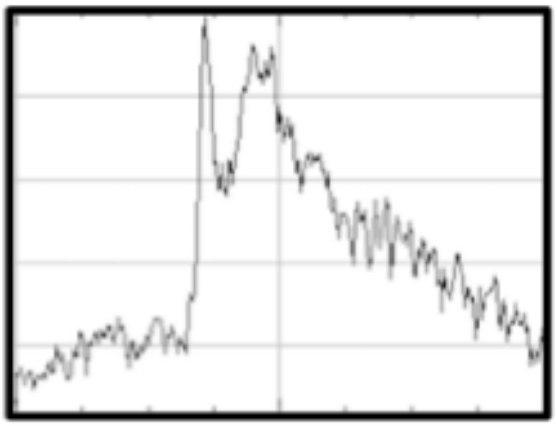

Figure 7.1 Wide initial peak

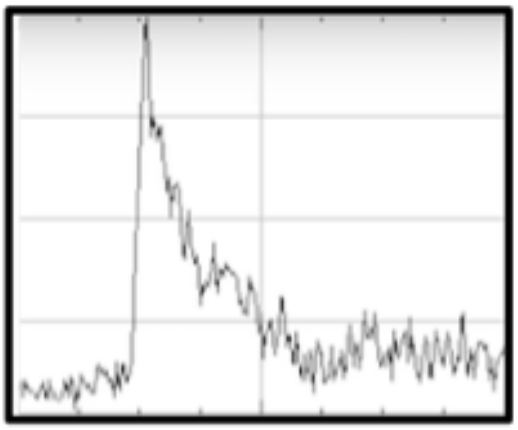

Figure 7.2 Narrow initial peak

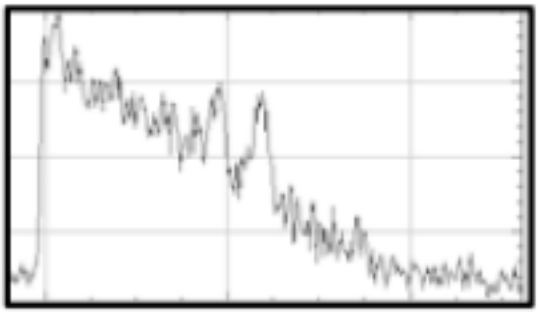

Figure 7.3 Jagged like appearance

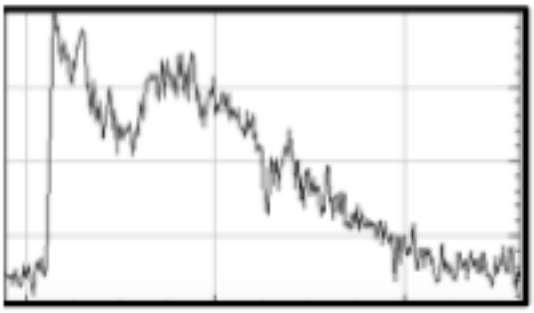

Figure 7.4 Wave like appearance

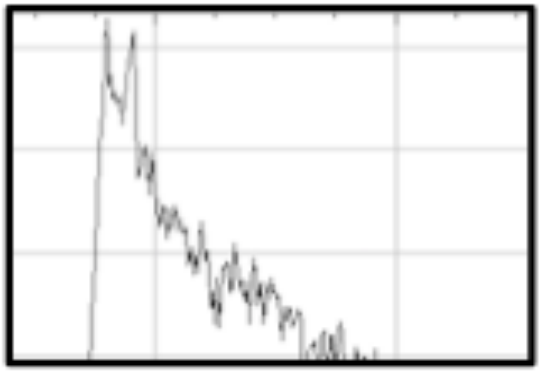

Figure 7.5 short vertical distance

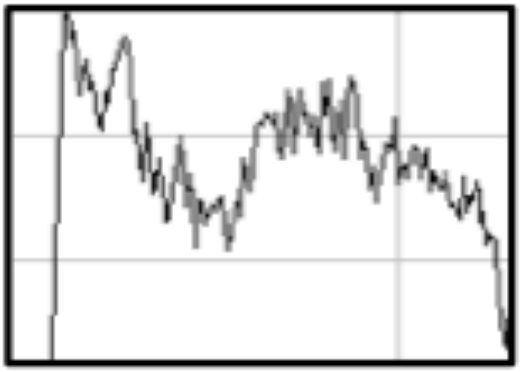

Figure 7.6 long vertical distance

Cycle 1

Consequently, the main author (examiner A) studied all 122 different A scans, and described them according to the characteristic features above, to see if they fit the criteria The examiner had to describe each lesion, without knowing which type it was, whether it had a narrow/ wide initial peak, long/ short vertical distance and if the scatter was more of a wave-like or jagged appearance. Later, the scans were de-blinded, and the markers were assessed to see if they did resemble lesion of interest. In addition, to understand how many of the markers were needed to diagnose a lesion, a Mlogit (multinomial logistic regression) was used to derive probabilities of each combination of markers and each related type, as it is the statistical test that is used to predict the probabilities of different categorical data.

Cycle 2

Examiner A repeated the exercise again a month later for the same 122 lesions, to assess intra-examiner reliability. The agreement was measured by the Cohen's Kappa index using stata15.

Kappa score

For data of population studies to be considered of good quality, it should be repeatable and reliable, i.e clinical examiners should have the ability to apply the diagnostic criteria and have consistent results when repeated (intra-examiner reliability), thus two different examiners were asked to repeat the exercise twice (one week apart), to test this. In addition, inter-examiner reliability is needed, which is consistency between different examiners, thus the 14 different examiners. In addition, calibration and training is needed to ensure that all examiners have understood the exercise properly, and to yield good results and to thus get a good

kappa score, which shows good agreement between examiners. Kappa score is defined as " a measure of true agreement. It indicates the proportion of agreement beyond that expected by chance" (Daly and Bourke 2000). It is calculated using the following formula, shown in figure 7.7.

$$\frac{\text{(observed agreement – expected treatment)}}{\text{(1- expected agreement)}}$$

Figure 7.7 Showing formula used to generate cohen's kappa

The value generated can then be used to analyse the strength of agreement between examiners. The values along with their strength of agreement are illustrated in table 7.1.

Cohen's Kappa values

Kappa Statistic	Strength of Agreement
<0.00	Poor
0.00-0.20	Slight
0.21-0.40	Fair
0.41-0.60	Moderate
0.61-0.80	Substantial
0.81-1.00	Almost Perfect

Table 7.1 illustrates interpretation of Cohen's Kappa (McHugh, M.L., 2012.).

7.1.2 Exercise 2: Inter-examiner reliability

Fourteen different A scans (4 of each type of defect) were randomly chosen, and given to three different examiners, two of who were the same mentioned previously (examiners B and C), plus a third examiner (examiner D) who had not seen the scans before. Each examiner had to study the scan, and fill in the table (table 7.2) according to the markers visible.

Lesion	Wide (A)	Narrow (B)	Jagged (C)	Wave (D)	Short (E)	Long (F)
1						
2						
3						
4						
5						
6						
7						
8						
9						
10						
11						
12						
13						
14						

Table 7.2 Showing lesions and markers for scoring each examiner filled in a table based on what the scans, and then an average of the three was formulated, as illustrated in the table below (table 7.2).

Lesion	Type	Wide (A)	Narrow (B)	Jagged (C)	Wave (D)	Short (E)	Long (F)
1	PEB		X		X	X	
2	1	X		X		X	
3	PEB		X		X	X	
4	1	X		X		X	
5	2		X		X		X
6	1	X		X		X	
7	PEB		X		X	X	
8	1	X		X		X	
9	1	X		X			X
10	PEB		X	X	X	X	
11	2		X		X		X
12	1	X		X		X	
13	2		X		X		X
14	2		X		X		X

Table 7.3 Showing the completed exercise

7.1.3 Exercise 3- Populating the Empirical Markers:

A calibration exercise was done for 14 different examiners, from both a scientific (some with previous experience with OCT) and non-scientific field, to make the sample more diverse. A presentation giving a brief summary explaining MIH (definition, clinical features and different types) and OCT (how it works, what it is) was done, an a-scan of each type of MIH (type 1, 2 and PEB) was shown and then the different markers were explained with illustrations.

The first two figures, (figures 7.1 and 7.2) show the difference between a wide and a narrow initial peak. Followed by figures 3 and 4, showing jagged and wave-like curved plots respectively, where jagged shows more uninterrupted peaks of different

sizes, and wave follows a more uniform pattern. Finally, figures 7.5 and 7.6 explaining the difference between a long and a short vertical distance between the 1st and 2nd peaks. If the distance was approximately less than a box, then it is considered short and vice versa.

A total of 30 different a-scans were then shown on a screen, 10 scans of each type of lesion (type 1, 2 and PEB), but randomly mixed. Each examiner was then asked to fill in the boxes of the table (table 7.2)) to assess inter-reliability a week later, 2 of the examiners were asked to repeat the exercise in order to check intra-reliability using cohen's kappa index.

7.2 Results:

7.2.1 Exercise 1:

- Cycle 1:

  60% of the scans showed that the markers truly resemble the type, with a total of 73 out of the 122 scans correctly fitting the criteria. Type 2 showed the most accurate results (76%) followed by type 1 (60%) and PEB (50%) respectively, illustrated in table 7.4.

Type	**Type 1**	**Type 2**	**PEB**
Number of lesions scanned	55	25	42
Fit criteria	33	19	21
Don't fit	22	6	21
Percentage	60%	76%	50%

Table 7.4 Showing summary of results of first cycle

For the type 1 lesions, the most prominent feature scored was a wide initial peak 44/55 (80%), while for type 2 it was a narrow peak 23/25 (92%), and for PEB a short vertical distance 37/42 (88%).

- Cycle 2:

50% of the scans in this cycle showed that the markers truly resemble the type, with a total of 61 out of the 122 scans correctly fitting the criteria. Type 2 showed the most accurate results (60%) followed by type 1 (51%) and PEB (42%) respectively, illustrated in table 7.5.

Type	**Type 1**	**Type 2**	**PEB**
Number of lesions scanned	55	25	42
Fit criteria	28	15	18
Don't fit	27	10	24
Percentage	51%	60%	42%

Table 7.5 Showing summary of results of second cycle

For the type 1 lesions, the most prominent feature scored was a wide initial peak 40/55 (72%), while for type 2 it was a narrow peak 23/25 (92%), and for PEB a short vertical distance 35/42 (83%).

Statistical analysis was then performed, using stata 15 software, to assess the intra-rater reliability of examiner A between the two cycles using kappa analysis (table 7.6); in addition, the intra-rater reliability in assessing each marker separately (tables 7.7-7.9). Note that the intra-rater reliability is the degree of agreement among repeated administrations of a diagnostic test performed by a single rater.

Agreement	Expected Agreement	Kappa	Std. Err	Z	Prob>Z
73.8%	49.5%	0.4809	0.0874	5.50	0.0000

Table 7.6 Showing intra-rater reliability in match of type to specified pattern of markers over cycle 1 and 2, measured by Kappa index. (single rater, 122 lesions)

Agreement	Expected Agreement	Kappa	Std. Err	Z	Prob>Z
81.1%	50.5%	0.6189	0.0904	6.84	0.0000

Table 7.7 Showing intra-rater reliability of assessment of width of initial peak (wide/ narrow) between cycle 1 and 2, measured by Kappa index. (single rater, 122 lesions)

Agreement	Expected Agreement	Kappa	Std. Err	Z	Prob>Z
78.7%	55.9%	0.5166	0.0905	5.71	0.0000

Table 7.8 Showing intra-rater reliability of assessment of height of initial peak (long/ short) between cycle 1 and 2, measured by Kappa index. (single rater, 122 lesions)

Agreement	Expected Agreement	Kappa	Std. Err	Z	Prob>Z
73.8%	50.11%	0.4743	0.0905	5.24	0.0000

Table 7.9 Showing intra-rater reliability of assessment of height of shape of curve (wave/ jagged) between cycle 1 and 2, measured by Kappa index. (single rater, 122 lesions)

In addition, probabilities of each combination of markers and if they truly fit their type was assessed using Stata procedure mlogit (Multinomial logistic statistical model). Results are illustrated in table 7.10 below, where 1= yes and 0=no.

The question that we wanted to answer is: How accurate are these markers in diagnosing the type of lesion?

Wide	**Short**	**Jagged**	**Probability (Type1)**	**Probability (Type2)**	**Probability (PEB)**
1	1	1	81%	2%	17%
1	1	0	62%	4%	35%
1	0	0	88%	10%	2%
1	0	1	78%	18%	4%
0	1	1	22%	9%	69%
0	1	0	10%	8%	83%
0	0	1	34%	56%	10%
0	0	0	20%	64%	16%

Table 7.10 Showing summary of probabilities (%) of each type of lesion with its pertaining markers, with the highest probabilities shaded in blue (type 1), green (type 2), yellow (PEB).

Source	Wald Chi-Square	Df	Sig.
Narrow/ Wide	23.636	1	0.0000
Short/ Long	15.488	1	0.0000
Jagged/ Wave	2.506	1	0.113

Table 7.11 Showing the significance of how much each marker adds to the diagnosis of the lesion

7.2.2 Exercise 2:

The average results of the 3 examiners was interpreted, as shown in table 7.12 below, for example, lesion 1, if examiner B assumed it was narrow, examiner C wide, but examiner D narrow, it would be scored as an overall narrow.

Lesion	Type	Wide (A)	Narrow (B)	Jagged (C)	Wave (D)	Short (E)	Long (F)
1	PEB		X		X	X	
2	1	X		X		X	
3	PEB		X		X	X	
4	1	X		X		X	
5	2		X		X		X
6	1	X		X		X	
7	PEB		X		X	X	
8	1	X		X		X	
9	1	X		X			X
10	PEB		X	X	X	X	
11	2		X		X		X
12	1	X		X		X	
13	2		X		X		X
14	2		X		X		X

Table 7.12 Shows the average of the results formulated between the 3 different examiners, with the correct markers highlighted in blue, green and yellow for type 1, 2 and PEB respectively.

Type	Type 1	Type 2	PEB
Number of lesions	4	4	4
Fit criteria	3	4	4
Don't fit	1	1	0
Percentage	75%	100%	100%

Table 7.13 Showing summary of results of exercise 2

7.2.3 Exercise 3:

Marker	Kappa	Z	Prob>Z
Narrow/ wide	0.5929	34.84	0.0000
Short/ Long	0.5667	34.67	0.0000
Wide/ Jagged	0.4318	25.91	0.0000

Table 7.14 illustrates Cohen's overall kappa values of assessment of markers between 14 different examiners (inter-rater reliability). (14 different raters, 30 lesions)

Agreement	Expected Agreement	Kappa	Std. Err	Z	Prob>Z
60%	64%	-0.1111	0.1794	-.062	0.7321

Table 7.15 illustrates Cohen's kappa values of intra-rater reliability of assessment of markers, examiner B (single rater, 1 week apart), (30 lesions)

Agreement	Expected Agreement	Kappa	Std. Err	Z	Prob>Z
100%	87.6%	1.000	0.1826	5.48	0.0000

Table 7.16 illustrates Cohen's kappa values of intra-rater reliability of assessment of markers, examiner C (single rater, 1 week apart), (30 lesions)

7.3 Discussion

MIH lesions pose a challenge to dentists in diagnosing the type of MIH and thus predicting the long-term prognosis. In this study a-scans of OCT were extracted from the *b*-scan images in an attempt to observe the behaviour of light as it travels through the depth of normal and MIH affected enamel. In previous studies (Al-Azri, K., et al., 2016), and earlier in this study it was found that MIH and sound enamel showed different a-scans, which was easily differentiated between. Nonetheless when looking at a-scans of different MIH lesions, each profile showed a distinctive behaviour of light scattering, which raised a question to my interest; “can one differentiate the type of MIH by observing the a-scans solely?”

7.3.1 Exercise 1:

Thus different examiners studied the scans and empirical markers were extracted to stereotype each defect. Results proved that by using the intensity of back-scattered light, these markers may lead toward a more systematic diagnostic dental application of the technique, and by that one can not only differentiate between healthy and affected enamel, but also make diagnosis of MIH easier and less subjective.

Based on our data, type 1 was the most prevalent (55 lesions), followed by PEB (42 lesions) and then type 2 (25 lesions) being the least. However this is only based on a minor number of lesions (122) and not considered as a universal prevalence. The characteristics were unique in stereotyping type 1 and 2 lesions type 1 lesion shows a scattering plot with a wide initial peak, jagged like appearance and a short vertical distance between first and second peak. For a type 2 lesion, the scattering plot shows a narrow initial peak, wave like appearance with a long vertical distance between first and second peak. However, in the case of PEB lesions, the scattering

plot showed a mixture between both, with a narrow initial peak and wave like appearance like type 2 lesions, however differentiated with a short vertical distance between first and second peak resembling type 1. This justifies that PEB is not an entity by itself, but a mixture between both as it can be either a type 1 or type 2, which has further deteriorated and ended up as PEB. These are summarised in table 7.17 below.

Type	Empirical markers
Type 1	Wide peak Short vertical distance Jagged appearance
Type 2	Narrow peak Long vertical distance Wave like appearance
Lesion with PEB	Narrow peak Short vertical distance Wave like appearance

Table 7.17 A summary of the empirical markers pertaining to each type of lesion

Statistical analysis was then done to see if the findings of the OCT data relate to the clinical picture of MIH. The results prove than one can not only diagnose MIH lesions using OCT and differentiate it from control teeth, but can also distinguish between the different types of lesions, when studying the A scan profile plots of different MIH lesions by looking at the characteristics and markers. However, these markers are only empirical, which means that they are based on the examiner's observations and assumptions rather than theory or pure logic, and have never been studied before.

Although empirical, the results showed an 81% agreement, with substantial intra-reliability (within same examiner), and moderate inter-reliability (between different examiners) agreement when compared using kappa analysis.

Furthermore, based on the data observed in both exercises 1 and 2, results show that the markers truly fit their criteria with a chance of 60% and 50% of them being accurate, respectively. In addition, we can draw an assumption that type 2 has the most accurate markers, followed by type 1 and PEB, respectively. Although the scores in exercise 2 were lower (50%), they both showed the same conclusion. The decrease in results can be explained either as inaccuracy of results or due to the fact that there has been a month interval between both exercises so a re-calibration should have been made as a reminder to the examiner before attempting the 2nd cycle.

According to the most prominent marker seen in the different scans, one can estimate the type of lesion based on the initial peak, so wide being type 1 and narrow being type 2. As PEB is a mixture clinically between type 1 and 2, the initial peak can sometimes be seen narrow and sometimes wide. However the most prominent feature of PEB was found to be a short vertical distance, which can also resemble type 1. In addition, based on the statistical analysis and probabilities composed illustrated in table 7.10, it shows that the markers extracted, although empirical still show statistical significance in diagnosing the lesion, with high chances ranging from 56-88%. This number shows a good prognosis for the sensitivity of this test, as the accuracy of dental diagnostics usually approximate around 40%. Therefore, this can be further studied using a larger sample, to confirm these findings.

It can be seen in table 7.10 (highlighted in blue) when we have a wide initial peak, regardless of the vertical height and shaped of curve, the probability of it being a type 1 lesion is always the highest (probability 62-88%). As for the type 2, probability of having narrow initial peak with a long interval, and a waved curve is 64%, whereas if it is jagged it is 56%. Thus when we have a narrow initial peak with a long interval, regardless of the curve the chance of it being a type 2 (highlighted in green) is above 56%. As for PEB, the probability of having a narrow initial peak, short interval and a wave-like appearance is 83%, whereas if it is jagged it is 69%. Thus in both situations, with or without the jagged/ wave appearance, having a narrow initial peak with a short interval mainly describes a lesion with PEB, with a chance equal to or higher than 69% (highlighted in yellow).

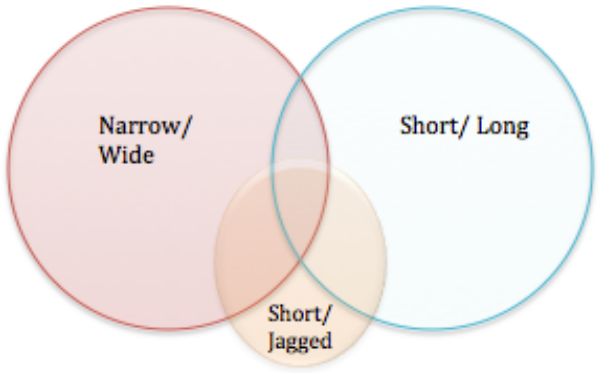

Figure 7.8 Showing a schematic diagram of the unique contributions of each marker to the diagnosis of a lesion based on p value (table 7.9)

Figure 7.8 explains how much each marker contributes to the diagnosis of a lesion, i.e. how significant is the marker? As illustrated, in pink we can see the narrow/ wide with a large unique contribution, the same as for the short/ long marker in blue. However, as for the short/ jagged it can aid in the diagnosis, however when viewed in solo it adds very minor information to the diagnosis, i.e. not significant.

Therefore, combining all results, we can conclude that even if we discard the wave or jagged appearance, we can also interpret the lesions by combining the following markers, illustrated below in table 7.18.

Type	**Markers**
Type 1	Wide initial peak, short vertical distance
Type 2	Narrow initial peak, long vertical distance
Lesion with PEB	Narrow initial peak, short vertical distance

Table 7.18 Summary of the final empirical markers related to each type of lesion

Additionally, PEB is easily diagnosed clinically as there will be evident loss of tooth structure, however the confusion is usually between type 1 and type 2 lesions; so for lesions other than PEB, even if we just look at the initial peak and describe its width (wide/ narrow), one can diagnose the lesion accurately, as the data showed highest agreement between raters, in describing the initial peak's width as being narrow or wide as described in table 7.11.

7.3.2 Exercise 2

This exercise was done as an initial step to question the markers by assessing inter-rater reliability, thus if it showed reliable results it would be taken further and populated into a larger exercise. It was found that when relating the profile to its lesion, results showed that 100% of the type 2 and PEB lesions fitted the related markers, while in the type 1 lesions only 75% were exact with 25% showing a variable of markers. The downside of this, was that only a-scans of lesions with defects were examined without comparing if the different examiners can differentiate between healthy and affected enamel.

7.3.3 Exercise 3

The preliminary data showed that the markers can be promising in actually identifying the type of MIH lesion based on a-scans, consequently populating these markers into a larger number of scans and examiners was performed to confirm the findings with a larger sample, as the larger the sample, the more accurate the results. To our knowledge, despite previous studies looking at MIH and OCT, this is the first study to consider extracting markers to analyse a-scans of different MIH lesions. Furthermore, as mentioned previously these markers are considered empirical as they were explored from studying different lesions and looking at different similarities between different examiners, thus these have not been studied or proved previously.

Based on cohen's kappa values (table 7.1), the inter-rater reliability results generated in this chapter show an overall moderate strength of agreement (0.41-0.60) between the 14 different examiners, with the narrow/wide being the highest and wide/jagged being lowest (table 7.14). This demonstrates that examiners can easily characterise the initial peak as being narrow or wide, with a moderate

agreement of kappa= 0.59. Furthermore, the differentiation between a short or long vertical distance showed approximately the same moderate agreement, with kappa being 0.57, thus giving high moderate agreement when it comes to describing the initial peak in width and height.

On the other hand, the kappa value demonstrated for wave/ jagged curve was lower, despite a moderate agreement yet low (kappa= 0.43). This lower value can additionally justify us discarding the wave or jagged curve (explained in exercise 1), and leave us with the final markers being based on the height and width of the initial peak only to differentiate between type 1, 2 and PEB lesions. Furthermore, when comparing the intra-rater reliability of assessment of markers for two different examiners (1 week apart), it was shown that rater 1 showed a 60% in consistency, while rater 2 scored 100%. Thus again proving the strong agreement, and adding to the conclusion that these markers can be clinically significant.

CHAPTER 8

Progression from 2-D to 3-D diagnostics of lesions

8. Progression of lesion, from 2-D to 3-D diagnostics

The previous chapters of this thesis were used as building blocks to analyse a 3-D image of the lesion as a whole i.e., reconstruction of data. After getting reliable markers from single a-scans, it was thought to take this further and understand the lesion as a whole, by getting a-scans across the complete lesion instead of a single one.

8.1 Methods

8.1.1 Mapping a-scans across the B-scan

Up-to now, our analysis involved choosing an empirical a-scan from all the possible B-scan available (600in total). To overcome, this fairly restrictive analysis, it is possible to extract more A-scans out of a single B-scan. Considering that we fixed our A-scan window to a 10pixel width (~45um), it is possible to effectively record up to 140 A-scans within a Bscan. Below is a series of A-scans windows recorded across a given B scan (figure 8.1).

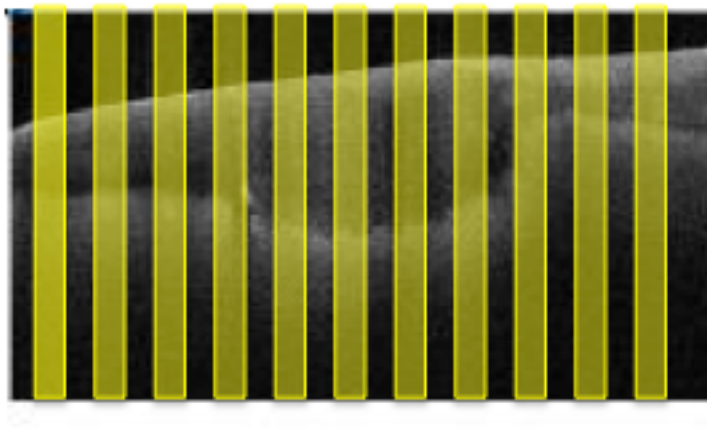

Figure 8.1 showing a schematic description of the distribution of the regions chosen throughout a b-scan, with the yellow boxes resembling a 10-pixel width of scan.

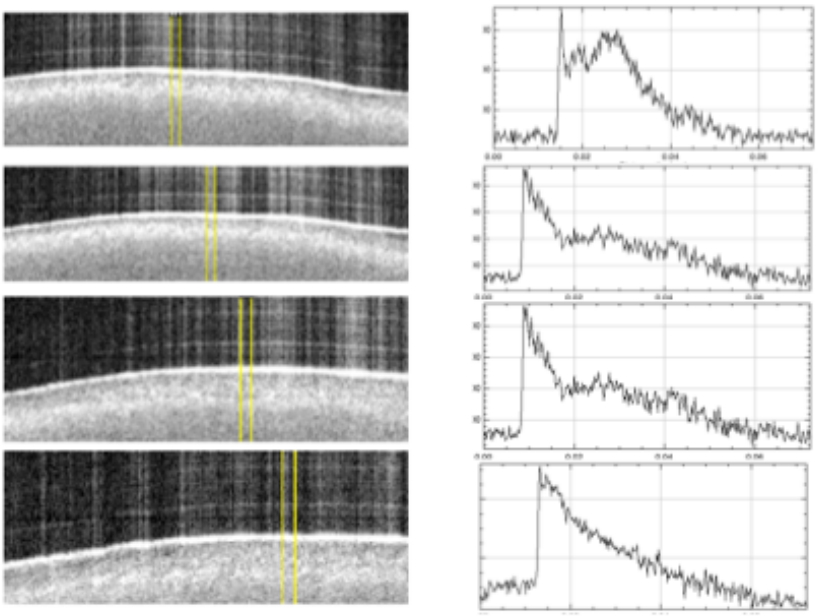

Figure 8.2 Showing consecutive regions of a-scans taken throughout a b-scan, with their corresponding a-scans.

8.1.2 Mapping A-scans across the C-scan

Instead of choosing a single A-scan to represent the whole lesion as performed in the previous chapter, we decided to review the evolution of A-scans across a given lesion. To do so, an A-scan at the centre of lesion was selected in a similar fashion as done in the previous chapter. The location of this A-scan within its original B-scan (called reference B-scan) was fixed for this approach. Following on this, series of A-scans were recorded in B-scans before and after the reference B-scan. Intervals of 10 frames were selected between each B-scan. This enabled us to plot a waterfall series of A-scan as displayed below (figures 8.4,8.5 and 8.6) from the data series data (figure 8.3).

	A	B	C	D	E	F	G	H	I	J	K	L
1	X	Y	Y	Y	Y	Y	Y	Y	Y	Y	Y	Y
2	0	19633.801	26476.801	10862.3	17315.4	17838	17164.699	18699.301	17477.801	20125.699	8418.3	4176.5
3	0.0001575	17252	29833.4	18635.6	20033.301	11699	14192	15192.7	18663.1	21613.301	8960.5	5882.7
4	0.000315	14762.6	27259.9	18001.6	23365.199	10688.6	16350.7	13661.8	19542.4	20145.9	9053	7419.7
5	0.0004724	17494.1	24172.1	12910.3	27096.5	15318.8	16144	16607.199	24219.199	20660.4	7401.5	5614.6
6	0.0006299	17057.4	26849	16048.7	22999	17515.6	10958	16067.3	20726.6	18892.9	8863.2	5794.9
7	0.0007874	21352.699	25507.1	12271.9	21900.301	16388.301	8315.8	16271.3	17962	15283	7424.2	4606.4
8	0.0009449	20347.801	31508.5	18937.301	23209.6	13850.6	14313.4	16059.4	22875.1	22545.4	6261.3	8157.7
9	0.0011024	14300.8	27947.801	21246.801	24103.301	16666.699	17711	11345.3	24258.9	25175.1	9103.9	7798.7
10	0.0012598	18755.1	22723.6	15624.9	29008.199	12955.7	14950.6	11602	16438.1	18619.9	8297.1	5950.9
11	0.0014173	21565.301	26997.6	16358.2	21928.801	20294.4	12292.8	12984.4	24240.199	18233.1	8862.2	8761.6
12	0.0015748	18342.9	28917.801	18036.199	19092.801	17646.5	13339.3	16144.8	18146.301	23977.1	6326.5	9383
13	0.0017323	20959.9	28005	17963.199	22715.301	14348.2	14683.3	15602.4	12527.1	20208.301	10965	10063.5
14	0.0018898	25122.801	31968.5	15885	22466.301	16507.6	16960.699	12179.9	17112.6	22359.9	10866.1	9662.4
15	0.0020472	23303.6	32931.301	21605.301	23329.699	18115.699	12779.1	15219.1	23121.6	23687.699	9182.5	9123
16	0.0022047	20274.6	27293.5	22958	29568.5	16542.199	11097.4	14527.5	21444.1	16277.2	10801.6	8566.7
17	0.0023622	18802.1	27041.699	20993.5	28786.5	20758	16369.5	18583.301	19597.6	15744.7	12120.8	6300.1
18	0.0025197	15808.5	24691.801	20061.6	26759.1	22199.5	15997.6	16628.6	23641.6	20347.801	10415.7	10846.4
19	0.0026772	15380.5	27091.9	18464.1	25041.301	19889.9	14144.6	13476.1	17297.801	22401.6	10990.9	7872.5
20	0.0028346	16761.699	26693.301	17409	21979.301	19434.301	19575.6	14115.6	22799.301	19600.301	9898.5	7495.9

Figure 8.3 illustrating how the data was fed to excel origin, with the x-axis being as a constant, and consecutively adding the y-axis data.

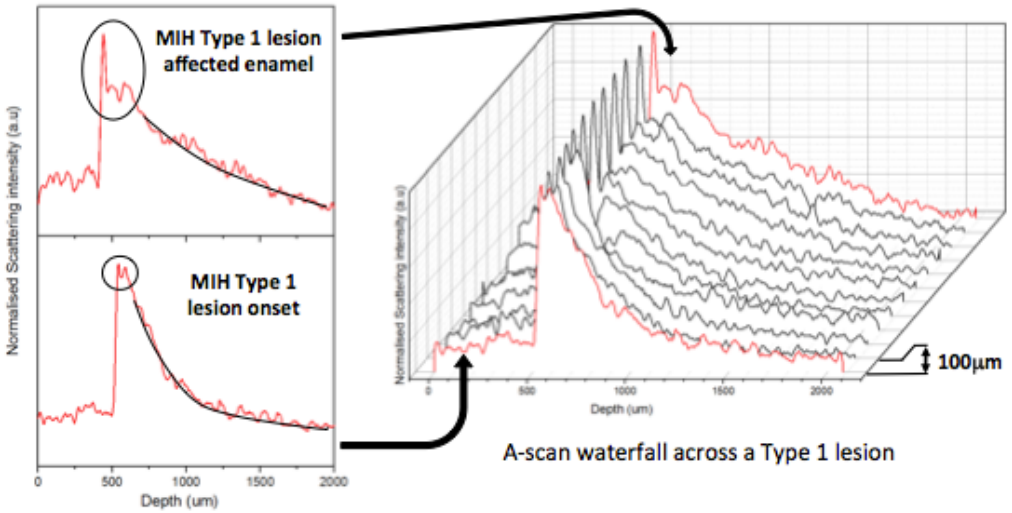

Figure 8.4 Showing a-scan waterfall (stacks of a-scans) across a Type 1 lesion

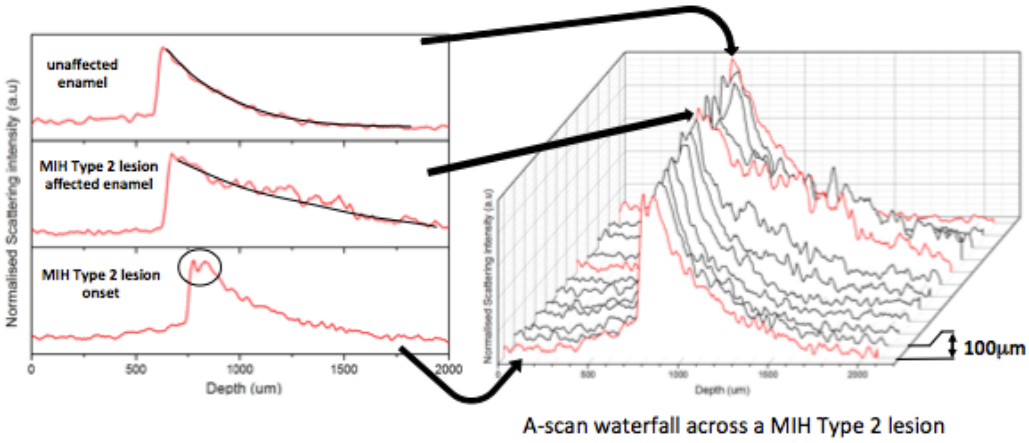

Figure 8.5 Showing a-scan waterfall (stacks of a-scans) across a Type 2 lesion

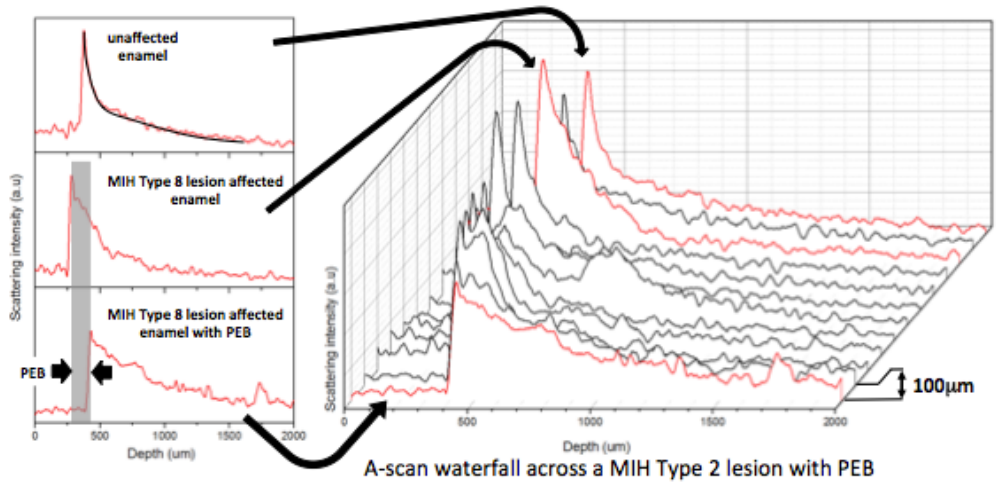

Figure 8.6 Showing a-scan waterfall (stacks of a-scans) across a lesion with PEB

8.3 Discussion

8.3.1 From building blocks to a whole image (cross-sectional analysis)

Reconstruction of scans from a 2 dimension perspective to a 3-d helped interpretation of data easier, thus one can understand exactly what is going on in a lesion instead of studying a single scan, from an arbitrary region. Data from the waterfall graph was more accessible, providing more structural details and made the reading more sophisticated.

A waterfall plot (figures 8.4-8.6) is a three-dimensional plot in which multiple curves of data, are displayed simultaneously. Typically the curves are staggered both across the screen and vertically, with 'nearer' curves masking the ones behind. The result is a series of mountain shapes that appear to be side by side. The waterfall plot is often used to show how two-dimensional information changes, or how lesions progress; it is useful in comparing a number of two-dimensional plots. When composing waterfalls in general, the horizontal axis is generally chosen to be a baseline measure (depth in enamel), and the bars may go either above or below the baseline, depending on the depth. On the other hand, the y-axis is generally used to quantify response to treatment; but in our case it is the back scattering of light from the tooth structure; therefore, if there is a change in refractive index, the more it scatters thus the higher the peak, while if there is loss of tooth structure it will have less backscattering thus a lower peak.

In the beginning of the thesis, a random ROI from different b-scans (type 1, 2 and PEB) was chosen to represent the lesion. Despite ensuring the region chose was free from any cracks/ fractures or increased reflectivity, some bias can be found. Thus when looking at a lesion in a whole, all areas which are relevant, i.e. tooth

structure and lesion, and irrelevant, i.e. air, curvature of tooth, can be scanned and compared to remove any sources of confounding.

The single a-scans (1D) were used as building blocks (slices) to build a larger picture (3D), just like the concept of magnetic resonance imaging, MRI (figure 8.7).

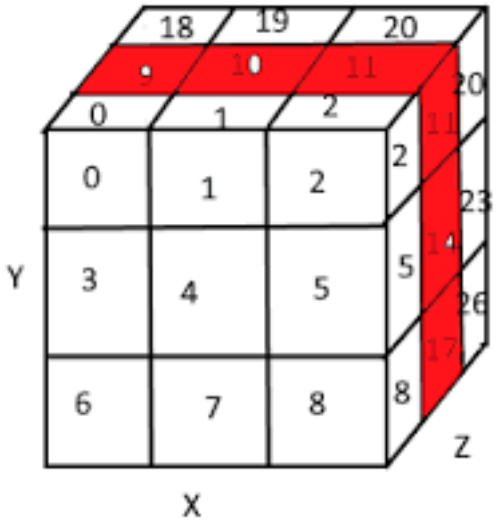

Figure 8.7 Showing an illustration of how using single blocks can build into a 3-D image.

Accordingly we are trying to reinforce the point that one random a-scan may not be able to represent a whole lesion, so sequentially we moved to scanning across a lesion, and then with every 10pixel width (~45um), move and plot a new a-scan, just to see how the a-scan varies as we move across the lesion. So what we can see for e.g. from a type 1 lesion (figure 8.4), we can see it in the beginning (the first red plot) as a typical type 1 graph, however as we go further it shows as it is much more affected (as you go further to the farthermost red plot); so this concluded that the a-scan we selected randomly may or may not be representative of a type 1 lesion. In addition, that within a single defect, different types can be found as going deeper intro a lesion (a mixture of type 1 and PEB, or type 1 and type), which cannot be diagnosed clinically or using plain 2d radiographs, hence we are not getting total

information of the defect, or can be looked in a different way as this can be the source of subjectivity as a clinician might diagnose it as a type 1 while another might see it as a type 2, leading to difference in diagnosis.

Thus if we wanted to take this further and look at all a-scans present in a single b-scan, however this is not feasible by hand. As when looking at a single b-scan of 6 mm x 6 mm, it is composed of 600 frames, and from each frame an a-scan can be generated. Moreover, a single a-scan of is composed of 1400 pixels, so we can generate 140 different a-scans of 10-pixel width each. Put in simpler words, a single lesion can give us 600 x 140 = 84,000 a-scans. Thus looking at a single scan, from a random point to study a whole lesion will not give us a full description of the lesion, and can miscue a lot of points, especially in PEB where we have a mixture of lesions. However, when considering studying all lesions in a full view, considering we have 137 lesions, this equals to 600 x 140 x 137 = 11,508,000; which is a very large number of scans, and is not feasible to study by hand. Thus this can be a starting point for further research, to populate the markers, program the generation of scans and accordingly put them together to have the diagnosis done in an automated way, moving towards reconstruction of volumetric data.

Another finding, when looking at figure 8.5 which shows a stack of a-scans of a type 2 lesion, however when studying it using 3-d graphs (waterfall), we can realise that what goes through a lesion is not always the same; i.e. the ultrastructure changes as we go across a lesion. In the beginning of figure 8.7 in red we can see a typical a-scan of unaffected enamel, however it was taken from a b-scan of a type 2 lesion, so when studying only one a-scan from a ROI, this can be misinterpreted as sound enamel, thus missing out the lesion. As we go more further across the lesion, shown in the second red graph, we can see the start of a wave-like appearance, which is a

typical marker of a type 2 lesion. Furthermore, in the farthermost red graph, deeper into the lesion, we can see the onset of a long vertical peak, indicating it as a type 2 lesion. Therefore, this justifies the point that in one lesion different defects can be present, plus the fact that a random ROI is not always representative of the lesion.

Moreover, when we look at a lesion with PEB (figure 8.7), we can see clearly a massive drop in the initial peak depth caused by less scattering of light, resembling loss of tooth structure (approximately 200 microns showed in grey). As explained early in the thesis, the initial peak starts with a change in refractive index (when light hits enamel, thus change in refractive index from air to teeth), so when we have PEB light travels further into air, due to the loss of enamel making the light further to reach to tooth structure.

8.3.2 Clinical needs for 3D volumetric data:

Having three-dimensional volumetric data generates clinically accurate and immediately available images from the full data set without extensive editing. Moreover, It permits the clinician to address specific questions concerning patient care by interactively exploring different aspects of the data set. In addition, it helps incorporate the patient with their treatment plan, as a 3D image is often easier for them to understand, as its generated by integrating a series of sections into a form that is often easier to interpret than the sections themselves (Calhoun, P.S et. al.,).

Carious lesions have been studied in 3-D data previously, showing good results. The idea of diagnosing dental caries using MRI was first mentioned by Lujik in 1981. The author suggested that using this will help in the future to enable detecting caries laying directly below a restoration that cannot easily be seen on a conventional dental radiograph (van Luijk, J.A., 1981). Advantages of having volumetric data for caries diagnosis include the three-dimensionality of lesion visualization and

quantification. This leads to the possibility to determine and monitor the relative position of the lesion in relation to the pulp, as well as close proximity and efficiency of margins of restorations (Tymofiyeva, O. et al., 2009).

CHAPTER 9

Clinical relevance

9. Clinical Relevance

9.1 Clinical relevance of MIH and OCT

MIH as a disease is increasing in prevalence, with a high global health burden, and the current diagnostic tools available have their limitations, therefore a better clinical diagnostic tool is needed. Continuing research and development are needed to prevent this important international health problem.

Dissemination of information and awareness regarding MIH is necessary in public education as well as in general clinics, to increase the chance of diagnosing it earlier and subsequently having the correct treatment to allow better long-term prognosis.

The use of OCT in clinical medicine has shown that this device is an invaluable technique in clinical diagnostics. It is currently used in many medical fields since the 1990s such as ophthalmology, dermatology and endoscopy. However, in dentistry the main use of OCT is in dental research (in vitro studies). It has not been investigated for potential clinical use especially for clinically diagnosing dental diseases. However, all dental studies involving OCT came to the same conclusion that OCT is an invaluable imaging tool.

Despite the large number of studies done on OCT, to our knowledge all results were based on studying the B and A scans, but none evaluated markers to stereotype each lesion differently. These markers composed help not only in diagnosing the MIH defect, but also in differentiating between lesions.

OCT is proven to be safe as it is non-ionising, nor destructing and has the advantage that it can be used at the chair side with real time imaging of the teeth. However, this can only be applicable if further research is done to compose a compatible device

that can be used intra-orally, thus this research is considered as a building block to build a bigger picture. As a result of bringing OCT to chairside, diagnosing dental conditions can be done at the same time as conventional clinical examination, which together would yield full information about the lesion, with minimal time. Other than that, having a 3-D real time image on a screen in front of the patient, helps to make it more comprehensible, and eases the treatment plan. The prognosis of the affected teeth can also be evaluated in the mean while. in addition, it does not require a large amount of space and can easily fit into the dental practice.

Other than diagnosing, OCT can be used to assess the efficiency of restorations and margins. On the other hand, while drilling the tooth one can see how much tooth structure is left over the pulp, to avoid pulp exposure. Thus the implementation of OCT into the dental field will open new doors for better diagnosis and treatment.

9.2 Limitations of OCT

It is important to highlight that OCT has its limitations, thus it may not totally replace the current diagnostic tools, but be added as an adjunct. First, the size of the current OCT scanner is too big and not convenient to be used intra-orally. There has been a dermatological probe implemented, which could be used on the anterior teeth only, however is too bulky thus would be difficult to be used posteriorly, especially in small mouths (i.e.. children). Moreover, it would be easy to scan buccal and lingual/ palatal areas, however mesial and distal surfaces are difficult due to the close proximity of teeth. In addition, occlusal surfaces are difficult to examine due to the tomography of the cusps. Furthermore, OCT scan can only penetrate 2mm in depth, thus it cannot scan deeper than 2mm into the tooth structure, limiting it to enamel.

Lastly, the cost of the device, as it is considered expensive compared to other

diagnostic tools, with an average 14,500 pounds.

CHAPTER 10

Conclusion

10. Conclusion

In conclusion, OCT has been proven to be a safe and useful diagnostic method when studying MIH lesions, which shows us a full understanding of the lesion with its depth and extent, in a 3 dimension, good clarity image that is not found in conventional methods. This helps in predicting the lesion's long-term prognosis; In addition, it helps in differentiating not only amongst MIH and sound teeth, but also even between different types of MIH lesions, in a non-destructive, objective and real time technique. The definition of specific scattering markers for each type of MIH lesions that was carried and will enable us to bring this technique one-step closer to the clinic.

CHAPTER 11

Future work

10. Future Work

The next step of this project will be to continue to understand MIH more by studying more lesions clinically, radiographically and under the OCT, therefore acting as a larger population study. In addition, investigating the ultra-structure of MIH enamel and comparing it to sound enamel in order to understand the observed signal intensity patterns described previously, and why they behave differently.

In addition, study the a-scans of a control tooth in order to make its comparison with the lesions easier. As in this study, markers were only extracted for different lesions, not control, it would be nice to have markers for control as well in order to measure their specificity and sensitivity.

Consequently, using the markers extracted and studying them in a larger sample, with more calibration to examiners and implementing more statistics in order to prove these markers as diagnostic. Furthermore, batch process the data analysis to remove the human bias in selecting a specific scan region, by comparing more markers and computerising it.

Finally, taking the OCT scan further into the clinical field of dentistry by designing an intra-oral scanning probe in a suitable size which is convenient for both the patient and the clinician. This design could be the same as that of an intra-oral camera or fibre-optic trans illuminator, which can be easily carried and used inside the mouth. This advancement in OCT would help diagnose MIH affected teeth in an objective, non-ionising, real time scan, with a 3-D demonstration of the tooth and lesion as a whole, which can be easily interpreted by patients.

CHAPTER 11

Scientific Dissemination

11. Scientific Dissemination

11.1 Presentations

11.1.1 Three-minute thesis (3MT) presentation, PhDs Annual Research Symposium, University College of London, UK in November 2017 (Appendix 4

Title: Seeing is Believing, A New Approach to Diagnostics in Dentistry

11.1.2 Poster presentation at the International Association of Dental Research (IADR) in London, UK in July 2017 (Appendix 5)

Title: Advanced imaging towards better diagnostics of Molar Incisor Hypomineralisation

CHAPTER 12

References

12. References

Al-Azri, K., Melita, L.N., Strange, A.P., Festy, F., Al-Jawad, M., Cook, R., Parekh, S. and Bozec, L., 2016. Optical coherence tomography use in the diagnosis of enamel defects. *Journal of biomedical optics*, *21*(3), p.036004.

Alaluusua, S., 2010. Aetiology of molar-incisor hypomineralisation: a systematic review. *European Archives of Paediatric Dentistry*, *11*(2), pp.53-58.

Alaluusua S, Lukinmaa P L, Koskimies M, Pirinen S, Holtta P, Kallio M, Holttinen T, Salmenpera L. Developmental defects associated with long breast feeding. Eur J Oral Scien.1996; 104: 493-7.

Allazzam, S.M., Alaki, S.M. and El Meligy, O.A.S., 2014. Molar incisor hypomineralization, prevalence, and etiology. *International journal of dentistry*, *2014*.

Avery J. Oral development and histology. 3rd edition. New York: Thieme Medical Publishers, Inc. 2002.

Balmer, R., Toumba, J., Godson, J. and Duggal, M., 2012. The prevalence of molar incisor hypomineralisation in Northern England and its relationship to socioeconomic status and water fluoridation. *International Journal of Paediatric Dentistry*, *22*(4), pp.250-257.

Baumgartner A., Hitzenberger C.K., Dicht S., Sattmann H., Moritz A., Sperr W., Fercher A.F. Optical Coherence Tomography or Dental Structures. Proc. SPIE. 1998;3248:130–136

Beentjes, V. E. V. M., Weerheijm, K. L. & Groen, H. J. 2002. Factors involved in the etiology of hypomineralized first permanent molars. *Nederlands tijdschrift voor tandheelkunde,* 109**,** 387-90.

Bezerra, H.G., Costa, M.A., Guagliumi, G., Rollins, A.M. and Simon, D.I., 2009. Intracoronary optical coherence tomography: a comprehensive review: clinical and research applications. *JACC: Cardiovascular Interventions*, *2*(11), pp.1035-1046.

Berkovitz, B. K. B., Holland, G. R. & Moxham, B. J. 2009. *Oral anatomy, histology and embryology*, Elsevier.

Brand, R.W., Isselhard, D.E. and Satin, E., 2013. *Anatomy of orofacial structures: a comprehensive approach*. Elsevier Health Sciences.

Chiego Jr, D.J., 2014. *essentials of Oral Histology and embryology: A clinical Approach*. Elsevier Health Sciences.

Calhoun, P.S., Kuszyk, B.S., Heath, D.G., Carley, J.C. and Fishman, E.K., 1999. Three-dimensional volume rendering of spiral CT data: theory and method. *Radiographics*, *19*(3), pp.745-764.

Cho SY, Ki Y, Chu V. Molar incisor hypomineralization in Hong Kong Chinese children. Int J Paediatr Dent 2008; 18: 348–352.

Chun, K.J., Choi, H.H. and Lee, J.Y., 2014. Comparison of mechanical property and role between enamel and dentin in the human teeth. *Journal of dental biomechanics*, *5*.

Clarkson, J., 1989. Review of terminology, classifications, and indices of developmental defects of enamel. *Advances in dental research*, *3*(2), pp.104-109.

Clarkson, J. and O'mullane, D., 1989. A modified DDE Index for use in epidemiological studies of enamel defects. *Journal of Dental Research*,*68*(3), pp.445-450.

Cobourne, M., Williams, A. and McMullan, R., 2009. A guideline for the extraction of first permanent molars in children. *Royal College of Surgeons of England*.

Colston, B.W., Everett, M.J., Da Silva, L.B., Otis, L.L., Stroeve, P. and Nathel, H., 1998. Imaging of hard-and soft-tissue structure in the oral cavity by optical coherence tomography. *Applied Optics*, *37*(16), pp.3582-3585.

Costa-Silva, D., Cristiane, M., Ambrosano, G., Jeremias, F., Souza, D., Juliana, F. and Mialhe, F.L., 2011. Increase in severity of molar–incisor hypomineralization and its relationship with the colour of enamel opacity: a prospective cohort study. *International Journal of Paediatric Dentistry*, *21*(5), pp.333-341.

Crombie, F., Manton, D. & Kilpatrick, N. 2009. Aetiology of molar-incisor

hypomineralization: a critical review. *International Journal of Paediatric Dentistry,*19**,** 73-83.

Cuy, J. L., Mann, A. B., Livi, K. J., Teaford, M. F. & Weihs, T. P. 2002. Nanoindentation mapping of the mechanical properties of human molar tooth enamel. *Archives of Oral Biology,* 47**,** 281-291.

Daly, L. and Bourke, G.J., 2008. *Interpretation and uses of medical statistics*. John Wiley & Sons.

Delpy, D. T., Cope, M., Vanderzee, P., Arrige, S., Wray, S. & Wyatt, J. 1988. Estimation of optical pathlength through tissue from direct time of flight measurement. *Physics in Medicine and Biology,* 33**,** 1433-1442. Dictionary, O.E., 2007. Oxford English dictionary online.

Dos Santos, M.P.A. and Maia, L.C., 2012. Molar incisor hypomineralization: morphological, aetiological, epidemiological and clinical considerations. In *Contemporary Approach to Dental Caries*. InTech.

Elfrink, M. E., Ten Cate, J. M., Jaddoe, V. W., Hofman, A., Moll, H. A. & Veerkamp, J. S. 2012. Deciduous molar hypomineralization and molar incisor hypomineralization. *J Dent Res,* 91**,** 551-5.

Fagrell, T.G., Dietz, W., Jälevik, B. and Norén, J.G., 2010. Chemical, mechanical and morphological properties of hypomineralized enamel of permanent first molars. *Acta Odontologica Scandinavica*, *68*(4), pp.215-222.

Farah RA, Swain MV, Drummond BK, Cook R, Atieh M. Mineral density of hypomineralised enamel. J Dent 2010; 38(1): 50−8

Fehrenbach, M.J. and Popowics, T., 2015. *Illustrated dental embryology, histology, and anatomy*. Elsevier Health Sciences.

Fercher AF. (1993); Ophthalmic Interferometry. In: von Bally G, Khanna S, editors. Optics in Medicine, Biology and Environmental Research. Selected Contributions to the First International Conference on Optics Within Life Sciences (OWLS I), Garmisch-Partenkirchen, Germany, 12–16 August 1990 (ICO-15 SAT). Amsterdam, London, New York, Tokyo: Elsevier; pages 221–8.

Fernandes, C.P. and Chevitarese, O., 1991. The orientation and direction of rods in dental enamel. *The Journal of prosthetic dentistry*, *65*(6), pp.793-800.

Fincham, A. G., LUO, W., Moradian-Oldak, J., Paine, M. L., Snead, M. L. & Zeichner-David, M. 2000. Enamel biomineralization: the assembly and disassembly of the protein extracellular organic matrix. *Development, Function and Evolution of Teeth.* Cambridge University Press.

Fragelli, C.M.B., Souza, J.F.D., Jeremias, F., Cordeiro, R.D.C.L. and Santos-Pinto, L., 2015. Molar incisor hypomineralization (MIH): conservative treatment management to restore affected teeth. *Brazilian oral research*, *29*(1), pp.1-7.

Fried, D., Xie, J., Shafi, S., Featherstone, J. D. B., Breunig, T. M. & Le, C. 2002. Imaging caries lesions and lesion progression with polarization sensitive optical coherence tomography. *Journal of Biomedical Optics,* 7**,** 618-627.

Freden, H. and Gronvik, M., 1980. Prenatal urinary infection and materialisation of permanent teeth. *Tandläkartidningen*, *72*, pp.1382-1383.

Fujimoto, J.G., Pitris, C., Boppart, S.A. and Brezinski, M.E., 2000. Optical coherence tomography: an emerging technology for biomedical imaging and optical biopsy. *Neoplasia*, *2*(1-2), pp.9-25.

Gambetta-Tessini, K., Mariño, R., Ghanim, A., Calache, H. and Manton, D.J., 2016. Knowledge, experience and perceptions regarding Molar-Incisor Hypomineralisation (MIH) amongst Australian and Chilean public oral health care practitioners. *BMC oral health*, *16*(1), p.75.

Garg N, Jain AK, Saha S, Singh J. Essentiality of Early Diagnosis of Molar Incisor Hypomineralization in Children and Review of its Clinical Presentation, Etiology and Management. Int J Clin Pediatr Dent 2012;5(3):190-196.

Ghanim, A., Morgan, M., Marino, R., Bailey, D. and Manton, D., 2011. Molar-incisor hypomineralisation: prevalence and defect characteristics in Iraqi children. *International Journal of paediatric dentistry*, *21*(6), pp.413-421.

Ghanim, A., Elfrink, M., Weerheijm, K., Mariño, R. and Manton, D., 2015. A practical method for use in epidemiological studies on enamel hypomineralisation. *European Archives of Paediatric Dentistry*, *16*(3), pp.235-246.

Ghanim, A., Silva, M.J., Elfrink, M.E.C., Lygidakis, N.A., Mariño, R.J., Weerheijm, K.L. and Manton, D.J., 2017. Molar incisor hypomineralisation (MIH) training

manual for clinical field surveys and practice. *European Archives of Paediatric Dentistry*, *18*(4), pp.225-242.

Gundappa, M., Ng, S.Y. and Whaites, E.J., 2014. Comparison of ultrasound, digital and conventional radiography in differentiating periapical lesions.*Dentomaxillofacial Radiology*.

Gutierrez-Salazar, M. D. P. & Reyes-Gasga, J. 2001. Enamel hardness and caries susceptibility in human teeth. *Revista Latinoamericana de Metalurgia y Materiales,* 21**,** 36-40.

Gutierrez-Salazar, M. D. P. & Reyes-Gasga, J. 2003. Microhardness and Chemical Composition of Human Tooth. *Material Research,* 6**,** 367-373.

Hsieh, Y.S., Ho, Y.C., Lee, S.Y., Chuang, C.C., Tsai, J.C., Lin, K.F. and Sun, C.W., 2013. Dental optical coherence tomography. *Sensors*, *13*(7), pp.8928-8949.

Jalevik, B. & Klingberg, G. A. 2002. Dental treatment, dental fear and behaviour management problems in children with severe enamel hypomineralization of their permanent first molars. *Int J Paediatr Dent,* 12**,** 24-32.

Jalevik B, Noren JG. Enamel hypomineralization of permanent first molars: A morphological study and survey of possible ae- tiological factors. Int J Paediatr Dent 2000; 10(4): 278−89.

Jälevik, B., 2010. Prevalence and diagnosis of Molar-Incisor-Hypomineralisation (MIH): a systematic review. *European Archives of Paediatric Dentistry*, *11*(2), pp.59-64.

Jan J, Vrbič V. Polychlorinated biphenyls cause developmental enamel defects in children. Caries Res 2000;34:469-473.

Jefferies, S.R., 2014. Advances in remineralization for early carious lesions: a comprehensive review. *Compend Contin Educ Dent*, *35*(4), pp.237-243.

Jones, R. S., Darling, C. L., Featherstone, J. D. B. & Fried, D. 2006b. Imaging artificial caries on the occlusal surfaces with polarization-sensitive optical coherence tomography. *Caries Research,* 40**,** 81-89.

Kleinerman, R.A., 2006. Cancer risks following diagnostic and therapeutic radiation exposure in children. *Pediatric radiology*, *36*(2), pp.121-125

Laisi S, Ess A, Sahlberg C, et al. Amoxicillin may cause molar incisor hypomineralisation. J Dent Res 2009;88:132-136

Leppaniemi, A., Lukinmaa, L. & Alaluusua, S. 2000. Nonfluoride hypomineralisation in permanent first molars. *European Academy of Paediatric Dentistry Congress Abstract number 100. Eur J Paediatr Dent***,** 1:128.

Leitgeb, R., Hitzenberger, C. K. & Fercher, A. F. 2003. Performance of fourier domain vs. time domain optical coherence tomography. *Optics Express,* 11**,** 889-894.

Li X, Wang J, Joiner A, Chang J. The remineralisation of enamel: a review of the literature. Journal of dentistry. 2014 Jun 30;42:S12-20

Li, X.D., Boppart, S.A., Van Dam, J., Mashimo, H., Mutinga, M., Drexler, W., Klein, M., Pitris, C., Krinsky, M.L., Brezinski, M.E. and Fujimoto, J.G., 2000. Optical coherence tomography: advanced technology for the endoscopic imaging of Barrett's esophagus. *Endoscopy*, *32*(12), pp.921-930.

Long, B.W., Rollins, J.H. and Smith, B.J., 2015. *Merrill's Atlas of Radiographic Positioning and Procedures-E-Book* (Vol. 3). Elsevier Health Sciences.

Lygidakis NA, Dimou G, Marinou D. Molar-incisor-hypomineralisation (MIH). A retrospective clinical study in Greek children. II. Possible medical aetiological factors. Eur Arch Paediatr Dent 2008;9:207-217.

Lynch, C.D., O'Sullivan, V.R., Dockery, P., McGillycuddy, C.T. and Sloan, A.J., 2010. Hunter-Schreger Band patterns in human tooth enamel. *Journal of Anatomy*, *217*(2), pp.106-115.

Mahoney EK, Rohanizadeh R, Ismail FS, Kilpatrick NM, Swain MV. Mechanical properties and microstructure of hypominer-alised enamel of permanent teeth. Biomaterials 2004; 25(20): 5091−100.

Mahoney, E., Kilpatrick, N. and Swain, M., 2005. Micromechanical and structural analysis of compromised dental tissues. *MRS Online Proceedings Library Archive*, *898*.

Margolis, H. C., Beniash, E. & Fowler, C. E. 2006. Role of macromolecular assembly of enamel matrix proteins in enamel formation. *Journal of Dental Research,* 85**,** 775-793.

Martinović, B., Ivanović, M., Milojković, Z. and Mladenović, R., 2015. Analysis of the mineral composition of hypomineralized first permanent molars. *Vojnosanitetski pregled*, (00), pp.71-71.

Mast, P., Rodrigueztapia, M.T., Daeniker, L. and Krejci, I., 2013. Understanding MIH: definition, epidemiology, differential diagnosis and new treatment guidelines. *Eur J Paediatr Dent*, *14*(3), pp.204-8.

Masterson, E.E., Fitzpatrick, A.L., Enquobahrie, D.A., Mancl, L.A., Conde, E. and Hujoel, P.P., Malnutrition-related early childhood exposures and enamel defects in the permanent dentition: A longitudinal study from the Bolivian Amazon. *American Journal of Physical Anthropology*.

Mathu-Muju, K. and Wright, J.T., 2006. Diagnosis and treatment of molar incisor hypomineralization. *Compendium of continuing education in dentistry (Jamesburg, NJ: 1995)*, *27*(11), pp.604-10.

McHugh, M.L., 2012. Interrater reliability: the kappa statistic. *Biochemia medica: Biochemia medica*, *22*(3), pp.276-282.

Mohd Noor, M., 2014. *Phenotypic properties of enamel in Molarincisor Hypomineralisation (MIH) and Amelogenesis imperfecta (AI) teeth* (Doctoral dissertation, University College London (University of London)).

Murray, D. and Whyte, A., 2002. Dental panoramic tomography: what the general radiologist needs to know. *Clinical radiology*, *57*(1), pp.1-7.

Nanci, A., 2007. *Ten cate's oral histology-pageburst on vitalsource: development, structure, and function*. Elsevier Health Sciences.

NANCI, A. 2013. *Ten Cate's Oral Histology Development, Structure and Function*, Elsevier.

Newbrun, E. and Pigman, W., 1960. The hardness of enamel and dentine. *Australian Dental Journal*, *5*(4), pp.210-217.

Ogden, A. R., Pinhasi, R. & White, W. J. 2007. Gross enamel hypoplasia in molars from subadults in a 16th-18th century London graveyard. *American Journal of Physical Anthropology,* 133**,** 957-966.

Oliver, K., Messer, L.B., Manton, D.J., Kan, K., Ng, F., Olsen, C., Sheahan, J., Silva, M. and Chawla, N., 2014. Distribution and severity of molar hypomineralisation: trial of a new severity index. *International Journal of Paediatric Dentistry*, *24*(2), pp.131-151.

Omar, S.I., 2013. Using resin infiltration to treat developmental defects of enamel: Three case reports. *Journal of Restorative Dentistry*, *1*(1), p.31.

Otis L.L., Matthew J.E., Ujwal S.S., Colson B.W., Jr. Optical coherence tomography: A new imaging technology for dentistry. J. Am. Dent. Assoc. 2000;131:511–514.

Pawlicki, R., Knychalska-Karwin, Z., Stankiewicz, D., Jakób-Dolezal, K. and Karwan, T., 1991. Disturbances of mineral metabolism in teeth of rats receiving corticosteroids for 3 generations. *Folia histochemica et cytobiologica/Polish Academy of Sciences, Polish Histochemical and Cytochemical Society*, *30*(2), pp.75-78.

Pinkham, J. R., Casamassimo, P. S., Mctigue, D. J., Fields, H. W. & Nowak, A. J. 2005. *Paediatric Dentistry Infancy Through Adolescence,* India, Elsevier.

Pitts, N.B., 1996. The use of bitewing radiographs in the management of dental caries: scientific and practical considerations. *Dentomaxillofacial Radiology*, *25*(1), pp.5-16.

Proffit, W.R. and Fields Jr, H.W., 1993. Contemporary Orthodontics. St Louis: Mosby-Year Book.

Prokocimer, T., Amir, E., Blumer, S. and Peretz, B., 2015. Birth-Weight, Pregnancy Term, Pre-Natal and Natal Complications Related to Child's Dental Anomalies. *Journal of Clinical Pediatric Dentistry*, *39*(4), pp.371-376.

Riederer, S.J., 2000. Current technical development of magnetic resonance imaging. *IEEE Engineering in Medicine and Biology Magazine*, *19*(5), pp.34-41.

Rodd, H. D., Boissonade, F. M., Day, P. F. & Dent, M. P. 2007. Pulpal status of hypomineralized permanent molars. *Pediatric Dentistry,* 29**,** 514-520.

ROBINSON, C., KIRKHAM, J., Brookes, S. J., Bonass, W. A. & Shore, R. C. 1995. The chemistry of enamel development. *Int J Dev Biol,* 39**,** 145-52.

Schneider, P.M. and Silva, M., 2018. Endemic Molar Incisor Hypomineralization: a Pandemic Problem That Requires Monitoring by the Entire Health Care Community. *Current osteoporosis reports*, *16*(3), pp.283-288.

Schneider, C.A., Rasband, W.S. and Eliceiri, K.W., 2012. NIH Image to ImageJ: 25 years of image analysis. *Nat methods*, *9*(7), pp.671-675.

Silva-Junior, M.F., Assis, R.I.F.D. and Pazinatto, F.B., 2016. Molar incisor hypomineralization: an aesthetic conservative restorative approach. *RGO-Revista Gaúcha de Odontologia*, *64*(2), pp.186-192.

Smith, J.C., 1971. Radiation: Its detection and its effects on taste preferences. *Progress in physiological psychology*, *4*, pp.53-118.

SIMMER, J. P. & HU, J. C. 2001. Dental enamel formation and its impact on clinical dentistry. *Journal of dental education,* 65**,** 896-905.

Soviero V, Haubek D, Trindade C et al. Prevalence and distribution of demarcated opacities and their sequelae in permanent 1st molars and incisors in 7 to 13-year-old Brazilian children. Acta Odontol Scand 2009; 67: 170–175.

Staines, M., Robinson, W.H. and Hood, J.A.A., 1981. Spherical indentation of tooth enamel. *Journal of materials science*, *16*(9), pp.2551-2556.

Strauss, K.J. and Kaste, S.C., 2006. The ALARA (As Low As Reasonably Achievable) Concept in Pediatric Interventional and Fluoroscopic Imaging: Striving to Keep Radiation Doses as Low as Possible during Fluoroscopy of Pediatric Patients—A White Paper Executive Summary 1. *Radiology*, *240*(3), pp.621-622.

Steffen, R., Krämer, N. and Bekes, K., The Würzburg MIH concept: the MIH treatment need index (MIH TNI). *European Archives of Paediatric Dentistry*, pp.1-7.

Tsai, M.T., Lee, C.K., Lee, H.C., Chen, H.M., Chiang, C.P., Wang, Y.M. and Yang, C.C., 2009. Differentiating oral lesions in different carcinogenesis stages with optical coherence tomography. *Journal of biomedical optics*, *14*(4), pp.044028-044028.

Tymofiyeva, O., Boldt, J., Rottner, K., Schmid, F., Richter, E.J. and Jakob, P.M., 2009. High-resolution 3D magnetic resonance imaging and quantification of carious lesions and dental pulp in vivo. *Magnetic Resonance Materials in Physics, Biology and Medicine*, *22*(6), p.365.

Vargas-Ferreira, F. and Ardenghi, T.M., 2011. Developmental enamel defects and their impact on child oral health-related quality of life. *Brazilian oral research*, *25*(6), pp.531-537.

Van Amerongen, W.E. and Kreulen, C.M., 1995. Cheese molars: A pilot study of the etiology of hypocalcifications in first permanent molars. *Journal of dentistry for children*, *62*.

van Luijk, J.A., 1981. NMR: dental imaging without x-rays?. *Oral Surgery, Oral Medicine, Oral Pathology*, *52*(3), pp.321-324.

Weerhejim, K. L., Jalevik, B. & Alaluusua, S. 2001. Molar-incisor hypomineralisation. *Caries Res,* 35**,** 390-1.

Weerheijm, K.L., Duggal, M., Mejàre, I., Papagiannoulis, L., Koch, G., Martens, L.C. and Hallonsten, A.L., 2003. Judgement criteria for Molar Incisor Hypomincralisation (MIH) in epidemiologic studies: a summary of the European meeting on MIH held in Athens, 2003. *European Journal of Paediatric Dentistry*, *4*, pp.110-114.

Welzel, J. 2001. Optical coherence tomography in dermatology: a review. *Skin Research and Technology,* 7**,** 1-9.

Whatling, R. & Fearne, J. M. 2008. Molar incisor hypomineralization: a study of aetiological factors in a group of UK children. *International Journal of Paediatric Dentistry,* 18**,** 155-162.

White, S.C. and Pharoah, M.J., 2014. *Oral radiology: principles and interpretation*. Elsevier Health Sciences.

White, S. & Mallya, S. M. 2012. Update on the biological effects of ionizing radiation, relative dose factors and radiation hygiene. *Australian Dental Journal,* 57 Suppl 1**,** 2-8.

Williams, J.K. and Gowans, A.J., 2003. Hypomineralised first permanent molars and the orthodontist. *European Journal of Paediatric Dentistry*, *4*, pp.129-132.

William, V., Messer, L.B. and Burrow, M.F., 2006. Molar incisor hypomineralization: review and recommendations for clinical management. *Pediatric dentistry*, *28*(3), pp.224-232.

Willmott, N. S., Bryan, R. A. E. & Duggal, M. S. 2008. Molar-incisor-hypomineralisation: a literature review. *European archives of paediatric* 166 *dentistry : official journal of the European Academy of Paediatric Dentistry,* 9**,** 172-9.

Woodward, G.L. and Leake, J.L., 1996. The use of dental radiographs to estimate the probability of cavitation of carious interproximal lesions. Part I: Evidence from the literature. *Journal (Canadian Dental Association)*, *62*(9), pp.731-736.

W. Sui, C. Boyd, and J. T. Wright, “Altered pH regulation during enamel

development in the cystic fibrosis mouse incisor," Journal of Dental Research, vol. 82, no. 5, pp. 388–392, 2003.

Zagdwon AM, Toumba KJ, Curzon ME. The prevalence of developmental enamel defects in permanent molars in a group of English school children. Eur J Paediatr Dent 2002; 3: 91–96.

CHAPTER 12

Appendices

12. Appendices

Appendix 1- Ethical approval

Miss Susan Parekh
Clinical Lecturer
UCL
Department of Paediatric Dentistry
Eastman Dental Hospital
London
WC1X8LD

National Research Ethics Service

NRES Committee London- Fulham

Fulham Palace Road
London
W68RF
Telephone: 020 3311 7282
Facsimile: 020 3311 7280

11 August 2011

Dear Miss

Study title: **A Study of the genotype and phenotype in AmelogenesisImperfecta& Molar Incisor Hypomineralization**

Thank you for your letter of 08 August 2011, responding to the Committee's request for further information on the above research and submitting revised documentation.

The further information has been considered on behalf of the Committee by the Chair.

Confirmation of ethical opinion

On behalf of the Committee, I am pleased to confirm a favourable ethical opinion for the above research on the basis described in the application form, protocol and supporting documentation as revised, subject to the conditions specified below.

Ethical review of research sites

NHS sites

The favourable opinion applies to all NHS sites taking part in the study, subject to management permission being obtained from the NHS/HSC R&D office prior to the start of the study (see "Conditions of the favourable opinion" below).

Non-NHS sites

The Committee has not yet been notified of the outcome of any site-specific assessment (SSA) for the non-NHS research site(s) taking part in this study. The favourable opinion does not therefore apply to any non-NHS site at present. We will write to you again as soon as one Research Ethics Committee has notified the outcome of a SSA. In the meantime no study procedures should be initiated at non-NHS sites.

Conditions of the favourable opinion

The favourable opinion is subject to the following conditions being met prior to the start of the study.

Statement of compliance

The Committee is constituted in accordance with the Governance Arrangements for Research Ethics Committees (July 2001) and complies fully with the Standard Operating

Procedures for Research Ethics Committees in the UK.

After ethical review

Reporting requirements

The attached document *"After ethical review - guidance for researchers"* give detailed guidance on reporting requirements for studies with a favourable opinion, including:

- Notifying substantial amendments
- Adding new sites and investigators
- Notification of serious breaches of the protocol
  Progress and safety reports
- Notifying the end of the study

The NRES website also provides guidance on these topics, which is updated in the light of changes in reporting requirements or procedures.

Feedback

You are invited to give your view of the service that you have received from the National Research Ethics Service and the application procedure. If you wish to make your views known please use the feedback form available on the website.

Further information is available at National Research Ethics Service website >After Review

11/LO/07
77

Please quote this number on all correspondence

With the Committee's best wishes for the success of this project

Yours sincerely

Charles Mackworth- Young

Chair

Email louise.moran2@imperial.

Management permission or approval must be obtained from each host organisation prior to the start of the study at the site concerned.

Management permission ("R&D approval'?should be sought from al/ NHS organisations involved in the study in accordance with NHS research governance arrangements.

Guidance on applying for **NHS** permission for research is available in the

Integrated Research Application System or at http://www.rdforum.nhs.uk.

Where a NHS organisation's role in the study is limited to identifying and referring potential participants to research sites ("participant identification centre"), guidance should be sought from the R&D office on the information it requires to give permission for this activity.

For non-NHS sites, site management permission should be obtained in accordance with the procedures of the relevant host organisation.

Sponsors are not required to notify the Committee of approvals from host organisations

It is the responsibility of the sponsor to ensure that all the conditions are complied with before the start of the study or its initiation at a particular site (as applicable).

Approved documents

The final list of documents reviewed and approved by the Committee is as follows:

Document	*Version*	*Date*
Covering Letter		09 May 2011
Investigator CV	1	22 September 2010
Other: CVs for student &other research team		
Participant Consent Form: Parent Consent Form	1	
Participant Consent Form: Patient Consent Form	1	
Participant Consent Form: Child Assent Form	1	
Participant Consent Form: Consent form for Phenodent database		
Participant Information Sheet: Main Study: Parent	3	08 August 2011
Participant Information Sheet: Main Study: Parent	2	07 July 2011
Participant Information Sheet: Main Study: Patient	2	07 July 2011
Participant Information Sheet: Colour Spectroscopy: Parent	1	04 July 2011
Participant Information Sheet: Colour Spectroscopy: Patient	1	04 July 2011
Participant Information Sheet: Main Study: First 20 Patients - Parent	2	07 July 2011
Participant Information Sheet: Main Study: First 20 Patients - Patient 2		07 July 2011
Participant Information Sheet: Main Study: Patient	3	08 August 2011
Protocol	2	07 July 2011
REC application	71904/212856/1/911	09 May 2011
Response to Request for Further Information		28 July 2011
Response to Request for Further Information		08 August 2011

Appendix 2- Patient Information leaflet

Research team:

Dr Susan Parekh,

Dr Agnes Bloch Zupan,

Dr Peter Brett,

Dr Laurent Bozec

Mashael Abdullatif

Nurjehan Ibrahim

Nabilah Harith

Amanda O'Donnell

Contact details:

Dr Susan Parekh

Tel: 020 3456 1067

Fax: 020 3456 2329

Unit of Paediatric Dentistry

The Eastman Dental Hospital and Institute

256 Gray's Inn Road

London WC1X 8LD

s.parekh@eastman.ucl.ac.uk

Website: www.uclh.nhs.uk

UCL HOSPITALS

If you need a large print, audio or translated copy of this document, please contact us on 0207 915 1022. We will try our best to meet your needs.

If you wish to discuss this study with a member of the research team or an independent expert who is not part of the research team, please ask Dr Susan Parekh

Thank you for taking the time to read this leaflet.

© University College London Hospitals NHS Foundation Trust

University College London Hospitals NHS

A study of the genetics and the physical properties of dental anomalies

Publication date: 08/08/11

Date last reviewed

Version number 3

UCL Hospitals cannot accept responsibility for information provided by external organisations.

Patient's Information Leaflet

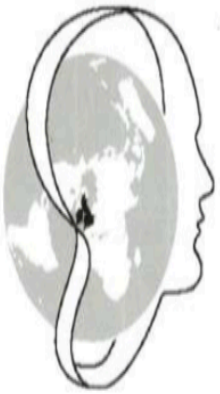

A Study of the genetics and the physical properties of dental anomalies

Invitation

You are being invited to take part in a research study. Before you make a decision, it is important that you know why the research is being done and what it would involve from you. Please take time to read the following information carefully and discuss it with others if you wish. Ask us if anything is not clear at any time before or after participating. If you need more information we are willing to spend more time to satisfy you before taking any decision.

What is the purpose of the study?

To obtain and gather more information about dental anomalies, such as Enamel defects (Amelogenesis Imperfecta AI), and dentine defects (Dentinogenesis Imperfecta DI). We want to use this information to improve our knowledge of genetics and the properties of the teeth, to provide better support and long term care.

Why has I have been chosen?

We are asking all patients who have been diagnosed with dental anomalies and members of their families with the same or other dental conditions to participate in the study

Do I have to take part?

No. It is up to you to decide. If you do decide to participate we will ask you to sign a consent form. If you change your mind, you are free to withdraw at any time, without giving a reason. The standard of care you will receive will not be affected in any way.

What will happen to me if I take part?

We will ask you some questions about your teeth and your medical history, and examine your teeth, take photographs, and a saliva sample. The saliva sample will be used to link your DNA with the physical properties of your teeth. If you require any teeth to be extracted as part of your treatment, these will be collected for laboratory testing of the teeth. You will not need to do anything else. If any member of your family has similar teeth, we will invite them to take part as well, as this will help to detect the common dental genes in families. If you do not want other members of your family to participate, you can refuse and your treatment will not be affected in any way.

What are the possible disadvantages or risks of taking part?

There are no risks anticipated. None of your answers will affect your treatment in any way.

What are the possible benefits?

The information from this study will hopefully be used to help us expand our knowledge about the genetics of dental anomalies, and relate this to the appearance of the teeth, identify affected families and provide better support and treatment.

What will happen with the results?

Any samples that we collect will be stored using a study ID number, so that they cannot be directly linked to you. We hope to publish the results of the study on completion. All confidential information will be coded and you will not be identifiable in any way.

Will my taking part in the study remain confidential?

Yes. All information that is collected about you during the research will remain strictly confidential and will be seen only by the investigators named on this sheet. The safety and security of the data will be the responsibility of the principal investigator (Miss Susan Parekh). This information will be recorded in such a way that it is completely anonymous and you cannot be individually identified in anyway.

The information will also be stored in a database developed by Strasbourg University (phenodent database), who we work closely with. All information will be anonymised before putting on the phenodent database.

Who has reviewed the study?

All research in the NHS is looked at by independent group, called a Research Ethics Committee to protect your safety, rights, wellbeing and dignity. This study has been reviewed and given favourable opinion by the Joint Research Ethics Committee. If you would like to see a summary of the findings from the study when it is completed, please tell Miss Parekh or any of the other dentists you see.

Appendix 3- Consent forms

University College London Hospitals NHS
NHS Foundation Trust

The Eastman Dental Hospital
256 Gray's Inn road
London
WC1X 8LD

Telephone: 020 3456 7899
Direct Line: 020-3456-1067
Fax: 020-3456-2329
Web-site: www.uclh.nhs.uk

Version 1
Study Number:....
Patient Identification Number for this trial: .....

PATIENT CONSENT FORM

Title of Project:

A Study of the genetics and the physical properties of dental anomalies.

Name of Researchers: Dr Susan Parekh, Dr Agnes Bloch-Zupan, Dr Peter Brett, Dr Laurent Bozec, Miss Amanda O`Donnell, Mashael Abdullatif, Nurjehan Mohamed Ibrahim and Nabilah Narith.

Please initial box

1. I confirm that I have read and understood the information sheet dated 21/12/10 (version 1) for the study. I have been allowed some time to think about this, ask questions, and have had these answered in a way that I understand. ☐

2. I understand that my participation is voluntary and that I am free to withdraw at any time, without giving any reason , without my medical care or legal rights being affected. ☐

3. I understand that sections of any medical notes may be looked at by the researchers and responsible individuals from regulatory authorities where it is relevant to my part in the research. I give permission for these individuals to have access to my records. ☐

4. I give permission to the investigators to pass clinical data collected from my examination to my General Practitioner or General Dental Practitioner ☐

5. I understand that the samples taken from me may be stored and used for the purpose of further research at a later date. I understand that these results will also remain anonymous. ☐

6. I understand that (this project or future research) will include genetic research aimed at understanding the genetic influences on dental defects in children. ☐

7. I agree for to take part in the above study. ☐

Name of Patient	Date	Signature of patient

Name of Person taking consent	Date	Signature

When completed, 1 for patient; 1 for researcher site file; 1 (original) to be kept in medical notes

UCL HOSPITALS

UCL Hospitals is an NHS Foundation Trust comprising: The Eastman Dental Hospital, The Heart Hospital, Hospital for Tropical Diseases, National Hospital for Neurology and Neurosurgery, The Royal London Homoeopathic Hospital and University College Hospital (incorporating the former Middlesex and Elizabeth Garrett Anderson Hospitals).

S Parekh Version 1

For further information about this study please contact Dr Susan Parekh
Phone : 020 3456 1067 email: s.parekh@eastman.ucl.ac.uk

UCLH welcomes feedback from their patients who have been involved in research. In the first instance, you should inform the Principal Investigator. If you are not satisfied with the response of the research team then you should address your complaints to the UCLH complaints manager at UCLH postal address or through our website http://www.uclh.nhs.uk/Contact+us/. To help us identify the research study you have been involved in, please mention the title and the name of the research doctor or principal investigator. You can find this information on the Patient Information Sheet.

Consent form for the Phenodent database

You/ your child have been asked to participate in the database project entitled "Diagnosing Dental Defects database D [4] / Phenodent.

The establishment of this registry has received the favorable opinion of CCTIRS 11.09.2008, and authorization of the CNIL on 18/05/2009 (Registration No. 908416).

I can at any time obtain additional information from Miss Susan Parekh (primary investigator) or Prof. Agnes Bloch-Zupan, Project Manager, the Reference Centre of dental manifestations of rare diseases, Department of Oral Health Care, University Hospital Strasbourg, Hôpital Civil, 1 place Hospital, F-67000 Strasbourg Cedex France or email: agnes.bloch@chru-strasbourg.fr

I authorize the registration of anonymous data and pictures in the database yes ☐ no ☐
and my ethnic background (via the collection of country and city of birth) yes ☐ no ☐
This information may also be used for teaching purposes

For data files, I authorize the possible dissemination of all images, yes ☐ no ☐
or only intraoral pictures yes ☐ no ☐

YOUR AGREEMENT TO PARTICIPATE IN THIS REGISTRY
My signature certifies that I clearly understood the information regarding my participation in this registry

Name of Patient	Date	Signature
Name of Parent	Date	Signature
Name of Person taking consent	Date	Signature

This document is to be performed in two original copies:
A copy kept by the person giving consent (or by the holders of parental authority if minor)
The other copy to be kept by the primary investigator, Miss Susan Parekh

Appendix 4- Dental anomaly proforma

Dental anomalies proforma

study ID:.....

Date of clinic:..... Pt sticker:

Clinician name:.....

Ethnicity: White Mixed Black Asian Chinese Other.....

Referred by: GDP CDS HDS GP Other:.....

c/o: Nil pain sens appearance Other:.....

Relevant medical history:.....

.....

Fluoride history: supp Y/N water Y/N toothpaste child/adult

Dental history: restn Y/N ext Y/N LA Y/N sed Y/N GA Y/N

Family history (inc family tree): Plaque score:

Extra-oral features: Skeletal pattern I II III

Hair: normal/sparse skin:.....

face:..... hands/nails:..... Other:.....

Intra-oral features: lips gingiva palate mucosa saliva

Teeth present (chart):

Eruption: early Y/N delayed Y/N infraoccluded Y/N impacted Y/N

General/local Mild/mod/sev; teeth:..... Teeth:.....

Occlusion: Class I Class II Class III Class III OJ = OB: complete / incomplete

AOB Y/N

Dentine:

discoloured: Y/N abscess: Y/N tooth wear: mild / mod / sev (which teeth):

Enamel:

18	17	16	15	14	13	12	11	21	22	23	24	25	26	27	28
DDE index: Location (L): 1 incisal ⅓; 2 gingival ⅓; 3 whole surface. Demarcation of defect (D): 1 demarcated; 2 diffuse; 3 both			55	54	53	52	51	61	62	63	64	65	Extent of defect(E): 1 < ¼; 2 ¼ – ½; 3 at least ½. Wear: mild mild; sev severe		
			85	84	83	82	81	71	72	73	74	75			
48	47	46	45	44	43	42	41	31	32	33	34	35	36	37	37

Type of defect: 0 normal; 1 opacity (white/cream); 2 opacity (yellow/brown); 3 hypoplasia (pits); 4 hypoplasia (horizontal grooves); 5 hypoplasia (vertical groves); 6 hypoplasia (missing enamel); 7 discoloured enamel (not assoc. with opacity); 8 post-eruptive breakdown; 9 other defects;

Number / form / size:

18	17	16	15	14	13	12	11	21	22	23	24	25	26	27	28
			55	54	53	52	51	61	62	63	64	65			
			85	84	83	82	81	71	72	73	74	75			
48	47	46	45	44	43	42	41	31	32	33	34	35	36	37	37

con conical; shov shovel; dbl double; rog rounded or bulbous; tap tapered; cet talon cusp; can abnormal cusp; noc notched; mic microdont; mac microdont; inv invagination; env evagination; mih enlarged mamelons; pem enamel pearls; sup supernumerary; hyp hypodontia

Radiographic findings: taurodont Y/N thin enamel Y/N short roots Y/N
pulp stones Y/N apical area Y/N resorption Y/N

Diagnosis:

Proposed treatment plan:

1.

2.

3.

4.

Treatment to date:

Allocated to:

Review on anomalies clinic: Y/N when?

Photographs Y/N **saliva** Y/N **Consent** Y/N

Appendix 5- Poster presentation at the International Association of Dental Research (IADR) in London, UK in July 2018

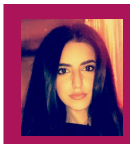

Advanced Imaging Towards Better Diagnostics of Molar Incisor Hypomineralisation

#3186

D. Al Sabah[1], K.Al Azri[1], S. Parekh[1] and L.Bozec[2]

[1] Eastman Dental Institute, University College of London (UCL), London, UK

[2] Division of Biomaterials & Tissue engineering, Eastman Dental Institute – University College London

UCL

Introduction:

Molar incisor hypomineralisation (MIH) is a qualitative developmental defect of enamel, defined as hypomineralisation of systemic origin affecting first permanent molars and less frequently associated with permanent central incisors. Currently, MIH lesions are diagnosed using conventional methods, clinical indices and radiographs, which both have their limitations, subjectivity and radiation respectively.

Aim of the study:

"Can optical coherence tomography (OCT) be used as an adjunct diagnosis for MIH?"

Objectives

➔Define empirical markers in the OCT scan and scattering profile intensity plot for different MIH lesions
➔Evaluate the progression of the lesions as a whole, from 1-D to 3-D

Materials and methods:

Ethical approval obtained and 34 teeth were collected, 3 control and 31 MIH affected FPMs. The MIH defects were characterised using both the modified developmental defects of enamel index (mDDE). All teeth were then imaged radiographically and using OCT (Vivosight, Michelson Diagnostics, Kent, UK).

Results:

a) Clinical assessment of Enamel Defects in MIH

Visual Assessment

- using related indices mDDE index

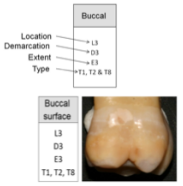

Radiographic Assessment

- Underestimates the lesion (2D)
- Involves ionising radiation

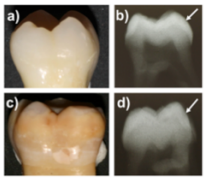

Figure 1 showing clinical and radiographic images of a first permanent molar (FPM)

a)MIH diagnosis with OCT

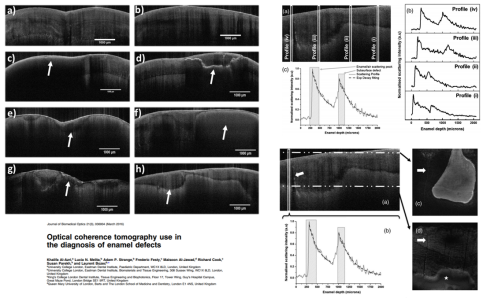

Figure 2 showing OCT scans of a FPM with their corresponding a-scans

c) From B-scan to disease markers:

Typical a-Scans

➔control

➔type 1

➔type 2

➔PEB

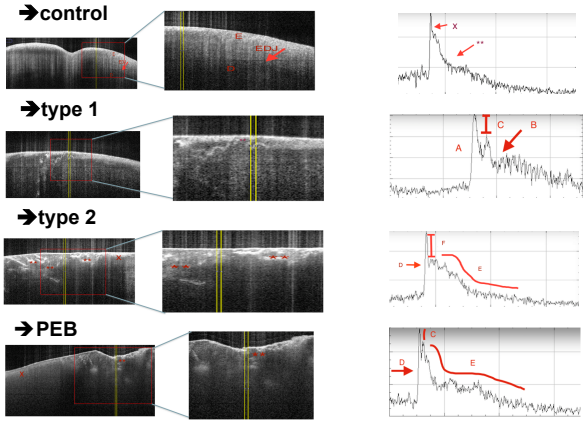

Figure 3 showing OCT scans of a control, type 1, type 2 and PEB MIH lesions with their corresponding a-scans

d) Markers assessments:

Wide	Short	Jagged	%Probability (Type1)	%Probability (Type2)	%Probability (PEB)
1	1	1	80.7	2.4	16.9
1	1	0	61.7	3.5	34.8
1	0	0	87.9	10.4	1.7
1	0	1	78.1	17.8	4.1
0	1	1	21.9	9.1	69.0
0	1	0	9.7	7.8	82.5
0	0	1	34.0	56.1	9.9
0	0	0	20.1	64.1	15.8

Type	Markers
Type 1	Wide
Type 2	Narrow, long
PEB	Narrow, short

Table 1 showing probabilities of markers relating to correct diagnosis (1= seen, 0= not seen)

e) From 1D to 3D diagnostics

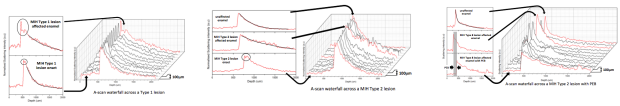

Figure 4 showing waterfall illustrations of type 1, type 2 and PEB lesions

Discussion:

- Conventional methods (figure 1) can not predict accurately the prognosis of MIH affected teeth before PEB occurs
- This is the first study to analyse markers (figure 3) to diagnose MIH lesions
- OCT can help us differentiate between different types of lesions (table 1) in a safe, non-ionising technique
- More accurate data can be seen in 3D images (figure 4)

Conclusion:

OCT has been proven to be a useful diagnostic method when studying MIH lesions, which shows us full understanding of the lesion with its depth and extent. OCT helps to differentiate between MIH and sound teeth, and additionally between different types of MIH lesions.

References

eastman DENTAL INSTITUTE

Appendix 6- Three minute thesis (3MT) presentation, PhDs Annual Research Symposium, University College of London, UK in November 2017

EASTMAN DENTAL INSTITUTE

UCL

Seeing is Believing

A New Approach to Diagnostics in Dentistry

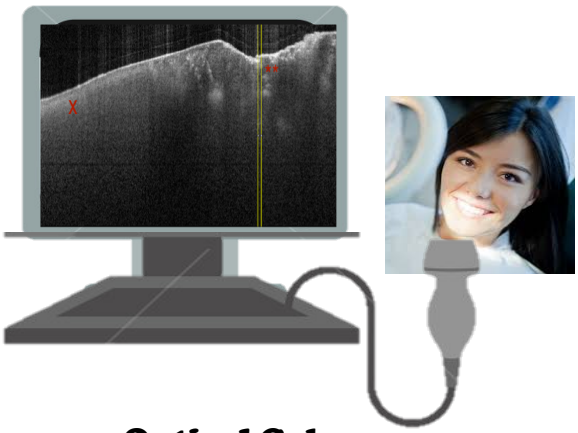

X-RAY

1895

Optical Coherence Tomography

2017